

Mid-Pliocene restriction of the Indonesian Gateway and its implication on ocean circulation and climate

Dissertation

Zur Erlangung des Doktorgrades
der Mathematisch-Naturwissenschaftlichen Fakultät
der Christian-Albrechts-Universität zu Kiel

vorgelegt von
Cyrus Karas

Kiel, 2010

Referent:.....PD Dr. Dirk Nürnberg

Koreferent:.....Prof. Dr. Ralf Tiedemann

Tag der Disputation:.....23.04.2010

Zum Druck genehmigt, Kiel den:.....23.04.2010

Der Dekan:.....Prof. Dr. Lutz Kipp

Erklärung

Hiermit erkläre ich Eides statt, dass die vorliegende Arbeit, abgesehen von der Beratung durch meine akademischen Lehrer, in Inhalt und Form meine eigene Arbeit darstellt. Ferner habe ich weder diese noch eine ähnliche Arbeit an einer anderen Hochschule im Rahmen eines Prüfungsverfahrens vorgelegt. Diese Arbeit ist unter Einhaltung der Regeln guter wissenschaftlicher Praxis der Deutschen Forschungsgemeinschaft entstanden.

Kiel, den 22. März 2010

Cyrus Karas

Abstract

The impacts of the constrictions of the Indonesian Gateway and the Central American Seaway on ocean circulation are among the keys to understand Pliocene climate evolution, including the intensification of the Northern Hemisphere Glaciation between 3.5 and 2.5 Ma. Plate tectonic reconstructions show that the main reorganization of one such seaway, the Indonesian Gateway, occurred between 4 and 3 Myr ago. Model simulations have suggested that this tectonic reorganization triggered far-reaching effects on ocean circulation and climate, including a switch in the source of waters feeding the Indonesian Throughflow into the Indian Ocean. This PHD thesis aims to elucidate the climatic and oceanographic changes related to the constriction of the Indonesian Gateway. It presents combined $\delta^{18}\text{O}$ and Mg/Ca ratios of planktonic foraminifera (marine protozoa) from surface and subsurface levels to reconstruct the thermal structure and changes in salinities at four following sensitive core sites in the Indian and Pacific Oceans from ~6 to 2 Myr ago: DSDP Site 214 in the tropical east Indian Ocean, ODP Site 709C in the west tropical Indian Ocean, ODP 763A in the subtropical east Indian Ocean under the influence of the Leeuwin Current, and DSDP Site 590B in the southwest Pacific Ocean at the Tasman Front:

In the outflow region of the Indonesian Throughflow (DSDP Site 214), sea surface conditions remained relatively stable throughout the mentioned Pliocene interval, while subsurface waters (300-450 m water depth) freshened and cooled by about 4°C between 3.5 and 2.95 Myr ago. After 2.95 Ma, constantly low subsurface temperatures and fresher conditions suggested a prevailing throughflow of North Pacific source waters through the Indonesian Gateway. These findings supported the hypothesis of Cane and Molnar (2001) that the constriction of the Indonesian Gateway (4-3 Ma) led to a major reorganization in the Indonesian Throughflow. The cooling and shoaling of the thermocline in the tropical Indian Ocean might have contributed to cooling in various (sub)tropical upwelling regions.

At Site 763, surface temperatures cooled by ~2°C compared to tropical Indian Ocean sites 214 and 709C during the mid-Pliocene, pointing to a Leeuwin Current, which weakened since ~3.3 Myr ago in line with the hydrographic changes in the Indonesian Throughflow region. Most likely, a reduced surface Indonesian Throughflow led to a diminished poleward heat transport resulting in a weakened Leeuwin Current and a cooling of the Benguela upwelling system. Thereby, by cooling the southern Indian and Atlantic Oceans this mechanism amplified the mid-Pliocene global development towards increased meridional temperature gradients.

The Tasman Front Site 590B is influenced by both, the Central American Seaway and the Indonesian Gateway. Gradual cooling of $\sim 2^{\circ}\text{C}$, and freshening of the sea surface during $\sim 4.6\text{-}4\text{ Ma}$ was related to the closing of the Central American Seaway, which reached a critical threshold during this time and presumably cooled the southwest Pacific through heat piracy by the Northern Hemisphere. After $\sim 3.5\text{ Ma}$, the ongoing restriction of the Indonesian Gateway might have amplified the southward heading East Australian Current, allowing still warm sea surface temperatures at Site 590B when the global climate gradually cooled. In contrast, the cooling and freshening of the subsurface level in line with a marked increase in the sand fraction points to a fostered northward circulation of Subantarctic Mode- and Antarctic Intermediate waters, possibly a first step towards the present Antarctic Frontal System.

Zusammenfassung

Die Auswirkungen der Einengungen der indonesischen Ozeanpassage und des Panamaseeweges auf die Ozeanzirkulation gehören zu den Schlüsseln die Pliozäne Klimaentwicklung zu verstehen, welche die Intensivierung der Nordhemisphärenvereisung zwischen 3.5-2.5 Millionen Jahren vor heute beinhaltet. Plattentektonische Rekonstruktionen zeigen, dass die vorwiegende Umgestaltung eines dieser Seewege, die indonesische Ozeanpassage, sich vor 4-3 Millionen Jahren vor heute vollzogen hat. Modellsimulationen haben nahegelegt, dass diese tektonische Umgestaltung weitreichende Folgen für die Ozeanzirkulation und das Klima verursachte, einschließlich eines Wassermassenwechsels im Indonesischen Durchfluss in den Indischen Ozean. Diese Studie beabsichtigt, die klimatischen und ozeanographischen Änderungen, die durch die Einengung der indonesischen Ozeanpassage entstanden sind aufzuklären. Kombinierte $\delta^{18}\text{O}$ - und Mg/Ca-Verhältnisse von planktonischen Foraminiferen (marine Einzeller) von der Oberfläche und von tieferen Wassermassen werden dargelegt, um die Wärmeverteilung und Änderungen der Salinität an den folgenden vier sensitiven Kernlokalationen im Indischen und Pazifischen Ozean im Zeitraum von 6-2 Millionen Jahren vor heute zu rekonstruieren: DSDP Site 214 im östlichen tropischen Indischen Ozean, ODP Site 709C im westlichen tropischen Indischen Ozean, ODP Site 763A im subtropischen östlichen Indischen Ozean im Einflußbereich des Leeuwin Stroms und DSDP Site 590B vom Südwest Pazifik an der Tasman Front.

In dem Ausflußbereich des indonesischen Durchflusses (DSDP Site 214) blieben die Oberflächentemperaturen während des gesamten Pliozäns relativ konstant, während die tiefen Wassermassen (Wassertiefe von 300-450 m) salzärmer wurden und eine Abkühlung von etwa 4°C während 3.5-2.95 Millionen Jahren vor heute zeigten. Nach 2.95 Millionen Jahren vor heute deuteten konstant kalte Temperaturen bei salzärmeren Bedingungen im tiefen Niveau den nun überwiegenden Durchfluß von Nordpazifischen Wassermassen durch die indonesische Ozeanpassage an. Diese Ergebnisse unterstützen die Hypothese von Cane and Molnar (2001), dass die Einengung der indonesischen Ozeanpassage (4-3 Millionen Jahre vor heute) zu einer wichtigen Umgestaltung des indonesischen Durchflusses geführt hat. Das Abkühlen und die Verflachung der Thermokline im tropischen Indischen Ozean könnte somit zur Abkühlung von verschiedenen (sub)tropischen Auftriebsgebieten beigetragen haben.

An Site 763 kühlten die Oberflächentemperaturen um etwa 2°C im mittleren Pliozän im Vergleich zu den Sites 214 und 709C ab, welche im tropischen Indischen Ozean liegen. Dies deutet darauf hin, dass sich der Leeuwin Strom seit etwa 3.3 Millionen Jahren vor heute in Übereinstimmung mit den hydrographischen Änderungen in der indonesischen

Durchflußregion abschwächte. Höchstwahrscheinlich führte ein reduzierter indonesischer Oberflächendurchfluß zu einem verminderten polwärts gerichteten Wärmetransport, der zu einem abgeschwächtem Leeuwin Strom und zu einer Abkühlung des Benguela Auftriebsgebietes führte. Durch die Abkühlung der südlichen Indischen und Atlantischen Ozeane verstärkte dieser Mechanismus die Entwicklung im Mittleren Pliozän zu ausgeprägteren meridionalen Temperaturgradienten.

Site 590B an der Tasman Front zeigt ozeanische Einflüsse von beiden Ozeanpassagen: Dem Panamaseeweg und der indonesischen Ozeanpassage. Ein sukzessives Abkühlen der Oberfläche um 2°C und salzärmere Bedingungen während etwa 4.6-4 Millionen Jahren vor heute wurden auf die Schließung des Panamaseeweges bezogen, welcher während dieser Zeit einen kritischen Schwellenwert erreichte und wahrscheinlich den Südwestpazifik durch die einsetzende "Wärmepiraterie" der Nordhemisphäre abkühlte. Nach etwa 3.5 Millionen Jahren vor heute verstärkte die anhaltende Einengung der indonesischen Ozeanpassage vermutlich den südwärtsgerichteten Ostaustralstrom, der an Site 590B weiterhin warme Oberflächentemperaturen erlaubte, als sich das globale Klima sukzessive abkühlte. Im Gegensatz dazu deutet das Abkühlen des tiefen Niveaus, bei gleichzeitig salzärmeren Bedingungen, im Einklang mit einem deutlichen Anstieg der Sandfraktion auf eine verstärkte nordwärtsgerichtete Zirkulation von subantarktischen Zwischen- und Intermediären Wassermassen. Dies war vielleicht der erste Schritt in Richtung des heutigen antarktischen Frontensystems.

Acknowledgements

In erster Linie möchte ich mich bei PD Dr. Dirk Nürnberg für die intensive Betreuung der Arbeit, die Unterstützung und für die zahlreichen Diskussionen bedanken. Ferner danke ich neben PD Dr. Dirk Nürnberg auch Prof. Dr. Ralf Tiedemann, ohne die es das Projekt Nu60/14-(1 und 2) nicht gegeben hätte. Hier noch mal großer Dank an Prof. Dr. Ralf Tiedemann für die nützlichen Ratschläge und Diskussionen.

Für die hilfreiche Unterstützung im Labor und bei der Probenaufbereitung bedanke ich mich ganz herzlich bei Nadine Gehre. Für die Unterstützung an der ICP bedanke ich mich bei Karin Kießling und Dieter Garbe-Schönberg. Lulzim Haxhiaj danke ich für die Hilfe im Isotopenlabor.

Für Ratschläge aller Art und Diskussionen möchte ich mich bei Dr. Jereon Groeneveld, Dr. Marcus Regenber, Dr. Johan Etourneau, Dr. André Bahr, Dr. Uwe Pflaumann, Nabil Khélifi und Prof. Dr. Martin Frank bedanken.

Für die Bereitstellung der Modellierungsergebnisse danke ich Dr. Uta Krebs-Kanzow und Prof. Dr. Birgit Schneider.

Ferner bedanke ich mich bei Prof. Dr. Wolf-Christian Dullo für die Bereitstellung des Arbeitsplatzes und allen Mitarbeitern des IFM-GEOMAR die zum Gelingen der Arbeit beigetragen haben. Hier natürlich auch Dank an Jan Riethdorf für das ein oder andere Korrekturlesen in den letzten Wochen.

Last but not least danke ich meiner Familie und meinen Freunden. Meinen Eltern bin ich für alle Unterstützung dankbar.

Contents

Abstract/ Zusammenfassung

Acknowledgements

Chapter I	Introduction: The Pliocene Epoch (~5-2 Ma) and oceanic gateways, main objectives, strategy and structure of the thesis	3
Chapter II	Materials and Methods: Sample preparation, $\delta^{18}\text{O}$ and Mg/Ca analysis and age models	13
Chapter III	Mid-Pliocene climate change amplified by a switch in Indonesian subsurface throughflow Cyrus Karas, Dirk Nürnberg, Anil K. Gupta, Ralf Tiedemann, Kuppusamy Mohan and Torsten Bickert (published in <i>Nature Geoscience</i> , 2009)	19
Chapter IV	Mid-Pliocene reduction in meridional heat transport amplified by Indonesian Throughflow changes Cyrus Karas, Dirk Nürnberg, Ralf Tiedemann and Dieter Garbe-Schönberg (<i>Paleoceanography</i> , in review)	45
Chapter V	Pliocene climate change of the southwest Pacific and the impact of ocean gateways Cyrus Karas, Dirk Nürnberg, Ralf Tiedemann and Dieter Garbe-Schönberg (submitted to <i>Earth and Planetary Science Letters</i>)	65
Chapter VI	General conclusions and perspectives	87
References	For chapters I, II and VI	93
Appendices	Data on the studied core sites presented in chapters III-V	

Chapter I

Introduction

The Pliocene Epoch (~5-2 Ma) and oceanic gateways

The early Pliocene (~5-3 Ma) is the most recent epoch in Earth's history with "Greenhouse" conditions. Although the atmospheric concentrations of CO₂ were comparable to modern conditions (Raymo et al., 1996; Pagani et al., 2010), global surface temperatures were ~3°C warmer and the sea level was ~25 m higher with less ice shields in the high northern latitudes (Mudelsee and Raymo, 2005; Ravelo et al., 2004; Dowsett et al., 1996). The tropical warm pool was greatly expanded with a weaker global atmospheric circulation that maintained "permanent El Niño-like" or "El Padre" conditions in the tropical Pacific Ocean (Brierley et al., 2009) with no or largely reduced east-west gradient in sea surface temperatures (SST). Consequently there was a deep thermocline in the equatorial east Pacific with the absence of a cold water tongue as today (Wara et al., 2005). Also, subsurface waters seem to have been globally warmer than today with distinctly warmer SST at present eastern boundary upwelling regions in the (sub)tropics (e.g., Marlow et al., 2000; Lawrence et al., 2006). Owing to different forcing mechanisms, these conditions have not changed synchronously when Earth experienced gradual global cooling towards the late Pliocene (Ravelo et al., 2004; Mudelsee et al., 2005). The impacts of the constriction of the Indonesian Gateway and the Central American Seaway on ocean circulation are thereby among the keys to understand the Pliocene climate evolution, including the intensification of the Northern Hemisphere Glaciation between 3.5 and 2.5 Ma (e.g., Haug et al., 1999; Cane and Molnar et al., 2001; Karas et al., 2009).

The closure of the Central American Seaway was intensively worked out by several paleoceanographic studies (e.g., Haug et al., 1999; Haug et al., 2001, Steph et al., in press), showing primarily oceanic effects during ~4.6-4 Ma. During this time, a critical threshold was reached with a significantly restricted Caribbean–Pacific surface water exchange. It was suggested that this restriction led to both, the development of the modern Atlantic-Pacific salinity contrast (Steph et al., 2006), and to a significant shoaling of the equatorial east Pacific thermocline (Steph et al., 2006; Steph et al., in press). The formation of the Isthmus of Panama should also have strengthened the Atlantic thermohaline circulation including the Gulf Stream, transporting more surface heat towards high northern latitudes (Haug et al., 1999).

In contrast, the restriction of the Indonesian Seaway was poorly defined due to the lack of paleoceanographic studies. Based on foraminiferal assemblages, Shrinivasan and Sinha (1998) assumed an early restriction at ~5.2 Ma, whereas other studies suggested significant shoaling since the middle or late Miocene (Kennett et al., 1985; Gaspari and Kennett, 1993).

From the plate tectonic history of the Indonesian Gateway it became evident that the early evolution of the Indonesian Gateway started at ~ 25 Ma, with major tectonic events during the Pliocene including the appearance of islands and mountain building (Hill and Hall, 2003; Kuhnt et al., 2004). However, the timing of a critical state, which might have acted as a threshold for profound ocean circulation, remained uncertain. Plate tectonic reconstructions and modelling studies pointed to a major reorganization in the Indonesian Throughflow (ITF) during ~ 4 -3 Ma (Cane and Molnar 2001; Rodgers et al., 2000). According to the study of Cane and Molnar (2001), the northward movement of New Guinea since 5 Ma switched the source of ITF surface waters from the warm and saline South Pacific to the cooler and fresher North Pacific. The postulated effects should have resulted in a distinct drop of SST ($\sim 2^\circ\text{C}$ in 100 m water depth) in the tropical eastern Indian Ocean (Fig. 1.1), which in turn might have initiated droughts in eastern Africa, affected hominid evolution, and contributed to the Northern Hemisphere Glaciation.

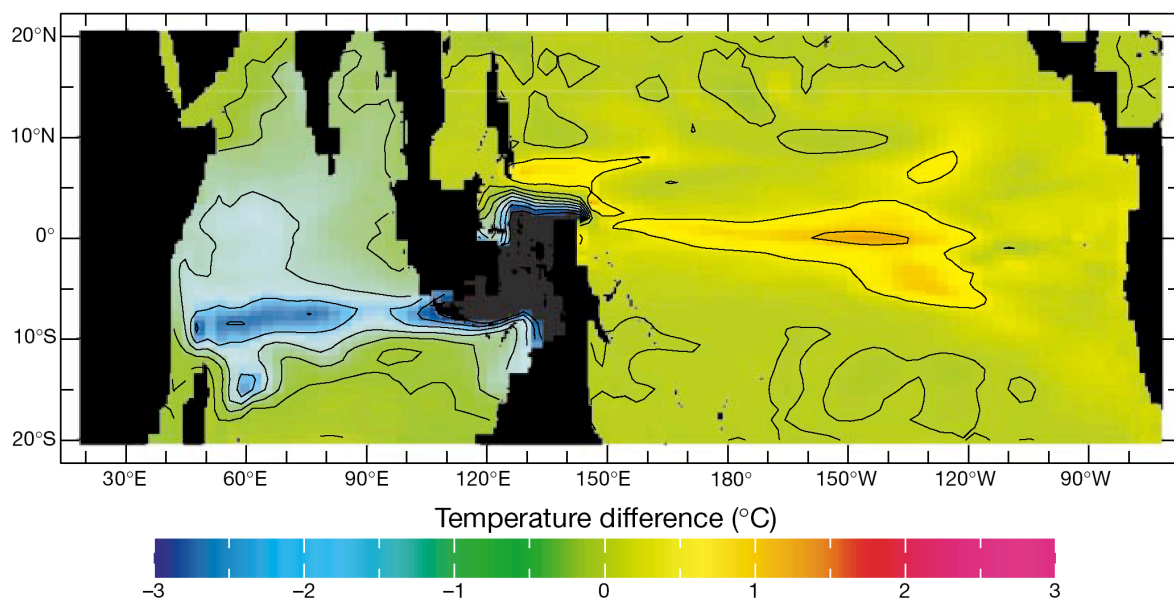


Figure 1.1 Modelled differences in seawater temperatures at ~ 100 m water depth between New Guinea's northward (2°N) and southward position (3°S ; Cane and Molnar, 2001). Note distinct cooling in the equatorial Indian Ocean at $\sim 10^\circ\text{S}$.

Modelling studies, which explored the influence of a closed *versus* an opened Indonesian Gateway on climate (Hirst and Godfrey, 1993; Godfrey, 1996) suggested notable changes in the warm surface ocean currents around Australia (Fig. 1.2). In the Indian Ocean, a weaker Leeuwin Current off northwest Australia was expected, whereas on the other side of the Gateway - in the southwest Pacific Ocean - a distinct weakening of the warm East Australian Current (EAC) was postulated.

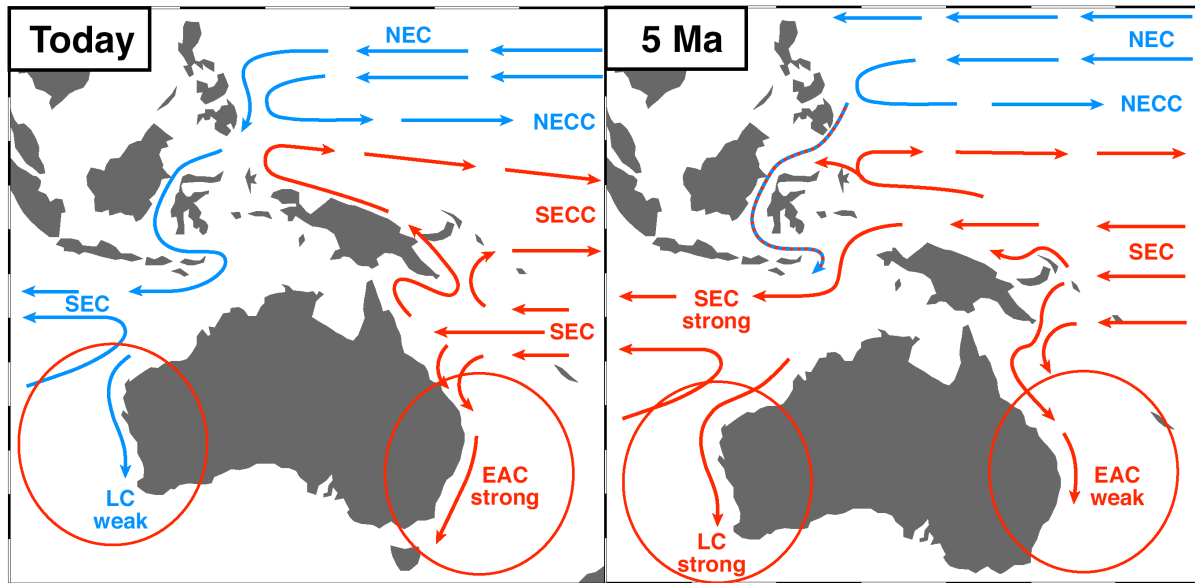


Figure 1.2 Schematic pattern of sea surface currents for today and 5 Ma. The hypothesized 5 Ma scenario is based on information from general ocean circulation models (Hirst and Godfrey, 1993; Godfrey, 1996; Rodgers et al., 1999; 2000). NEC=North Equatorial Current, NECC=North Equatorial Counter Current; SECC=South Equatorial Counter Current; SEC=South Equatorial Current. Changes in the Leeuwin Current (LC) and East Australian Current (EAC) are indicated by a circle. Figure modified from Nürnberg and Tiedemann (DFG-Project proposal Nu60/14-1).

Main objectives of the thesis

The overall aim of this thesis is to examine of the closure history of the Indonesian Gateway and its impact on the upper ocean circulation and climate for the time interval from ~6 to 2 Ma. The research presented here focused on the following objectives:

- To reconstruct closure-related changes (sea surface temperatures and salinities) within the surface layer.
- To test the hypothesis of Cane and Molnar (2001), suggesting that the constriction of the Indonesian Gateway from ~4 to 3 Ma switched the source of ITF waters from the warm and saline South Pacific to the cooler and fresher North Pacific, leading to a cooling of the tropical Indian Ocean. This cooling might in turn have initiated droughts in eastern Africa and contributed to the Northern Hemisphere Glaciation.
- To explore closure-related changes (temperatures and salinities) at subsurface depths, especially in the Indian Ocean, to test the proposed switch of ITF source waters at subsurface depths and infer the development of the modern cold and fresh Australasian Mediterranean Water tongue.

- To determine changes of the Leeuwin Current, which has been predicted to weaken in response to a closed Indonesian Gateway. And to clarify the implications for the pole ward heat transport.
- To examine the development of the warm EAC in the southwest Pacific, which was suggested to increase upon closing the Indonesian Gateway.
- To explore a possible interplay between the oceanographic changes associated with the constriction of the Indonesian Gateway and the shoaling of the Central American Seaway. It is possible distinguish between both effects between 5 and 3 Ma?

Strategy of the thesis

Selection of core sites and modern oceanography

To elucidate the closure history of the Indonesian Gateway and to test its modelled effects on ocean circulation and climate (Hirst and Godfrey, 1993; Godfrey, 1996; Cane and Molnar, 2001) we selected four core sites in the Indian Ocean (DSDP/ODP sites 214, 709C, and 763A) and Pacific Ocean (DSDP Site 590B), located in key regions sensitive to changes upon closing the Indonesian Gateway (Fig 1.3).

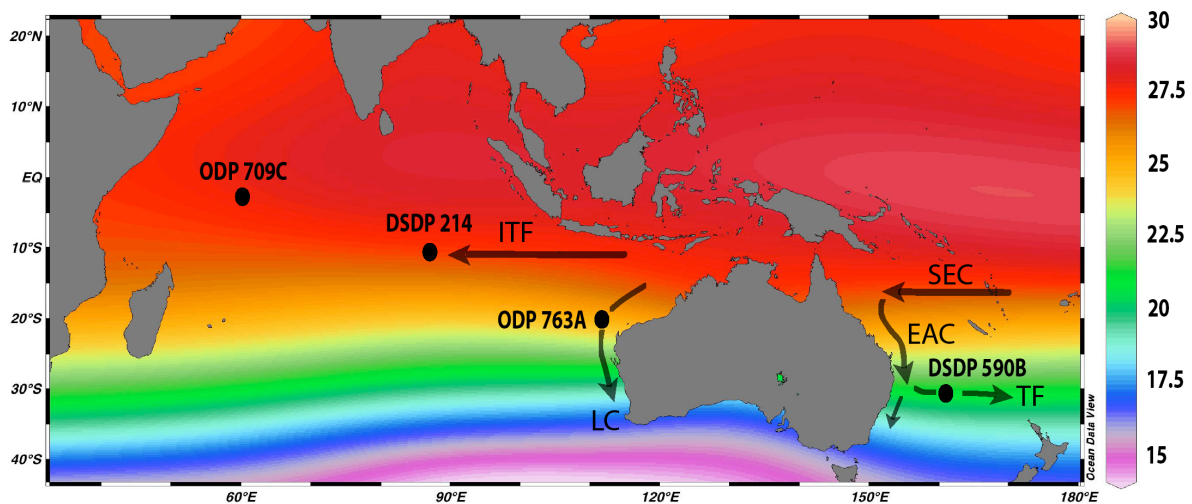


Figure 1.3 Modern annual ocean temperatures (in °C) at 20 m water depth (Locarnini et al., 2006). Studied core sites 214, 709C, 763A, 590B (black dots) and surface ocean currents are indicated. ITF=Indonesian Throughflow, SEC=South Equatorial Current, LC=Leeuwin Current, EAC=East Australian Current, TF=Tasman Front.

Site 214

Deep Sea Drilling Program (DSDP) Site 214 ($11^{\circ}20.21'S$, $88^{\circ}43.08'E$; 1665 m water depth) is located in the tropical eastern Indian Ocean on the Ninety East Ridge. Site 214 is at a key location to monitor changes in the ITF, as surface waters are within the ITF and record conditions of the Indian-Pacific Warm Pool (Fig. 1.3), whereas subsurface waters belong to the cold and fresh Australasian Mediterranean Water, which originates from the ITF area (Fig. 1.4). Today it can be traced at water depths of ~ 300 -450 m far into the Indian Ocean (Tomczak and Godfrey, 1994). This core site is essential to test the hypothesis of Cane and Molnar (2001), as it lies within the predicted area of distinct surface cooling due to the constriction of the Indonesian Gateway.

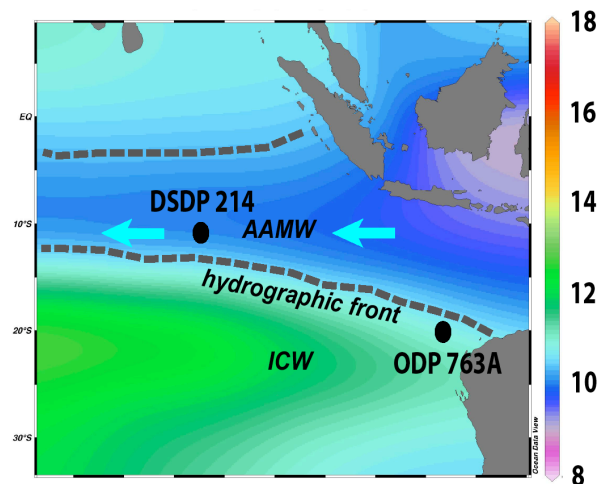


Figure 1.4 Oceanographic chart showing subsurface annual temperatures (in $^{\circ}C$) at 400 m water depth in the eastern Indian Ocean. Site 214, 763A, and different water masses are indicated. AAMW=Australasian Mediterranean Water, ICW=Indian Ocean Central Water. (Locarnini et al., 2006). Note the hydrographic front between both water masses at Site 763A.

Site 709C

ODP Site 709C ($3^{\circ}54.9'S$; $60^{\circ}33.1'E$, 3041 m water depth, Fig. 1.3) is located in the tropical western Indian Ocean. It was selected to monitor the development of the Indian Ocean Warm Pool.

Site 763A

ODP Site 763 ($20^{\circ}35.20'S$, $112^{\circ}12.50'E$; 1367 m water depth) is located in the subtropical eastern Indian Ocean close to the Indonesian Gateway northwest of Australia. Today this site lies within the influence of the warm Leeuwin Current off western Australia, whereas at subsurface depths it is situated at the southernmost reaches of the Australasian

Mediterranean Water from the Indonesian region (Fig. 1.3, 1.4; Tomczak and Godfrey, 1994). Therefore this site is sensitive to changes in the Indonesian Throughflow at both, the surface and subsurface level. This site location was selected to test Ocean General Circulation Models (Hirst and Godfrey, 1993; Godfrey, 1996), which suggest a marked reduction of the Leeuwin current upon closing the ITF with consequences for the polar heat transport.

Site 590B

DSDP Site 590B (31°10.02'S; 163°21.51'E; 1308 m water depth) is located in the southwestern Pacific close to the Tasman Front (Fig. 1.3). Nowadays the Tasman Front is a thermal front separating warm subtropical waters to the north from temperate waters to the south (Kennett, 1986). This front is fed by the EAC, being a branch of the South Equatorial Current off southwestern Australia. Occasionally, some water is transported all along the east coast of Australia towards Tasmania (Hamilton, 2006) forming warm eddies there (Cresswell, 1987). Site 590B is ideally located to infer changes of the warm EAC, the corresponding Tasman Front and the meridional heat gradient between the tropics and the subtropics. Modelling studies suggest a weakening of the warm EAC upon closing of the Indonesian Gateway (Hirst and Godfrey, 1993; Godfrey, 1996). At subsurface and bottom depths, Site 590B was suitable to monitor changes in Subantarctic Mode and Antarctic Intermediate Waters (for details see Chapter V).

Structure of the thesis

To address the abovementioned objectives, this thesis is divided into six chapters:

Chapter I contains a general introduction into the Pliocene climate and the restriction of the Indonesian Gateway. It further presents the main objectives of the thesis and discusses the selection of sites and their modern oceanographic settings.

Chapter II gives an overview of the methods, which were applied to reconstruct the closing history of the Indonesian Gateway. It contains general information on the age models used, sample preparation, and foraminiferal Mg/Ca- and $\delta^{18}\text{O}$ analyses. Detailed information is given in the respective chapters.

Chapter III is an already published article in *Nature Geoscience* that presents Pliocene (sub)surface ocean temperature and salinity reconstructions from the tropical eastern Indian

Ocean Site 214. Here, we test the hypothesis of Cane and Molnar (2001) predicting a switch in ITF source waters along the restriction of the Indonesian Gateway.

Chapter IV corresponds to a manuscript in *Paleoceanography* (in review) that elucidates the effects of the restricted Indonesian Gateway on the surface heat flux towards the Southern Ocean. In particular, it focuses on the response of the warm Leeuwin Current off northwestern Australia, which is crucial for the southward heat transport.

Chapter V is submitted to *Earth and Planetary Science Letters* and presents the Pliocene climatic evolution at southwest Pacific Site 590B and discusses possible influences from both gateways: The Central American Seaway and the Indonesian Gateway. Most notably, this chapter shows changes in Subantarctic Mode Water and Antarctic Intermediate Water due to climatic changes in the Southern Ocean.

Chapter VI summarizes the main conclusions from chapters III-V and provides perspectives for future studies, exploring the climatic effects from the restriction of the Indonesian Gateway.

The **Appendices** present the data on the studied core sites shown in chapters III-V.

Chapter II

Materials and Methods

Sample preparation for $\delta^{18}\text{O}$ and Mg/Ca analysis

All samples analysed in this study were provided by IODP. Bulk sediment samples (~10cm³) from Sites 590B, 709C, and 763A were freeze-dried and washed over a 63 μm sieve. The remaining >63 μm sediment fraction was dried at 50°C, sieved and separated into six fraction sizes: >400 μm , 350-400 μm , 315-350 μm , 250-315 μm , 125-250 μm , and 63-125 μm .

Subsequently, ~30-50 specimens were selected from shallow dwelling planktonic foraminifera *G. sacculifer* (without sac-like chamber) and *G. ruber* (only at Site 214), which both calcify in the upper 50 m water depth (Anand et al., 2003). From the deep dwelling planktonic foraminifera *G. crassaformis* (calcification depth of ~300-450 m; Elderfield et al., 2002), 20-40 specimens were selected. At Site 214, 20-40 specimens of deep mixed layer species *G. venezuelana* were picked. Only in few cases, the number had to be reduced to ~10 specimens. Specimens were selected from the 315-355 μm size fraction to avoid size effects in $\delta^{18}\text{O}$ values and Mg/Ca (Elderfield et al., 2002). At Site 214, we used the 300-400 μm size fraction. Subsequently, sample material was gently crushed, mixed, and optically divided into two thirds used for Mg/Ca analyses, and one third for stable isotope measurements.

$\delta^{18}\text{O}$ analysis

For stable isotope analyses, samples were rinsed with Ethanol and ultrasonically cleaned for a few seconds. Measurements were either conducted on a Finnigan MAT-252 (at IFM-GEOMAR, Kiel) or on a Finnigan MAT-251 mass spectrometer (at the Leibniz-Laboratory for Radiometric Dating and Stable Isotope Research, Kiel), both equipped with a fully automated carbonate preparation device. Both machines have an analytical precision better than $\pm 0.07\%$ for $\delta^{18}\text{O}$; $\pm \sigma$. All values are reported relative to Pee Dee Belemnite (PDB, based on calibration directly to National Bureau of Standards (NBS-19)).

Mg/Ca analysis

For Mg/Ca analyses, samples were cleaned according to the established cleaning protocol of Barker et al. (2003) (non reductive). To remove clay particles, the material was rinsed 5 times with distilled deionized water, each time interrupted by 1-2 minutes of ultrasonic cleaning. To remove further clay, the samples were washed two times with distilled methanol, alternating with ultrasonic cleaning. Methanol residues were removed with distilled deionized water. Thereafter, a treatment with a 1% *NaOH* / *H₂O₂* oxidizing solution (10 mL

0.1 N NaOH (analytical grade); 100 μL 30% H_2O_2 (suprapure) at $\sim 100^\circ\text{C}$ followed. Every 2.5 minutes vials were rapped on the bench top to release gaseous build. To enhance the reaction after 5 min, vials were placed in an ultrasonic bath for a few seconds. The treatment was repeated once. Residues of the solution were removed by 3 times rinsing of distilled deionized water. Samples were then transferred into new vials, and 250 μL of a 0.001 M HNO_3 solution (subboiled distilled) was added. Repeated rinsing with distilled deionized water followed. Afterwards, each sample was dissolved with 350 μL of a 0.075 M HNO_3 solution (subboiled distilled) in an ultrasonic bath, interrupted by releasing gaseous buildup. Samples were transferred into 500 μL vials diluted with 2,5 ml distilled deionized water.

Measurements were performed on a simultaneous, radially viewing ICP-OES (Ciros CCD SOP, Spectro A.I., Germany, Inst. of Geosciences, Univ. of Kiel) with an analytical error of $\sim 0.1\%$. Replicate analysis on the same samples, cleaned and analysed during different sessions, showed a standard deviation of ~ 0.1 mmol/mol (rel. std. dev. $< 3\%$). Monitoring of Fe/Ca and Mn/Ca indicated that contamination with clays or Mn-carbonates after cleaning was not an issue.

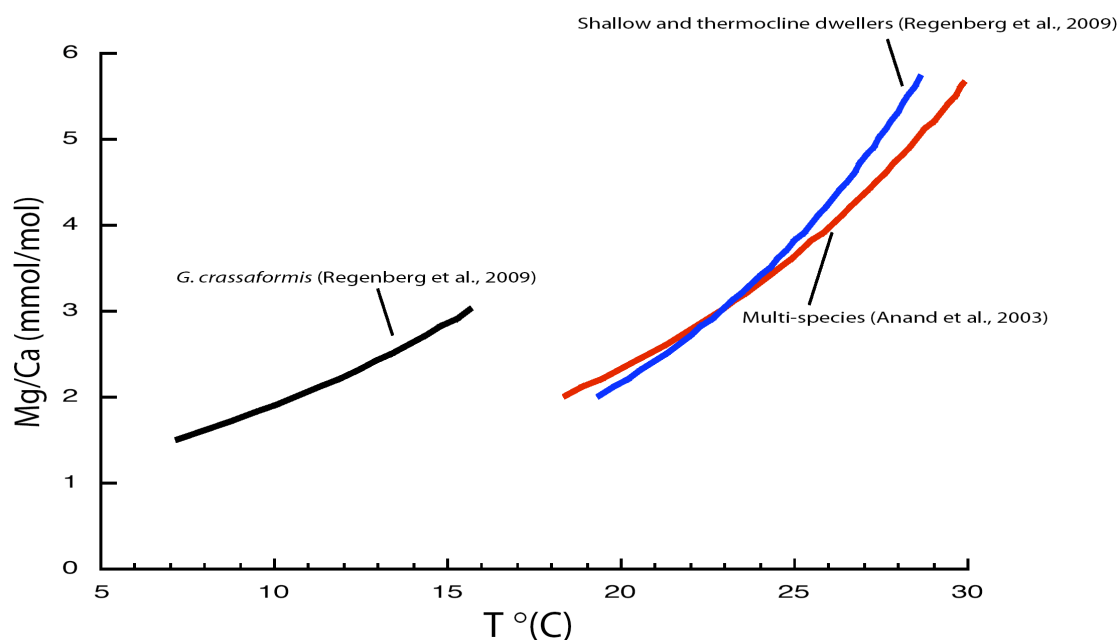


Figure 2.1 Multi-species dependencies of foraminiferal Mg/Ca on temperature. Calibrations used in this study are indicated. For further explanations see text.

Mg/Ca ratios of *G. sacculifer* and *G. ruber* were converted into temperatures (Fig. 2.1) by using the multispecies calibration of Anand et al. (2003): $\text{Mg/Ca} = 0.38 \exp(0.09 \times \text{SST})$. The conversion from *G. crassaformis* Mg/Ca ratios into temperatures (Fig. 2.1) was conducted by using a species-specific calibration of Regenberg et al. (2009): $\text{Mg/Ca} = 0.83 \exp(0.082 \times T)$. For *G. venezuelana* Mg/Ca ratios, we used the shallow/thermocline dweller calibration of Regenberg et al. (2009; Fig. 2.1): $\text{Mg/Ca} = 0.22 \exp(0.113 \times T)$.

When establishing Mg/Ca derived SST records, it is most crucial to assess the impact of calcite dissolution on foraminiferal Mg/Ca, the effect of which varies regionally as well as spatially. Consequently, this study eagerly assessed the impact of possible calcite dissolution at each core site, and if it was necessary, the initial Mg/Ca ratios were corrected after Regenberg et al. (2006) (see chapters III-V). Regenberg et al. (2006) suggested critical ΔCO_3^{2-} levels of $\sim 20 \mu\text{mol/kg}$, when Mg^{2+} loss starts, and proposed correction equations.

The calculation of planktonic foraminiferal $\delta^{18}\text{O}_{\text{seawater}}$ and $\delta^{18}\text{O}_{\text{ivc-seawater}}$ values were used to infer ancient changes in (sub)surface salinities. We thereby used the combined $\delta^{18}\text{O}$ and Mg/Ca-temperature records (Nürnberg, 2000; Fig. 2.2) from the surface dwelling planktonic species *G. sacculifer* and from the deep dwelling *G. crassaformis*. Details for the calculations are given in chapters III-V.

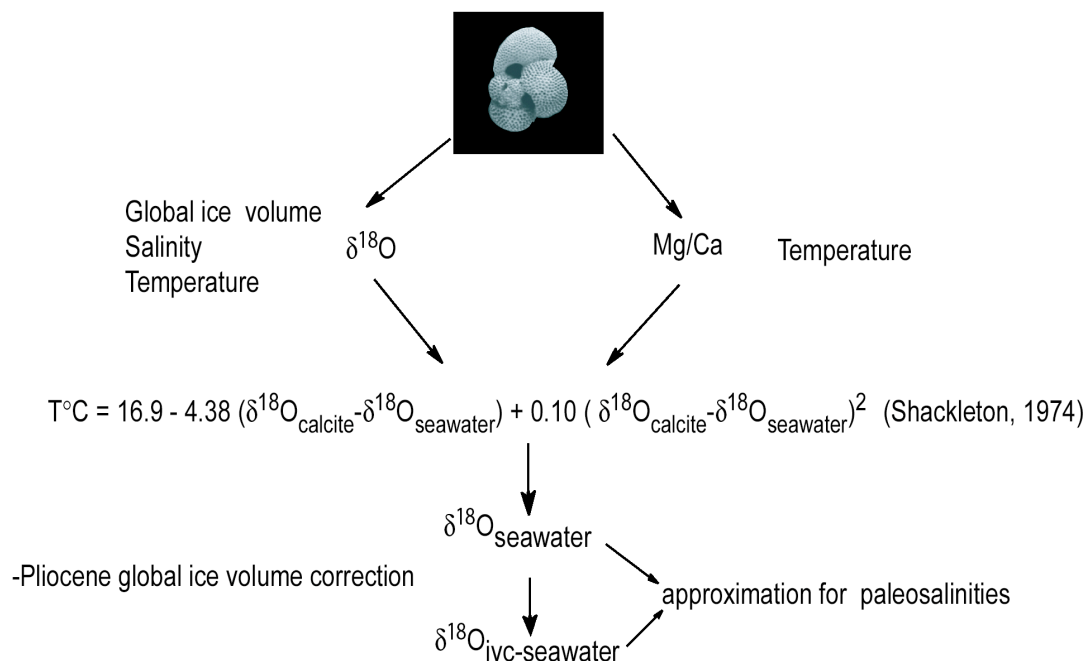


Figure 2.2 Schematic description to assess paleo (sub)surface salinities (after Nürnberg, 2000). The combined analyses of Mg/Ca and $\delta^{18}\text{O}$ on the same biotic carrier allows to extract $\delta^{18}\text{O}_{\text{seawater}}$ by the usage of the equation of Shackleton et al. (1974). This formula describes the dependency of $\delta^{18}\text{O}_{\text{calcite}}$, $\delta^{18}\text{O}_{\text{seawater}}$, and ocean temperature ($T^{\circ}\text{C}$). Note that the foraminiferal $\delta^{18}\text{O}$ signal is dependent from the global ice volume, the salinity, and the ocean temperature, whereas the foraminiferal Mg/Ca ratio is predominantly determined by the ocean temperature. By subtracting an estimation of the Pliocene global ice volume signal, the ice volume corrected seawater values ($\delta^{18}\text{O}_{\text{ivc-seawater}}$) were calculated. Both, $\delta^{18}\text{O}_{\text{seawater}}$ and $\delta^{18}\text{O}_{\text{ivc-seawater}}$ served as an approximation for paleosalinities.

Age models

A well-established and accurate age control for sediment cores is essential for all interpretations concerning the history of ocean circulation and climate. Especially, when comparing proxy records from different core sites, it is necessary to establish a consistent stratigraphic framework. Keeping this in mind, new age models were established or existing age controls were improved from all core sites studied. Thereby, benthic $\delta^{18}\text{O}$ records from sites 214, 590B, and 763A were produced during time periods, when significant oceanographic changes due to the restricted Indonesian Gateway were expected. The development of benthic isotope records provided most reliable stratigraphic information, as the deep ocean is largely unaffected by temperature and salinity changes. Subsequently, the tuning to the widely accepted benthic reference record “LR04” from Lisiecki and Raymo (2005) warranted the usage of the same age scale for all studied core sites. In this respect this holds also true for Site 709C. We here tuned the planktonic $\delta^{18}\text{O}$ record from Shackleton and Hall (1990) to Site 806, which age control is also based on the LR04 stack (see Chapter IV). Further age test was achieved by the usage of existing nannofossil biostratigraphy and magnetic reversal ages, which were all updated to the latest age scale of ATNTS 2004 (Lourens et al., 2004). At Site 763A further astronomical tuning supported our established age model. All tuning, astronomical tuning, and filtering was carried out with Analyseries 1.2 (Paillard et al., 1996). Each age model is explained in detail in chapters III-V.

Chapter III

Mid-Pliocene climate change amplified by a switch in Indonesian subsurface throughflow

Mid-Pliocene climate change amplified by a switch in Indonesian subsurface throughflow

Cyrus Karas¹, Dirk Nürnberg¹, Anil K. Gupta², Ralf Tiedemann³, Kuppusamy Mohan² and Torsten Bickert⁴

¹ Leibniz Institute of Marine Sciences (IFM-GEOMAR), University of Kiel, Wischhofstrasse 1-3, D-24148 Kiel, Germany

² Department of Geology & Geophysics, Indian Institute of Technology, Kharagpur 721302, India

³ Alfred Wegener Institute for Polar and Marine Research, Am Alten Hafen 26, D-27568 Bremerhaven, Germany

⁴ Zentrum für Marine Umweltwissenschaften, Universität Bremen, D-28334 Bremen, Germany

The tectonically driven closure of tropical seaways during the Pliocene epoch (5–2 million years (Myr) ago) altered ocean circulation and affected the evolution of climate. Plate tectonic reconstructions show that the main reorganization of one such seaway, the Indonesian Gateway, occurred between 4 and 3 Myr ago. Model simulations have suggested that this would have triggered a switch in the source of waters feeding the Indonesian Throughflow into the Indian Ocean, from the warm salty waters of the South Pacific Ocean to the cool and relatively fresh waters of the North Pacific Ocean. Here we use paired measurements of the $\delta^{18}\text{O}$ and Mg/Ca ratios of planktonic foraminifera to reconstruct the thermal structure of the eastern tropical Indian Ocean from 5.5 to 2 Myr ago. We find that sea surface conditions remained relatively stable throughout the interval, whereas subsurface waters freshened and cooled by about 4°C between 3.5 and 2.95 Myr ago. We suggest that the restriction of the Indonesian Gateway led to the cooling and shoaling of the thermocline in the tropical Indian Ocean. We conclude that this tectonic reorganization contributed to the global shoaling of the thermocline recorded during the Pliocene epoch, possibly contributing to the development of the equatorial east Pacific cold tongue.

The importance of the Central American Seaway (Haug et al., 2001) and the Indonesian Throughflow (ITF) (Cane and Molnar, 2001) with respect to Pliocene global climatic reorganizations is intensively debated. The closing of the Central American Seaway was thought to have affected tropical climate and might have pre-conditioned or delayed Northern Hemisphere Glaciation (NHG) by supplying heat and moisture to high northern latitudes, although major oceanographic and climatic responses terminated more than 1 Ma before

NHG (Haug et al., 2001; Driscoll and Haug, 1998; Steph et al., 2006). The mid-Pliocene climate transition (Mudelsee and Raymo, 2005) marks the gradual change from a climate with little or no ice in the Northern Hemisphere and $\sim 3^{\circ}\text{C}$ warmer global surface temperatures (Ravelo et al., 2004) to a climate state with extended continental ice sheets at high northern latitudes (Shackleton et al., 1984). The onset of significant NHG (Mudelsee and Raymo, 2005) was accompanied by the initiation of strong winter monsoons in India (Gupta and Thomas, 2003) and a shift in African vegetation (deMenocal, 1995). This time was also marked by enhanced sea surface temperature (SST) cooling in (sub)tropical upwelling regions and the development of a tropical Pacific west-to-east SST gradient, especially after 3 Ma (Marlow et al., 2000; Lawrence et al., 2006; Dekens et al., 2007; Ravelo et al., 2007; Wara et al., 2005). These changes in (sub)tropical SST were taken as evidence for the termination of the early Pliocene “permanent El Niño-like” climate conditions (Philander and Fedorov, 2003; Fedorov et al., 2006). However, the timing of major tropical reorganizations during the Pliocene, which also include significant shoaling of the thermocline in the equatorial east Pacific cold tongue (Steph et al., 2006; Wara et al., 2005; Chaisson and Ravelo, 2000) does not appear to have taken place synchronously. This makes it difficult to define and to allocate the driving mechanisms, especially if the response has different regional expressions, due to different regional sensitivities (Ravelo et al., 2004). Here, we examine whether the gradual constriction of the Indonesian Gateway from 4-3 Ma appears as a viable process to reorganize the tropical Indian and Pacific oceanography and hence, tropical climate (Cane and Molnar, 2001).

Testing the theory of Cane and Molnar (2001)

According to Cane and Molnar (2001), the northward movement of New Guinea since 5 Ma switched the source of ITF surface waters from the warm and saline South Pacific to the cooler and fresher North Pacific. The postulated effects should have resulted in a distinct drop of SST ($\sim 2^{\circ}\text{C}$ in 100 m water depth) in the tropical eastern Indian Ocean and a reorganization of the Pacific SST from an El Niño-like towards a La Niña-like pattern which in turn both initiated droughts in eastern Africa and contributed to the NHG (Cane and Molnar, 2001; Rodgers et al., 2000). In order to test this hypothesis (Cane and Molnar, 2001) we here present combined planktonic foraminiferal Mg/Ca and $\delta^{18}\text{O}$ data from tropical eastern Indian Ocean Deep Sea Drilling Program (DSDP) Site 214 ($11^{\circ}20.21'\text{S}$, $88^{\circ}43.08'\text{E}$, 1665 m water depth) spanning the time period from 5.5 to 2 Ma. Site 214 is at a key location, as surface waters record conditions of the Indian-Pacific Warm Pool (Fig. 3.1A), whereas subsurface

waters belong to the cold and fresh Australasian Mediterranean Water, which originates from the ITF area. Today, it can be traced at water depths of ~300-450 m far into the Indian Ocean (Tomczak and Godfrey, 1994; You and Tomczak, 1993) (Fig. 3.1B, C). We selected surface dwelling planktonic foraminifera *Globigerinoides ruber* and *Globigerinoides sacculifer*, deep mixed layer species *Globoquadrina venezuelana*, and deep dwelling *Globorotalia crassaformis* to reconstruct oceanographic changes at different depth levels (Supplementary Information). In particular, *G. crassaformis* allowed us to monitor variations of the thermocline associated with the cold and fresh Australasian Mediterranean Water (Fig. 3.1B, C; Supplementary Information). We combined $\delta^{18}\text{O}$ and Mg/Ca derived temperatures of surface dwelling *G. ruber* and *G. sacculifer* and of deep dwelling *G. crassaformis* to calculate $\delta^{18}\text{O}$ of seawater (Shackleton, 1974). Ice volume corrected records ($\delta^{18}\text{O}_{\text{ivc-seawater}}$) that approximate local salinity were deduced from $\delta^{18}\text{O}_{\text{seawater}}$ by subtracting an estimation of the Pliocene global ice volume (Supplementary Information).

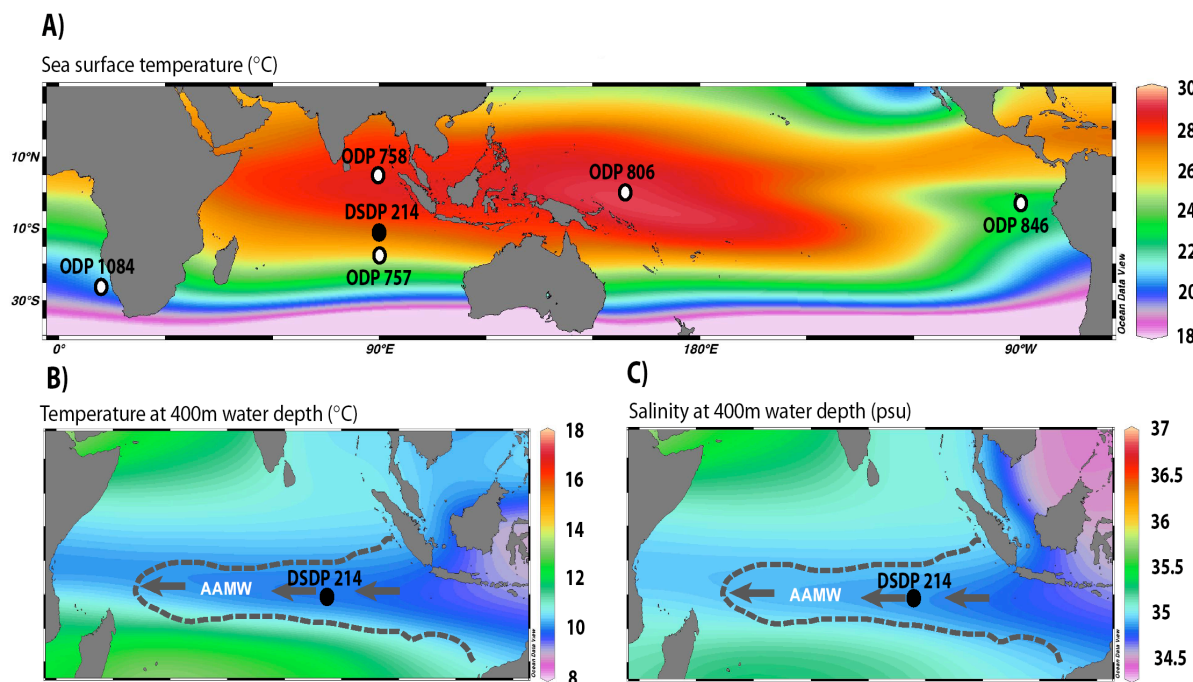


Figure 3.1 Annual ocean temperatures and salinities at (sub)surface levels. (A) Chart of annual ocean temperatures (in °C) at 20 m water depth (Locarnini et al., 2006; Schlitzer, 2007). Paleooceanographic proxy data were generated for (DSDP) Site 214. Locations of sediment cores discussed in the text are indicated. Annual temperatures (B) and salinities (C) at 400 m water depth (Locarnini et al., 2006; Schlitzer et al., 2007) show the westward expansion of relatively cold and less-saline Australasian Mediterranean Water (AAMW, dotted line) that originates from the ITF area (Tomczak and Godfrey, 1994; You and Tomczak, 1993).

At tropical eastern Indian Ocean Site 214, the $\delta^{18}\text{O}$ and $\text{SST}_{\text{Mg/Ca}}$ records of the surface dwelling foraminifera *G. ruber* and *G. sacculifer* (Supplementary Information) show similar trends between 5.5 and 2.0 Ma, indicating that the $\delta^{18}\text{O}$ signal to a large part reflects

variations in SST_{Mg/Ca} (Figs 3.2A, B, 3.3A). The SST_{Mg/Ca} records vary from 24°C to 26.5°, showing a warming trend of ~1.5°C during the early Pliocene from 5.5 to 3.8 Ma and then a slight cooling of ~1°C during the Pliocene climate transition from 3.8-2.5 Ma. The deep mixed layer Mg/Ca temperature record from *G. venezuelana* (spanning the time interval from 5.5 to 3.5 Ma) is 1-2°C cooler than the SST_{Mg/Ca} record but clearly resembles the warming trend during the early Pliocene (Fig. 3.3A). The sea surface δ¹⁸O signature as well as the pattern of SST_{Mg/Ca} variability at Site 214 are very similar to that of West Pacific Warm Pool Site 806 (Wara et al., 2005). This indicates that the long-term SST_{Mg/Ca} evolution between both sites developed almost identical between 5.5 and 2 Ma, although the absolute temperatures are different. SST_{Mg/Ca} in the tropical eastern Indian Ocean are consistently ~3.5°C cooler than in the West Pacific Warm Pool (Fig. 3.2A; Supplementary Information). This difference is similar to the modern SST offset of ~2°C between both core locations (Locarnini et al., 2006; Fig. 3.1A). Our SST_{Mg/Ca} record from Site 214, provides no evidence for pronounced surface cooling in the tropical eastern Indian Ocean between 4 and 3 Ma, which has been suggested as a response to the constriction of the Indonesian seaway (Cane and Molnar, 2001). The slight cooling trend at Site 214 of ~1°C from ~3.8-2.5 Ma most likely reflects global climate cooling as similar trends are also registered at Site 806 and at eastern Indian Ocean Site 758 (Dekens et al., 2006).

In contrast to the conditions at the sea surface, the Mg/Ca temperature record of the deep-dwelling *G. crassaformis* suggests a distinct cooling of the subsurface level of ~4°C between ~3.5 and 2.95 Ma with an abrupt component from ~3.3 to 3 Ma. (Fig. 3.3A) This pattern is also reflected by the δ¹⁸O_{*G. crassaformis*} record (Fig. 3.2C). Most notably is the rapid ~1‰ increase in δ¹⁸O_{*G. crassaformis*} from ~3.5 to 2.95 Ma. Evidently, the most intense hydrographic changes in the tropical eastern Indian Ocean occurred during the mid-Pliocene transition at ~3.5-2.95 Ma within the subsurface level rather than at the surface. The decoupled evolution of subsurface and surface water masses caused an increasing temperature and δ¹⁸O gradient between shallow and deep dwelling species after ~3.5 Ma and point to a shoaling and cooling of the thermocline (Ravelo and Fairbanks, 1992; Ravelo and Andreasen, 1999) in the tropical eastern Indian Ocean. Similar to the modern situation, we assume that the Pliocene ITF was rather characterized by changes in the subsurface flow than at the surface (Gordon and Fine, 1996; Gordon et al., 1999). This is supported by our δ¹⁸O_{ivc-seawater} reconstructions, which point to a gradual change of the source of ITF waters (Cane and Molnar, 2001) during ~3.5-2.95 Ma. The deep-dwelling *G. crassaformis* δ¹⁸O_{ivc-seawater} record

(Fig. 3.3D) reveals an overall freshening trend from ~ 4.3 to 2.5 Ma indicated by a $\delta^{18}\text{O}_{\text{ivc-seawater}}$ change from ~ 0.4 ‰ to ~ -1.2 ‰, interrupted by sudden and stepwise changes towards more saline conditions at ~ 3.3 – 3.15 Ma. These rapid subsurface changes might have been due to a reduction in ITF as the throughflow waters would have been replaced by warmer and saltier Indian Ocean waters. Alternatively, the ITF source might have switched back to more warm and saline South Pacific waters (Fig. 3.3A, D). Rapid and gradual freshening of subsurface waters started again at ~ 3.15 Ma, with a $\delta^{18}\text{O}_{\text{ivc-seawater}}$ amplitude of ~ 1 ‰ until ~ 2.95 Ma (Fig. 3.3D). The shallow-dwelling *G. ruber* and *G. sacculifer* $\delta^{18}\text{O}_{\text{ivc-seawater}}$ records (Fig. 3.3D) also exhibit a long-term continuous freshening from ~ 5.2 Ma to ~ 2 Ma, although with a much smaller $\delta^{18}\text{O}_{\text{ivc-seawater}}$ amplitude.

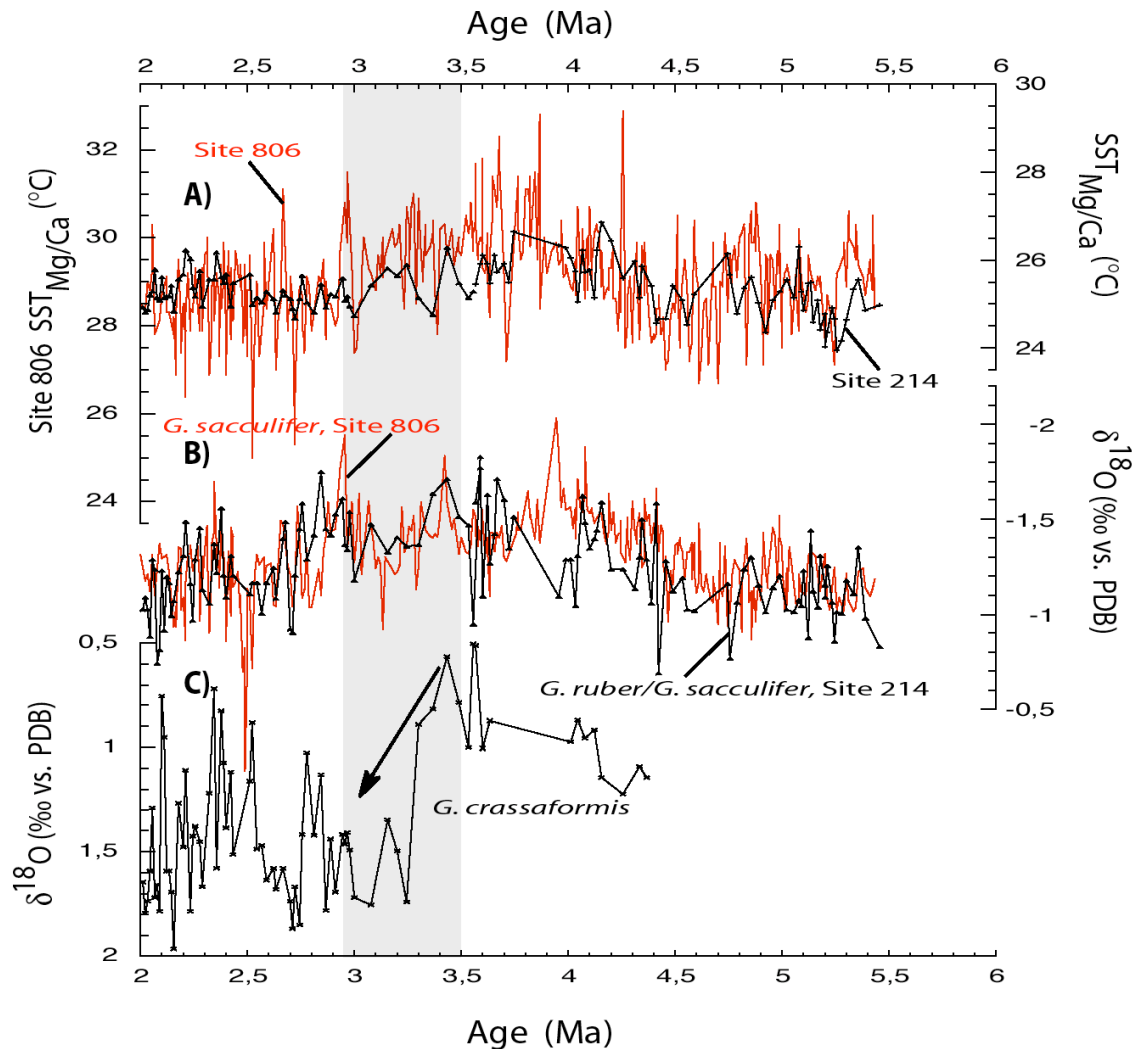


Figure 3.2 Pliocene proxy records from Site 214 and Site 806. (A) $\text{SST}_{\text{Mg/Ca}}$ derived from *G. ruber* (black triangles) and *G. sacculifer* (black crosses) from Site 214 and $\text{SST}_{\text{Mg/Ca}}$ *G. sacculifer* (red) from Site 806 (Wara et al., 2005). (B) $\delta^{18}\text{O}$ records from Sites 214 (black triangles) and 806 (Wara et al., 2005) (red; stratigraphy of Site 806 was changed based on additional $\delta^{18}\text{O}_{\text{benthic}}$ data; Supplementary Information). Site 214 $\delta^{18}\text{O}_{G. ruber}$ values were adjusted to the $\delta^{18}\text{O}_{G. sacculifer}$ record by adding 0.25 ‰ (Supplementary Information). (C) Site 214 $\delta^{18}\text{O}_{G. crassaformis}$ record. Note different temperature scales for Sites 214 and 806.

We appraise the gradual freshening from ~4.3 to 2.5 Ma and the related cooling (~4°C) of subsurface waters - with most prominent changes at ~3.5-2.95 Ma - to be a consequence of the gradual constriction of the Indonesian seaway and the related switch in the source of subsurface ITF waters (Cane and Molnar, 2001). The long- and short-term variability in subsurface salinity after 2.95 Ma, however may partly reflect oceanic changes in response to global climate variability. Sea surface conditions of the tropical eastern Indian Ocean and of the equatorial west Pacific, instead, developed equally (Figs 3.2A, B, 3.3D). In this respect, our data do not support Cane and Molnar's (2001) prediction of a surface cooling in the tropical eastern Indian Ocean synchronous to a relative sea surface warming in the equatorial west Pacific and the initiation of the West Pacific Warm Pool. Our notion on the freshening/cooling of tropical eastern Indian subsurface waters during ~3.5-2.95 Ma is supported by ϵNd data from eastern Indian Ocean Site 757 (Martin and Scher, 2006) (located south of Site 214) which were discussed in terms of a switch from southern to northern Pacific source waters in the ITF.

The timing of subsurface events largely coincides with eastern African climate proxy data, which indicate a change from formerly wet to dry conditions between ~4 and 3 Ma (deMenocal, 1995). It might indeed be speculated that the prominent temperature drop in the tropical eastern Indian Ocean subsurface waters affected the surface temperature in the west Indian Ocean *via* equatorial and/or coastal upwelling off Somalia, which is partly fed by thermocline waters being supplied by the Indonesian Throughflow (Bruce et al., 1980; Schott et al., 2002). A SST drop in the west Indian Ocean triggered by upwelling of cooler tropical eastern Indian Ocean subsurface waters might have caused a reduction in evaporation and hence, less precipitation over east Africa and in consequence, a change in hominid evolution (Cane and Molnar, 2001; deMenocal, 1995). During this time, the gradual slight freshening of surface waters in the tropical eastern Indian Ocean may have resulted from enhanced precipitation in line with the strengthening of the Monsoon system (after ~3.6 Ma; Gupta and Thomas, 2003; Zheng et al., 2004) rather than being a result of changing throughflow at the surface. This notion is corroborated by the good correlation between the surface $\delta^{18}\text{O}_{\text{ivc-seawater}}$ records from Site 806 (*G. sacculifer* SST_{Mg/Ca} and $\delta^{18}\text{O}$ data from Wara et al., 2005) and Site 214 in particular during the critical time period 3.5-2.95 Ma (Fig. 3.3D).

Pliocene global cooling and the Indonesian Gateway

The distinct change in the tropical eastern Indian Ocean thermocline structure during the mid-Pliocene (~3.5-2.95 Ma) occurs within a long-term sequence of paleoceanographic

events (~4.8-3 Ma; Steph et al., 2006; Marlow et al., 2000; Lawrence et al., 2006; Dekens et al., 2007; Ravelo et al., 2007; Wara et al., 2005; Chaisson and Ravelo, 2000), leading to the cooling and shoaling of the thermocline and the appearance of cold surface waters in various ocean regions (Philander and Fedorov, 2003). In the tropical east Pacific this process already started at ~4.8 Ma and has been related to the gradual closing of the Central American Seaway (Steph et al., 2006; Chaisson and Ravelo, 2000) which might have preconditioned the cooling of the equatorial east Pacific cold tongue (Lawrence et al., 2006). In consequence, this process marked the start of the gradual termination of permanent El Niño-like conditions. Alternatively, Philander and Fedorov (2003) related the termination of permanent El Niño-like conditions to global cooling inducing overall thermocline shoaling.

In the tropical eastern Indian Ocean (Site 214), the cooling and freshening of subsurface waters rather took place at ~3.5-2.95 Ma and appear to be quasi-synchronous to the plate tectonic northward drift of New Guinea and the postulated change in the source of ITF waters towards a cool and fresh North Pacific source (Cane and Molnar, 2001). At the same time, benthic $\delta^{18}\text{O}$ values were globally low and small in amplitude (Lisiecki and Raymo, 2005) (Fig. 3.3C), and benthic Mg/Ca implies low and hardly changing deep ocean temperatures (Billups and Schrag, 2002). Accordingly, we argue that the relative abrupt cooling of subsurface waters is not the result of “cooling from below” due to global cooling that strengthened NHG (Philander and Fedorov, 2003) but instead, rather amplified global climate change by contributing to a shoaling/cooling of the thermocline in various ocean areas.

At ~3.2 Ma, the previously uniform SST_{Mg/Ca} evolution at Site 214 and within the Benguela Upwelling cell (Site 1084 SST U^K₃₇ data from Marlow et al., 2000; age model revised by Johan Etourneau et al., in prep.; Fig. 3.3A) started to deviate, suggesting that the relative cooling of the Benguela Upwelling system might have been preconditioned by the continuously cooled tropical eastern Indian Ocean thermocline, the temperature signal of which would have been transported westward towards Site 1084. Today, the Benguela Current system transports ~25 Sverdrup (Sv) of water, 15 Sv of which can be related to Indian Ocean thermocline water (Gordon et al., 1992). Ventilation of the Indian Ocean thermocline is driven by the Australasian Mediterranean Water, which mixes with Indian Ocean Central Water before being transported in the South Atlantic Ocean via the Agulhas Current (You and Tomczak, 1993; Gordon, 1986). The dramatic cooling in the Benguela upwelling cell observed after ~2.4 Ma (Fig. 3.3A), however, was most likely related to the occurrence of more intense glacials (Marlow et al., 2000; Lisiecki and Raymo, 2005).

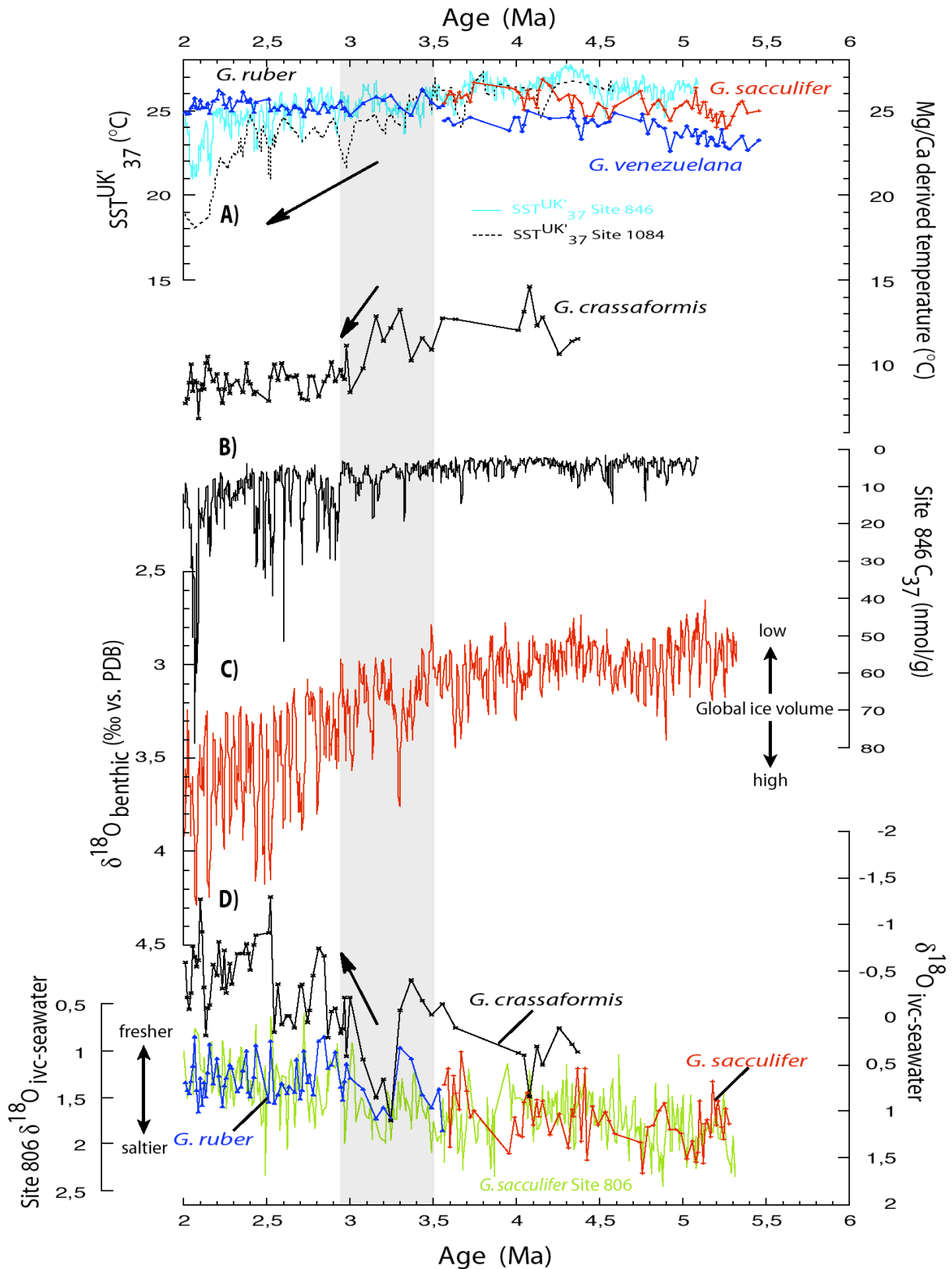


Figure 3.3 Pliocene (sub)surface changes in the tropical eastern Indian Ocean in relation to other ocean areas. (A) Mg/Ca derived temperatures of *G. ruber* (blue triangles), *G. sacculifer* (red crosses), *G. venezuelana* (blue diamonds) and *G. crassaformis* (black crosses) from Site 214; SST^{UK}₃₇ records from Sites 846 (light blue; Lawrence et al., 2006) and 1084 (dashed; Marlow et al., 2000; Johan Etourneau et al. in prep.). (B) C₃₇ alkenones concentrations of Site 846 (Lawrence et al., 2006). (C) The LR04 global benthic δ¹⁸O stack (Lisiecki and Raymo, 2005). (D) Site 214 δ¹⁸O_{ivc-seawater} records from *G. ruber* (blue triangles), *G. sacculifer* (red crosses), *G. crassaformis* (black crosses) and Site 806 δ¹⁸O_{ivc-seawater} *G. sacculifer* record (green; SST_{Mg/Ca} and δ¹⁸O values from Wara et al., 2005), (Supplementary Information). Arrows indicate trends.

When constant and low subsurface temperatures finally point to prevailing North Pacific source waters passing through the Indonesian Gateway since ~ 2.95 Ma, we observe a significantly increasing number of high productivity/upwelling events occurring in the equatorial east Pacific (Site 846) indicated by C_{37} alkenones, and accompanied by distinct drops in SST U_{37}^K (Lawrence et al., 2006) (Fig. 3.3A, B). Both the high productivity/upwelling events and the increasing gradient in ocean surface temperatures between the tropical eastern Indian Ocean and the equatorial east Pacific evolving after 2.95 Ma are taken as evidence for the manifestation of the equatorial east Pacific cold tongue, presumably amplified by strengthened wind stress in line with the intensification of NHG (Philander and Fedorov, 2003; Timmerman et al., 2004). A viable mechanism linking the ITF dynamics to east Pacific upwelling might come through the Equatorial Undercurrent. A Modelling study (Rodgers et al., 2000) suggest that the plate tectonic northward drift of New Guinea would change the source of the Equatorial Undercurrent in the Pacific towards a stronger Southern Ocean component. In fact, upwelled waters in the equatorial east Pacific cold tongue today originate from the lower levels of the Equatorial Undercurrent that is fed by cold Subantarctic Mode Water (Toggweiler et al., 1991). The Subantarctic Mode Water serves as the main contributor of nutrients fueling the east Pacific thermocline from below and enhancing primary productivity (Sarmiento et al., 2003). As this relation most likely held true throughout the Pliocene (Marlow et al., 2000; Dekens et al., 2007), we suspect that after 2.95 Ma a larger portion of Subantarctic Mode Water transported via “ocean tunnels” to equatorial regions (Liu and Yang, 2003) amplified the shoaling of the east Pacific thermocline, the cooling of upwelled water and the increase in productivity (Fig. 3.3A, B).

Our reconstructions of tropical eastern Indian Ocean surface and subsurface temperatures and $\delta^{18}O_{\text{IVC-seawater}}$ shed new light on the hydrographic changes in the Indonesian Gateway and its implications for the mid-Pliocene climate transition. Our results support the hypothesis of Cane and Molnar (2001) that the constriction of the Indonesian seaway (4-3 Ma) led to a major reorganization in the ITF. Although their assumption of a change in the surface throughflow and the proposed drop in tropical eastern Indian Ocean SST is not registered, our data reveal a pronounced cooling of $\sim 4^\circ\text{C}$ at the subsurface level from ~ 3.5 -2.95 Ma. This points to a switch in ITF source waters from initially South Pacific to North Pacific subsurface waters. After 2.95 Ma, constantly low subsurface temperatures and fresher conditions suggest a prevailing throughflow of North Pacific source waters through the Indonesian Gateway. The associated changes in the thermocline might have preconditioned the cooling of the Benguela Upwelling system at ~ 3.2 Ma and contributed to the global

cooling of the thermocline. We suggest that the plate tectonic constellation in the Indonesian Throughflow area after 2.95 Ma allowed for bringing a larger portion of Subantarctic Mode Water via “ocean tunnels” into the Equatorial Undercurrent (Liu and Yang, 2003) thereby supporting the final formation of the equatorial east Pacific cold tongue.

Acknowledgements

Samples for this study were provided by the IODP. Funding of this research was provided by the German Science Foundation (DFG) within project Nu60/14-1. We thank J. Etourneau, S. Steph, D. Garbe-Schönberg, J. Groeneveld, M. Regenberg, N. Gehre and K. Kiesling for valuable comments and technical support. KM was supported by IIT Kharagpur fellowship.

References

- Billups, K., and D. P. Schrag (2002), Paleotemperatures and ice volume of the past 27 Myr revisited with paired Mg/Ca and $18\text{O}/16\text{O}$ measurements on benthic foraminifera, *Paleoceanography* 17, PA000567.
- Bruce, J. G., D. R. Quadfasel, and J. C. Swallow (1980), Somali eddy formation during the commencement of the southwest monsoon, 1978, *J. Geophys. Res.*, 85, 6654–6660.
- Cane, M., and P. Molnar (2001), Closing of the Indonesian seaway as a precursor to east African aridification around 3–4 million years ago, *Nature*, 411, 157–162.
- Chaisson, W., and A. C. Ravelo (2000), Pliocene development of the East-West hydrographic gradient in the Equatorial Pacific, *Paleoceanography*, 15, 497–505.
- Dekens, P. S., A. C. Ravelo, and M. W. Wara (2006), Indo-Pacific evidence for cooling subsurface water, stable Indo-Pacific warm pool temperatures, and cooling upwelling regions through the Plio-Pleistocene transition. *AGU, Fall Meeting 2006 abstract*, PP12A-07.
- Dekens, P. S., A. C. Ravelo, and M. D. McCarthy (2007), Warm upwelling regions in the Pliocene warm period, *Paleoceanography* 22, PA3211, doi:10.1029/2006PA001294.
- deMenocal, P. B. (1995), Plio-Pleistocene African climate, *Science* 270, 53–59.
- Driscoll, N. W., and G. H. Haug (1998), A short circuit in the ocean's thermohaline circulation: A cause for northern hemisphere glaciation?, *Science* 282, 436–438.
- Fedorov, A. V. et al. (2006), The Pliocene Paradox (Mechanisms for a Permanent El Niño). *Science* 312, 1485–1489.
- Gordon, A. L. (1986), Interocean Exchange of Thermocline Water, *J. Geophys. Res.* 91, 5037–5046.

- Gordon, A. L., and R. A. Fine (1996), Pathways of water between the Pacific and Indian Oceans in the Indonesian Seas, *Nature* 379, 146-149.
- Gordon, A. L., R. D. Susanto, and A. Field (1999), Throughflow within Makassar straight, *Geophys. Res. Lett.* 26, 3325-3328.
- Gordon, A. L., R. L. Weiss, W. M. Smethie Jr., and M. J. Warner (1992), Thermocline and intermediate water communication between the South Atlantic and Indian Ocean, *J. Geophys. Res.* 97, 7223-7240.
- Gupta, A. K., and E. Thomas (2003), Initiation of northern hemisphere glaciation and strengthening of the northeast Indian monsoon: Ocean drilling program site 758, eastern equatorial Indian ocean, *Geology*, 31, 47-50.
- Haug, G. H., D. M. Sigman, R. Tiedemann, T. F. Pedersen, and M. Sarnthein (1999), Onset of permanent stratification in the subarctic Pacific, *Nature* 401, 779-782.
- Haug, G. H., R. Tiedemann, R. Zahn, and A. C. Ravelo (2001), Role of Panama uplift on oceanic freshwater balance, *Geology* 29, 207-210.
- Lawrence, K. T., Z. Liu, and T. D. Herbert (2006), Evolution of the eastern tropical Pacific through Plio-Pleistocene glaciation, *Science* 312, 79-83.
- Lisiecki, L. E., and M. E. Raymo (2005), A Pliocene-Pleistocene stack of 57 globally distributed benthic $\delta^{18}\text{O}$ records, *Paleoceanography* 20, PA1003, doi:10.1029/2004PA001071.
- Liu, Z., and H. Yang (2003), Extratropical control of tropical climate, the atmospheric bridge and oceanic tunnel, *Geophys. Res. Lett.*, 30, 1230, doi:10.1029/2002GL016492.
- Locarnini, R. A. et al. (2006), *World Ocean Atlas 2005*, Vol. 1: Temperature. S. Levitus, Eds. NOAA Atlas NESDIS 61, (U.S. Gov. Printing Office, Washington, D.C., 2006) 182 pp.
- Marlow, J. R., C. B. Lange, G. Wefer, and A. Rosell-Melé (2000), Upwelling intensification as part of the Pliocene-Pleistocene climate transition, *Science*, 290, 2288-2291.
- Martin, E. E., and H. A. Scher (2006), Nd isotopic study of southern sourced waters and Indonesian Throughflow at intermediate depths in the Cenozoic Indian Ocean, *Geochem. Geophys. Geosyst.* 7, Q09N02, doi:10.1029/2006GC001302.
- Mudelsee, M., and M. E. Raymo (2005), Slow dynamics of the Northern Hemisphere glaciation. *Paleoceanography*, 20, PA4022, doi:10.1029/2005PA001153.
- Philander, S. G., and A. V. Fedorov (2003), Role of tropics in changing the response to Milankovich forcing some three million years ago, *Paleoceanography*, 18, doi:10.1029/2002PA000837.

- Ravelo, A. C., and D. H. Andreasen (1999), Using planktonic foraminifera as monitors of the tropical surface ocean. In *Reconstructing Ocean History- A window into the future*. Abrantes, F., and A. Mix, Eds., (Plenum Press, New York, 1999) 217-244.
- Ravelo, A. C., D. H. Andreasen, M. Lyle, A. O. Lyle, and M. W. Wara (2004), Regional climate shifts caused by gradual global cooling in the Pliocene epoch, *Nature*, 429, 263-267.
- Ravelo, A. C., K. Billups, P. S. Dekens, T. D. Herbert, and K. T. Lawrence (2007), Onto the ice ages: proxy evidence for the onset of Northern Hemisphere Glaciation, in *Deep-time perspectives on climate change: marrying the signal from computer models and biological proxies*. Williams, M., A.M. Haywood, J. Gregory, and D. Schmidt, Eds. (The Geol. Soc. of London & The Micropal. Soc., 2007).
- Ravelo, A. C., and R. G. Fairbanks (1992), Oxygen isotopic composition of multiple species of planktonic foraminifera: recorders of the modern photic zone temperature gradient. *Paleoceanography* 7, 815-832.
- Rodgers, K. B., M. Latif, and S. Legutke (2000), Sensitivity of equatorial Pacific and Indian Ocean watermasses to the position of the Indonesian throughflow, *Geophys. Res. Lett.* 27, 2941-2944.
- Sarmiento, J. L., N. Gruber, M. A. Brzezinski, and J. P. Dunne (2003), High-latitude controls of thermocline nutrients and low latitude biological productivity, *Nature* 427, 56-60.
- Schott F. A., M. Dengler, and R. Schoenefeld (2002), The shallow overturning circulation of the Indian Ocean. *Progress in Oceanography*, 53 57–103.
- Shackleton, N. J. (1974), Attainment of isotopic equilibrium between ocean water and the benthonic foraminifera genus *Uvigerina*: isotopic changes in the ocean during the last glacial, *Colloq. Int. Cent. Natl. Rech. Sci.* 219, 203-209.
- Shackleton, N. J. et al. (1984), Oxygen isotope calibration of the onset of ice-rafting and history of glaciation in the North Atlantic region, *Nature* 307, 620-623.
- Schlitzer, R. (2007), Ocean Data View, <http://odv.awi.de>.
- Steph, S., R. Tiedemann, J. Groeneveld, A. Sturm, and D. Nürnberg (2006), Pliocene changes in tropical east Pacific upper ocean stratification: response to tropical gateways? In *Proc. ODP, Sci. Results*, 202 Tiedemann, R., A. C. Mix, C. Richter, and W.F. Ruddiman, Eds. (College Station, TX 2006) pp. 1-51.
- Timmermann, A., F. B. Justino, F.-F. Jin, and H. Goosse (2004), Surface temperature control in the North and tropical Pacific during the last glacial maximum, *Clim. Dyn.* 23, 353-370.

- Toggweiler, J. R., K. Dixon, and W. S. Broecker (1991), The Peru upwelling and the ventilation of the South Pacific thermocline. *J. Geophys. Res.* *96*, 20467-20497.
- Tomczak, M., and J. S. Godfrey (1994), *Regional Oceanography: an Introduction* (Pergamon, 1994) 422pp.
- Wara, M. W., A. C. Ravelo, and M. L. Delaney (2005), Permanent El Niño-Like Conditions During the Pliocene Warm Period, *Science*, *309*, 758-761.
- You, Y., and M. Tomczak (1993), Thermocline circulation and ventilation in the Indian Ocean derived from water mass analysis, *Deep-Sea Research* *1.*, *40*, 13-56.
- Zheng, H., McA. Powell, D. K. Rea, J. Wang, and P. Wang (2004), Late Miocene and mid-Pliocene enhancement of the East Asian monsoon as viewed from the land and sea, *Global Planet. Change* *41*, 147-155.

Supplementary Information

$\delta^{18}\text{O}$ and Mg/Ca analysis

For stable oxygen isotope and Mg/Ca analyses, ~40-50 specimens were selected from shallow dwelling planktonic foraminifera *G. ruber* (white variety) and *G. sacculifer* (without sac-like chamber) which both calcify in the upper 50 m water depth (Anand et al., 2003). From the deep dwelling planktonic foraminifera *G. crassaformis* (calcification depth of ~300-450 m; Elderfield et al., 2002) and deep mixed layer species *G. venezuelana*, 20-40 specimens were selected. Only in few cases the number had to be reduced to ~10 specimens. All specimens were selected from the 300-400 μm size fraction to avoid size effects in $\delta^{18}\text{O}$ values and Mg/Ca (Elderfield et al., 2002). Subsequently sample material was gently crushed, mixed and optically divided into two thirds used for Mg/Ca- analyses, and one third for stable isotope measurements. Isotope measurements were conducted on a Finnigan MAT-252 mass spectrometer equipped with a fully automated Kiel-Carbo-II carbonate preparation device. Analytical precision was better than $\pm 0.07\%$ for $\delta^{18}\text{O}$; $\pm \sigma$. All values are reported relative to Pee Dee Belemnite (PDB, based on calibration directly to National Bureau of Standards (NBS-19)).

For Mg/Ca analyses, samples were cleaned according to an established cleaning protocol (Barker et al., 2003; non reductive). Measurements were performed on a simultaneous, radially viewing ICP-OES (Ciros CCD SOP, Spectro A.I., Germany). The analytical error for the Mg/Ca ratios was ~0.1% (~300 samples). Replicate analysis on the same samples, cleaned and analysed during different sessions, showed a standard deviation of <0.1 mol/mol (rel. std. dev. <3%) introducing a temperature error of ~0.5°C. We converted Mg/Ca ratios of *G. ruber* and *G. sacculifer* into temperatures by using the multispecies calibration of Anand et al. (2003): $\text{Mg/Ca} = 0.38 \exp(0.09 \times \text{SST})$, because we found no significant Mg/Ca offset between both species. As Gasperi and Kennett (1993) showed from the Pacific Ocean that since 7.5 Ma *G. venezuelana* is a planktonic foraminifer that lives in the deep mixed layer, we converted Mg/Ca ratios into deep mixed layer temperatures by using a shallow/thermocline dweller calibration (Regenberg et al., 2009): $\text{Mg/Ca} = 0.22 \exp(0.113 \times T)$. The conversion from *G. crassaformis* Mg/Ca ratios into temperatures was conducted by using a species-specific calibration (Regenberg et al., 2009): $\text{Mg/Ca} = 0.83 \exp(0.082 \times T)$.

Compatibility of Mg/Ca measurements

When comparing different Mg/Ca data sets it is essential to consider the cleaning techniques applied, the temperature *vs.* Mg/Ca calibrations used and differences in calcite dissolution. For example, to account for different foraminiferal cleaning techniques prior to Mg/Ca analyses, the foraminiferal Mg/Ca data derived from reductive cleaning are commonly lower by ~10% than those using only the oxidative cleaning step (Barker et al., 2003). Inconsistencies in Mg/Ca determination between laboratories (Greaves et al., 2008) add to the problem of comparability of Mg/Ca analyses. Most crucial is the impact of calcite dissolution on foraminiferal Mg/Ca, the effect of which varies regionally as well as spatially. Dekens et al. (2002) proposed Mg/Ca *vs.* temperature equations, which include a dissolution correction. From core-top studies Regenberg et al. (2006) suggested species-specific calcite saturation levels critical for Mg/Ca removal and proposed correction equations. Both studies (Dekens et al., 2002; Regenberg et al., 2006) are in general accordance suggesting that Mg²⁺ loss starts below ΔCO_3^{2-} levels of ~20 $\mu\text{mol/kg}$.

Keeping in mind these problems, we did not hesitate to compare the Indian Ocean Site 214 Mg/Ca data to those from the deep (~2520 m water depth) west Pacific Site 806 (Wara et al., 2005). For the shallow dwelling *G. ruber*/*G. sacculifer* of Site 214, we applied the Anand et al. (2003) calibration, which is almost identical to the Dekens et al. (2002) equation used by Wara et al. (2005) for Site 806 without the dissolution correction part of that equation. This seems appropriate as throughout the studied time interval (Peirce et al., 1989) Site 214 was located far above the lysocline. Today, the carbonate lysocline is at 4400 m water depth in the central Indian Ocean (Banakar et al., 1998), and indeed the Site 214 location is above critical ΔCO_3^{2-} levels of ~20 $\mu\text{mol/kg}$ (Dekens et al., 2002; Regenberg et al., 2006) (Data from World Ocean Circulation Experiment-transect 102E were used to calculate ΔCO_3^{2-} levels; Lewis and Wallace, 1998). As the deep west Pacific Site 806, instead, is dissolution-affected, Wara et al. (2005) applied the Dekens et al. (2002) calibration including the correction for ΔCO_3^{2-} related Mg-removal. The according Pliocene SST_{Mg/Ca} are on average ~3.5°C warmer than those for Site 214, a pattern that even holds for the modern temperature gradient between the west Pacific Warm Pool and the eastern Indian Ocean (~2°C; Locarnini et al., 2006). The Dekens et al. (2002) approach to correct foraminiferal Mg/Ca for dissolution effects, however, is considerably improved by Regenberg et al. (2006). If the Site 806 Mg/Ca data were added by 10% to consider for different cleaning methods (Barker et al., 2003), then corrected for dissolution effects according to Regenberg et al. (2006) (assuming a ΔCO_3^{2-} level of -10.5 $\mu\text{mol/kg}$; Wara et al., 2005), and finally converted into SST_{Mg/Ca} using the Anand et al. (2003)

calibration, we would end up with almost the same SST_{Mg/Ca} as reported by Wara et al. (2005) (on average a deviation of $\sim 0.2^{\circ}\text{C}$). Apart from the absolute temperature differences, the relative changes between both SST_{Mg/Ca} records are not influenced by using different calibrations (Anand et al., 2003; Regenberg et al., 2009; Dekens et al., 2002), which we aim to resolve in this study.

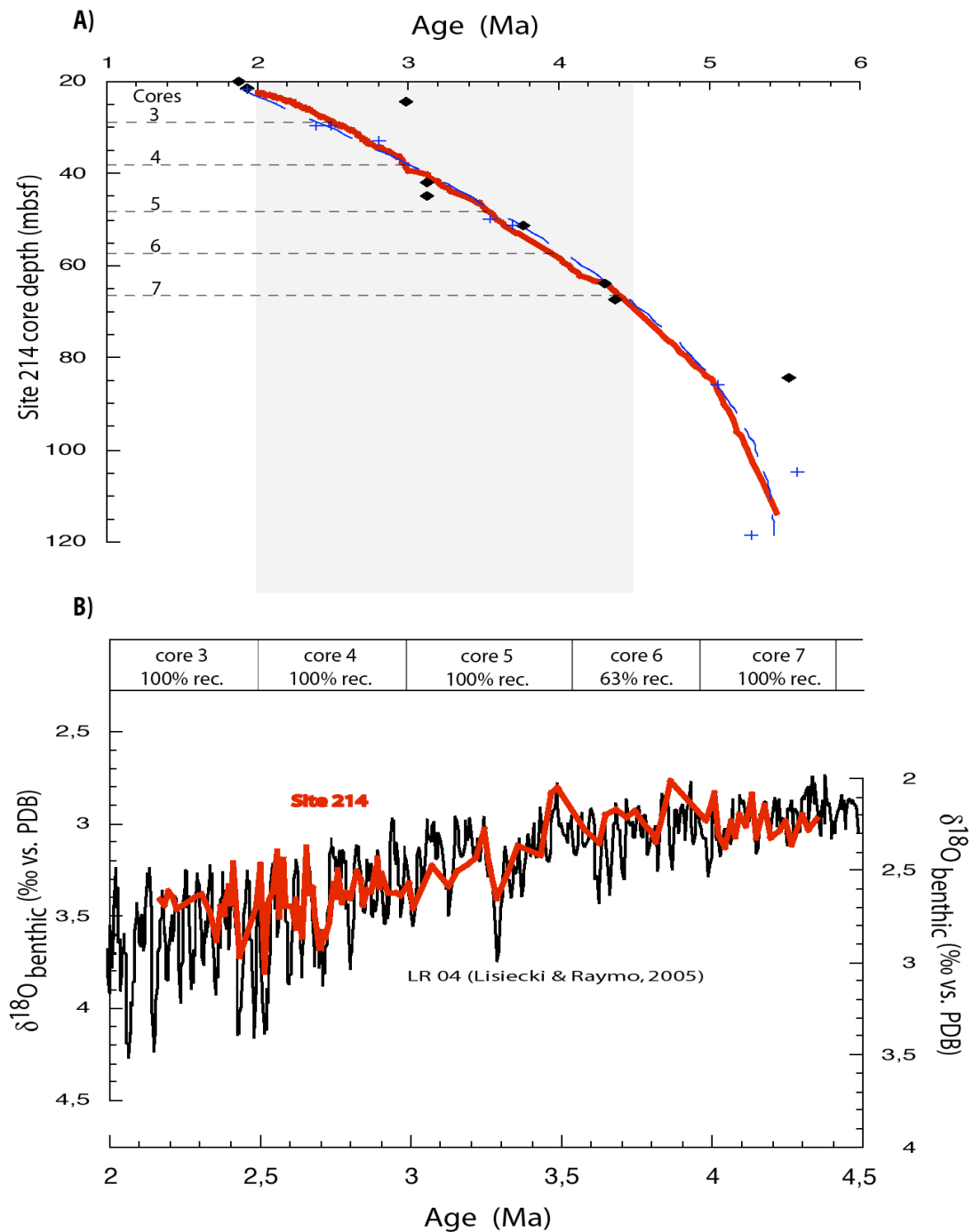
Age models

Site 214

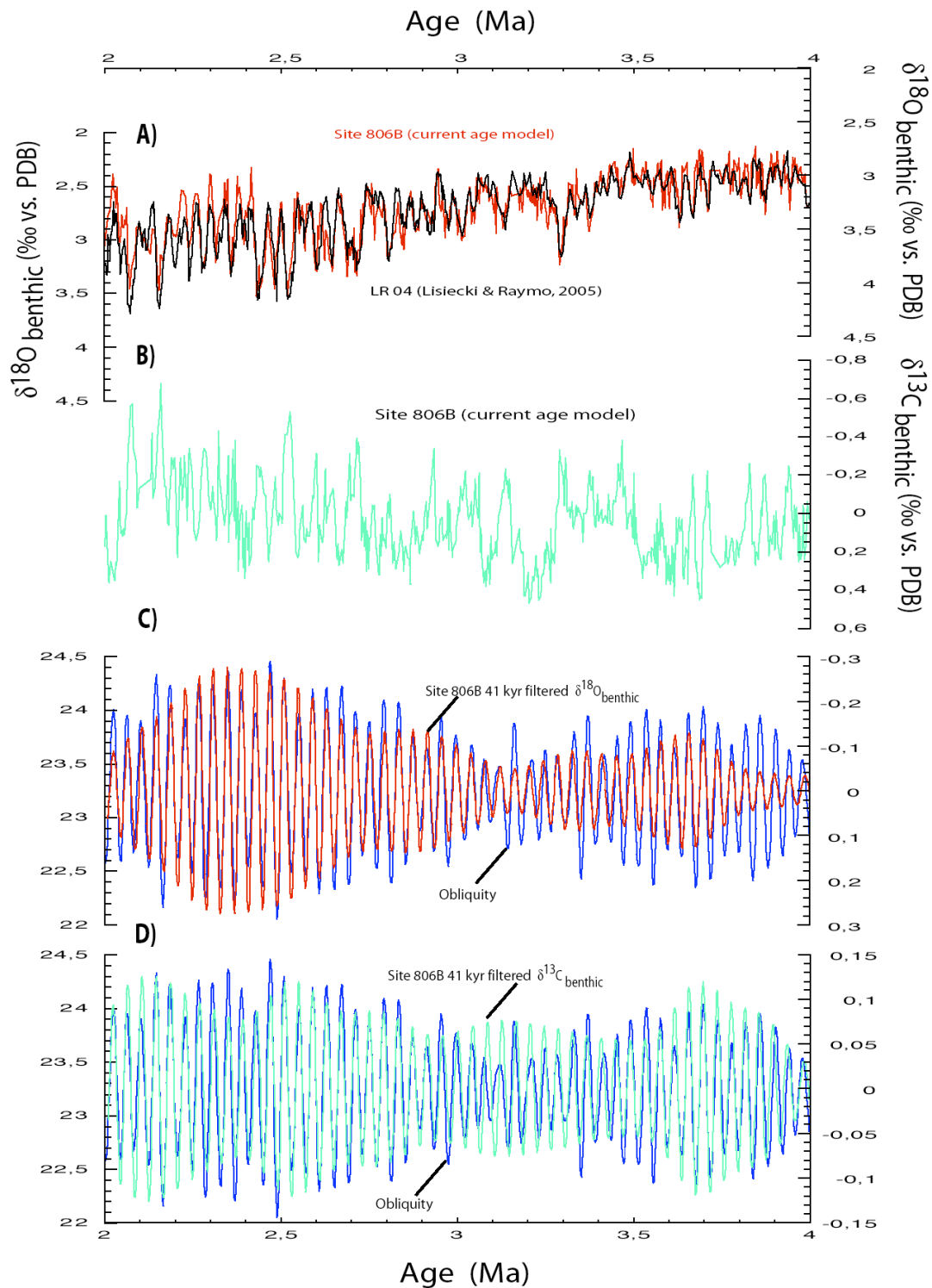
The initial age control is based on several nanofossil biodatums (depths were taken from Srinivasan and Chaturverdi, 1990; www.odsn.de). All biodatums were updated to the ATNTS 2004 time scale (Lourens et al., 2004). In a next step, we calculated a polynomial fit through those nanofossil biodatums which are supported by foraminiferal biodatums (depths from Srinivasan and Chaturverdi, 1990; Srinivasan and Sinha, 1992; ages are according to the ATNTS 2004 time scale; Lourens et al., 2004; S-Fig. 3.1A). To further improve our stratigraphy during the critical time period 4.5 – 2 Ma, we generated a benthic $\delta^{18}\text{O}_{C. wuellerstorfi}$ record (S-Fig. 3.1B), which was then fine-tuned to the LR04 stack (Lisiecki and Raymo, 2005). Both records correspond well (S-Fig. 3.1B). The resulting depth/age curve is almost similar to the polynomial fit of the nanofossil biodatums (S-Fig. 3.1A). The combined use of well constrained nanofossil biodatums and tuning of the benthic isotope record from 4.5 to 2 Ma to the LR04 stack (Lisiecki and Raymo, 2005), hence, produces a reliable age model for Site 214.

Site 806

As the comparison of Site 214 west of the ITF to Site 806 east of it is essential to our study, we established a consistent stratigraphic framework for both sites. The initial chronostratigraphy of Site 806 (Wara et al., 2005), is based on several nanofossil biodatums (revised age scale in the older part (>1.8 Ma) of the core; Shackleton et al., 1990). From ~ 3 to 1.8 Ma, the age model was improved by using planktonic $\delta^{18}\text{O}_{G. sacculifer}$ data (Jansen et al., 1993) where isotope stages were defined (Mayer et al., 1993). As benthic $\delta^{18}\text{O}$ data provide more reliable stratigraphic information because the deep ocean is largely unaffected by temperature and salinity changes, we produced a high-resolution (~ 3 kyr) benthic $\delta^{18}\text{O}_{C. wuellerstorfi}$ record for the time period 4-2 Ma. We then tuned the $\delta^{18}\text{O}_{C. wuellerstorfi}$ record to the global benthic reference stack LR04 (Lisiecki and Raymo, 2005) using Analyseries 1.2 (Paillard et al., 2000; $r=0.89$; S-Fig. 3.2A). For the time period 4-2 Ma, the 41 kyr filtered



S-Figure 3.1 Stratigraphic framework of Site 214. (A) Diagram showing the age/depth relationship of Site 214 (red line). Dashed blue curve represents the polynomial fit of all nannofossil biostratigraphy (crosses) used that were updated to the ATNTS 2004 time scale (Lourens et al., 2004). Foraminiferal biostratigraphy is indicated as diamonds. Dashed lines mark core breaks from 4.5-2 Ma (von der Borch et al., 1974). (B) Comparison of the benthic $\delta^{18}\text{O}_{C. wuellerstorfi}$ record (red line) from 4.5-2 Ma and the benthic LR04 stack (Lisiecki and Raymo, 2005) (black line) for the age model established here. Core sections are indicated, implying that the critical time period 3.5-2 Ma shows 100% recovery (von der Borch et al., 1974).



S-Figure 3.2 Revised stratigraphic framework of ODP Site 806 from 4 to 2 Ma. (A) Tuning of the high resolution benthic $\delta^{18}\text{O}_{C. wuellerstorfi}$ record to the global benthic reference stack LR04 (Lisiecki and Raymo, 2005). The $\delta^{13}\text{C}_{C. wuellerstorfi}$ record is shown in (B). The age model is corroborated by the filtered 41 kyr components of both the benthic $\delta^{18}\text{O}_{C. wuellerstorfi}$ (C) and the benthic $\delta^{13}\text{C}_{C. wuellerstorfi}$ records (D) being in accordance to the obliquity solutions (Laskar, 1993).

components of the benthic $\delta^{18}\text{O}_{C. wuellerstorfi}$ and $\delta^{13}\text{C}_{C. wuellerstorfi}$ records are in accordance to the obliquity solution of Laskar (1993) (S-Fig. 3.2C, D). The obliquity filter has a frequency of 0.025 cycles/kyr and a bandwidth of 0.003 cycles/kyr. We observed and corrected phase lags of 8 and 10 kyr between obliquity and obliquity-controlled variations in the benthic $\delta^{18}\text{O}_{C. wuellerstorfi}$ and $\delta^{13}\text{C}_{C. wuellerstorfi}$ records, respectively. The difference of 2 kyr in phase lags between the obliquity controlled variations in $\delta^{18}\text{O}_{C. wuellerstorfi}$ and $\delta^{13}\text{C}_{C. wuellerstorfi}$ records was also observed in the eastern Pacific (Mix et al., 1995). In the older sections of Site 806 (5.5-4 Ma) we updated the nanofossil biostratigraphy to the ATNTS 2004 time scale (Lourens et al., 2004)

Adjusting the $\delta^{18}\text{O}$ and Mg/Ca records of *G. ruber* to *G. sacculifer*

As in the older (>3.4 Ma) sections of Site 214, specimens of *G. ruber* became absent we combined $\delta^{18}\text{O}$ and Mg/Ca records of *G. ruber* from ~3.4 to ~2.4 Ma with those of *G. sacculifer* from ~6.7 to ~3.4 Ma. In order to account for habitat differences (Anand et al., 2003) we run $\delta^{18}\text{O}$ and Mg/Ca analyses for both species for the short time interval of 3.5-3 Ma where both species occur. The interspecific $\delta^{18}\text{O}$ difference amounts to 0.25‰ being similar to that reported by Shackleton and Hall (1990) from the western Indian Ocean. We therefore adjusted our $\delta^{18}\text{O}_{G. ruber}$ record to the $\delta^{18}\text{O}_{G. sacculifer}$ record by adding 0.25‰. In contrast to Regenberg et al. (2006), who reported on a 15‰ habitat-related difference between *G. ruber* and *G. sacculifer* for recent core-top specimens, the Mg/Ca-difference for the Pliocene species is <0.1 mmol/mol. We therefore did not adjust the Mg/Ca values.

Calculation of $\delta^{18}\text{O}_{\text{ivc-seawater}}$

To assess ancient sea surface salinities from different water depths, we used the combined $\delta^{18}\text{O}$ and Mg/Ca temperature records from surface dwelling planktonic foraminifera *G. ruber* and *G. sacculifer* and from the thermocline dwelling species (S-Fig. 3.3A). $\delta^{18}\text{O}_{\text{seawater}}$, which reflects a combination of ice-volume controlled $\delta^{18}\text{O}_{\text{seawater}}$ changes plus local variations in $\delta^{18}\text{O}_{\text{seawater}}$ due to regional hydrological changes, was calculated (Shackleton, 1974; S-Fig. 3.3B).

Variations in local sea surface salinities expressed as ice volume corrected records ($\delta^{18}\text{O}_{\text{ivc-seawater}}$) were deduced by subtracting an estimation of the Pliocene global ice volume signal (Groeneveld et al., 2006). In this respect we used the benthic $\delta^{18}\text{O}$ record of Lisiecki and Raymo (2005) (S-Fig. 3.3C, D). We first normalized the benthic $\delta^{18}\text{O}$ record to the

modern value. Subsequently, we reduced the benthic $\delta^{18}\text{O}$ record with its initial $\sim 1.6\text{‰}$ last glacial/interglacial amplitude to 75% to account for the $\sim 1.2\text{‰}$ last glacial/interglacial difference in global ice volume (Lisiecki and Raymo, 2005; Groeneveld et al., 2006). We assume that this relationship between the global ice volume, sea surface salinity and temperature also holds true for the Pliocene. Finally, we subtracted the modified benthic $\delta^{18}\text{O}$ record from our $\delta^{18}\text{O}_{\text{seawater}}$ records leading to $\delta^{18}\text{O}_{\text{ivc-seawater}}$ values (S-Fig. 3.3D). We are aware that this approach introduces slight errors, but it still is a reliable approximation that produces qualitatively correct results.

Supplementary References

- Anand, P., H. Elderfield, and M. H. Comte (2003), Calibration of Mg/Ca thermometry in planktonic foraminifera from a sediment trap time series, *Paleoceanography*, 18, doi:10.1029/2002PA000846.
- Banakar, V. K., G. Parthiban, and P. Jauhari (1998), Chemistry of surface sediments along a north-south transect across the equator in the central Indian basin: An assessment of biogenic and detrital influences on elemental burial on the seafloor, *Chem. Geol.*, 147, 217-232.
- Barker, S., M. Greaves, and H. Elderfield (2003), A study of cleaning procedures used for foraminiferal Mg/Ca paleothermometry, *Geochem., Geophys., Geosyst.*, 4 (9), doi:10.1029/2003GC000559.
- Dekens, P. S., D. W. Lea, D. K. Pak, and H. J. Spero (2002), Core top calibration of Mg/Ca in tropical foraminifera: Refining paleotemperature estimation, *Geochem., Geophys., Geosyst.*, 3, doi: 10.1029/2001GC000200.
- Elderfield, H., M. Vautravers, and M. Cooper (2002), The relationship between shell size and Mg/Ca, Sr/Ca, $\delta^{18}\text{O}$, and $\delta^{13}\text{C}$ of species of planktonic foraminifère, *Geochem., Geophys., Geosyst.*, 3, doi: 10.1029/2001GC000194.
- Gasperi, J. T., and J. P. Kennett (1993), Vertical thermal structure of Miocene surface waters: Western equatorial Pacific DSDP Site 289, *Mar. Micropaleontology* 22, 235-254.
- Greaves, M. et al. (2008), Interlaboratory comparison study of calibration standards for foraminiferal Mg/Ca thermometry, *Geochem. Geophys. Geosyst.* 9, Q08010, doi:10.1029/2008GC001974.
- Groeneveld, J. et al. (2006), in *Proc. ODP, Sci. Results 202*, Tiedemann, R., A. C. Mix, C. Richter, and W. F. Ruddiman, Eds. (College Station, TX, 2006),

- 10.2973/odp.proc.sr.202.209.2006.
- Jansen et al. (1993), in *Proc. ODP, Sci. Results 130*, Berger, W.H., L. W. Kroenke, L. A. Mayer et al., Eds., 349-362 (College Station, TX, 1993).
- Laskar, J. (1993), The chaotic motion of the solar system: a numerical estimate of the chaotic zones, *Icarus*, 88, 266-291.
- Lewis, E., and D. W. R. Wallace (1998), co2sys -Program Developed for CO2System Calculations, oRNL/CDIAC-105, Carbon Dioxide Information Analysis Center, Oak Ridge Natl. Lab., (U.S. Dep. of Energy, Oak Ridge, Tenn., 1998).
- Lisiecki, L. E., and M. E. Raymo (2005), A Pliocene-Pleistocene stack of 57 globally distributed benthic $\delta^{18}\text{O}$ records, *Paleoceanography*, 20, PA1003, doi:10.1029/2004PA001071.
- Locarnini, R. A. et al. (2006), *World Ocean Atlas 2005*, in Vol. 1: Temperature. S. Levitus, eds., NOAA Atlas NESDIS 61, (U.S. Government Printing Office, Washington, D.C., 2006) 182 pp.
- Lourens, L. J. et al. (2004), in *A Geologic Time Scale 2004*: Cambridge. Gradstein, F.M., J. Ogg et al., Eds. (Cambridge Univ. Press, 2004), Appendix 2.
- Mayer, L. A., E. Jansen, J. Backman, and T. Takayama (1993), in *Proc. ODP, Sci. Results 130*, Berger, W.H., L. W. Kroenke, L. A. Mayer, et al., Eds., 623–639 (College Station, TX, 1993).
- Mix, A. C. et al. (1995), in *Proc. ODP, Sci. Results 138*, Pisisas, N.G., L. A. Mayer, T. R. Janecek, Eds., 371-412 (College Station, TX, 1995).
- Paillard, D., L. Labeyrie, and P. Yiou (1996), Macintosh program performs time-series analysis, *Eos, Transactions AGU*, 77, 379.
- Peirce, J. et al. (1989), Site 758, in *Proc. ODP, Sci. Results 121*, Peirce, J. et al., Eds., Shipboard Scientific Party (College Station, TX, 1989), pp. 359-453.
- Regenberg, M., D. Nürnberg, S. Steph, J. Groeneveld, D. Garbe-Schönberg, R. Tiedemann, and W.-C. Dullo (2006), Assessing the effect of dissolution on planktonic foraminiferal Mg/Ca ratios: Evidence from Caribbean core tops, *Geochem., Geophys., Geosyst.*, 7, doi: 10.1029/2005GC001019.
- Regenberg, M., S. Steph, D. Nürnberg, R. Tiedemann, and D. Garbe-Schönberg (2009), Calibrating Mg/Ca ratios of multiple planktonic foraminiferal species with $\delta^{18}\text{O}$ -calcification temperatures: Paleothermometry for the upper water column, *Earth Planet. Sci. Lett.*, 278, 324-336, doi:10.1016/j.epsl.2008.12.019.

- Shackleton, N. J. (1974), Attainment of isotope equilibrium between ocean water and the benthonic foraminiferal genus *Uvigerina*. Isotopic changes in the ocean during the last glacial, *Cent. Nat. Rech. Sci. Colloq. Int.*, 219, 203.
- Shackleton, N. J., A. Berger, and W. R. Peltier (1990), An alternative astronomical calibration of the lower Pleistocene timescale based on ODP Site 677. *Trans. R. Soc. Edinburgh, Earth Sci.*, 81, 251-261.
- Shackleton, N. J., and M. A. Hall (1990), in Proceedings ODP, Science Results, v. 115, Duncan, R. A., J. Backman, and L. C. Peterson, Eds. (College Station, Texas, 1990).
- Srinivasan, M. S., and S. N. Chaturverdi (1990), in *Pacific Neogene Events: Their Timing, Nature and Interrelationship*, R. Tsuchi, Eds. (Univ. of Tokyo Press, 1990), pp. 65-73.
- Srinivasan M. S., and D. K. Sinha (1992), in *Pacific Neogene: Environment, Evolution and Events*, R. Tsuchi, Eds. (Univ. of Tokyo Press, 1992) pp. 203–220.
- von der Borch, C. C., et al. (1974), in *Init. Rep. 22*, von der Borch et al., Eds., Site 214, Shipboard Scientific Party, (College Station, TX, 1974), doi:10.2973/dsdp.proc.22.105.1974.
- Wara, M. W., A. C. Ravelo, and M. L. Delaney (2005), Permanent El Niño-Like Conditions During the Pliocene Warm Period, *Science*, 309, 758-761.

Chapter IV

Mid-Pliocene reduction in meridional heat transport amplified by Indonesian Throughflow changes

Mid-Pliocene reduction in meridional heat transport amplified by Indonesian Throughflow changes

Cyrus Karas¹, Dirk Nürnberg¹, Ralf Tiedemann² and Dieter Garbe-Schönberg³

¹ Leibniz Institute of Marine Sciences (IFM-GEOMAR), University of Kiel, Wischhofstrasse 1-3, D-24148 Kiel, Germany

² Alfred Wegener Institute for Polar and Marine Research, Am Alten Hafen 26, D-27568 Bremerhaven, Germany

³ Institute of Geosciences, University of Kiel, D-24118 Kiel, Germany

Understanding the gradual global cooling during the mid-Pliocene (3.5–2.5 Ma ago) needs to consider the tectonical constriction of tropical seaways, which affected ocean circulation and the evolution of climate. Here, we use paired measurements of $\delta^{18}\text{O}$ and Mg/Ca ratios of planktonic foraminifera to reconstruct the Pliocene hydrography of the western tropical Indian Ocean (Site 709C) and changes in the Leeuwin Current in the eastern subtropical Indian Ocean (Site 763A) in response to Indonesian Gateway dynamics. Today, the warm southward flowing Leeuwin Current off western Australia is essential for the polar heat transport in the Indian Ocean. While subsurface waters in the Leeuwin Current area do not show a cooling during 3.5-3 Ma, sea surface temperatures significantly drop, becoming since ~ 3.3 Ma 2-3°C cooler than the rather unchanged sea surface temperatures from the eastern and western tropical Indian Ocean. We refer this drop in sea surface temperatures to a weakened Leeuwin Current with severe climatic effects on western Australia induced by a tectonically reduced surface Indonesian Throughflow. These oceanographic processes in the Indian Ocean might have contributed to the global development of increased meridional temperature gradients during the mid-Pliocene.

1. Introduction

During the mid-Pliocene, earth gradually changed from greenhouse with globally warmer temperatures and minor ice coverage at high northern latitudes to icehouse with the prominent Northern Hemisphere Glaciation and the extension of continental ice sheets (Ravelo et al., 2004; Mudelsee and Raymo, 2005). This climate transition was accompanied by a main tectonic reorganization of the Indonesian Gateway triggering a change in the throughflow from initially South Pacific to North Pacific subsurface waters as indicated by a

significant cooling at subsurface niveau in the tropical East Indian Ocean (Cane and Molnar, 2001; Karas et al., 2009). A tectonically induced effect on the meridional heat transport towards the southern hemisphere was not yet proven, although today the Indonesian Throughflow (ITF) is assumed to be responsible for the largest poleward heatflux in the southern Ocean (Talley, 2003; Gordon, 2005). The Leeuwin Current, which is important for the poleward heat transport in the Indian Ocean, is mainly driven by the ITF (Feng et al, 2003). At modern conditions the Leeuwin Current transports up to 5 Sverdrups (1 Sverdrup= $10^6 \text{ m}^3 \text{ s}^{-1}$) of relatively warm and less saline tropical waters in the upper 200-250 m from the ITF region southward along the west coast of Australia, predominantly against equatorward winds (Fig. 4.1A; Smith et al., 1991). It thereby suppresses coastal upwelling (Morrow et al., 2003) and leads to distinctly warmer sea surface temperatures (SST) than at any other subtropical eastern boundary zone commonly characterized by strong upwelling.

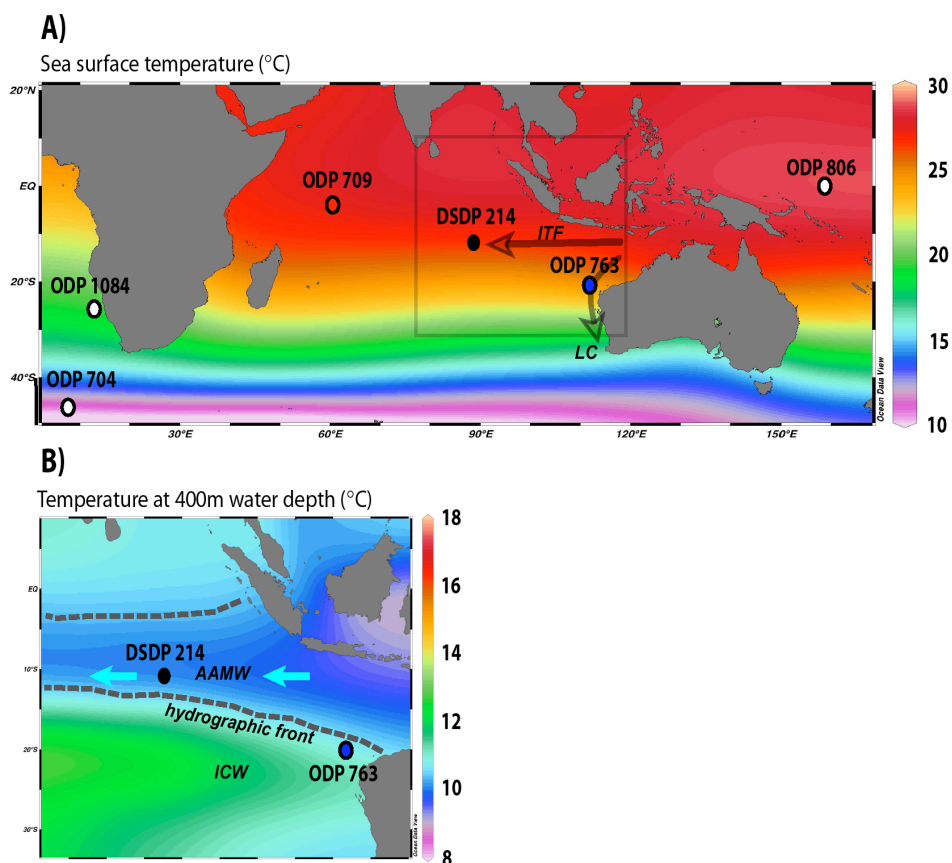


Figure 4.1 (A) Chart of annual ocean temperatures (in °C) at 20 m water depth; Locarnini et al., 2006). Paleooceanographic proxy data were generated for ODP Sites 763A and 709C. The pathways of the Indonesian Throughflow (ITF) and Leeuwin Current (LC) and locations of sediment cores discussed in the text are indicated. (B) Chart showing annual temperatures at 400 m water depth in the eastern Indian Ocean (Locarnini et al., 2006). Note the hydrographic front near Site 763A. AAMW (Australasian Mediterranean Water) and ICW (Indian Ocean Central water) are indicated.

We here present combined planktonic foraminiferal Mg/Ca and $\delta^{18}\text{O}$ data spanning the time period from 6-2 Ma from ODP sites 763A in the subtropical east Indian Ocean within the present influence of the Leeuwin Current (20°35.20'S, 112°12.50'E, 1367 m water depth, Fig. 4.1A) and 709C (03°54.9'S, 60°33.1'E, 3041 m water depth, Fig. 4.1A) in the tropical western Indian Ocean (isotope data from Shackleton and Hall, 1990). We used the combined $\delta^{18}\text{O}$ - and Mg/Ca-derived temperatures to calculate $\delta^{18}\text{O}$ of seawater that approximate changes in ancient salinities (see section 2.4). The analysis of the surface-dwelling planktonic foraminifera *Globigerinoides sacculifer* allow us to monitor changes in the surface-near Leeuwin Current compared to the Indo-Pacific Warm Pool. The geochemical signature of the deep-dwelling *Globorotalia crassaformis* (habitat depth of ~300-450 m; see section 2.2) sheds light on the Pliocene subsurface water oceanography. Specifically at these water depths, Site 763A is at modern times at the hydrographic front between the cold and less saline Australasian Mediterranean Water (AAMW) from the ITF region and the warmer Indian Ocean Central Water (ICW) originating from the Subtropical Front (Tomczak and Godfrey, 1994; Fig. 4.1B).

2. Materials and Methods

2.1. Age models of studied DSDP/ODP sites

Site 709C

To improve the initial age control from Shackleton and Hall (1990), we tuned the corrected *G. ruber/ G. sacculifer* $\delta^{18}\text{O}$ record (Shackleton and Hall, 1990) to the *G. sacculifer* $\delta^{18}\text{O}$ record of Site 806 (Wara et al., 2005) using Analyseries 1.2 (Paillard et al., 1996) (Fig. 4.2A). We selected Site 806 for tuning because of the following aspects. First, as both sites lie within the Indo-Pacific Warm Pool, we can assume a similar development of both $\delta^{18}\text{O}$ signals over time. Second, the resolution of the *G. sacculifer* $\delta^{18}\text{O}$ record of Site 806 is high enough (~8 kyrs) to serve as a tuning reference. Third, the age model of Site 806 was already improved by Karas et al. (2009), who tuned the high-resolution benthic $\delta^{18}\text{O}$ record (4-2 Ma) to the LR04 stack (Lisiecki and Raymo, 2005). As a result, both $\delta^{18}\text{O}$ records correspond quite well (Fig. 4.2A). The resulting depth/age curve is supported by the good fit with the nannofossil biostratigraphy reported by Shackleton and Hall (1990), the ages of which were updated to the ATNTS 2004 time scale (Lourens et al., 2004; Fig. 4.2B). Therefore, the combined use of tuning of the planktonic isotope record to Site 806 and well constrained nannofossil biostratigraphy produces a reliable age model for Site 709C.

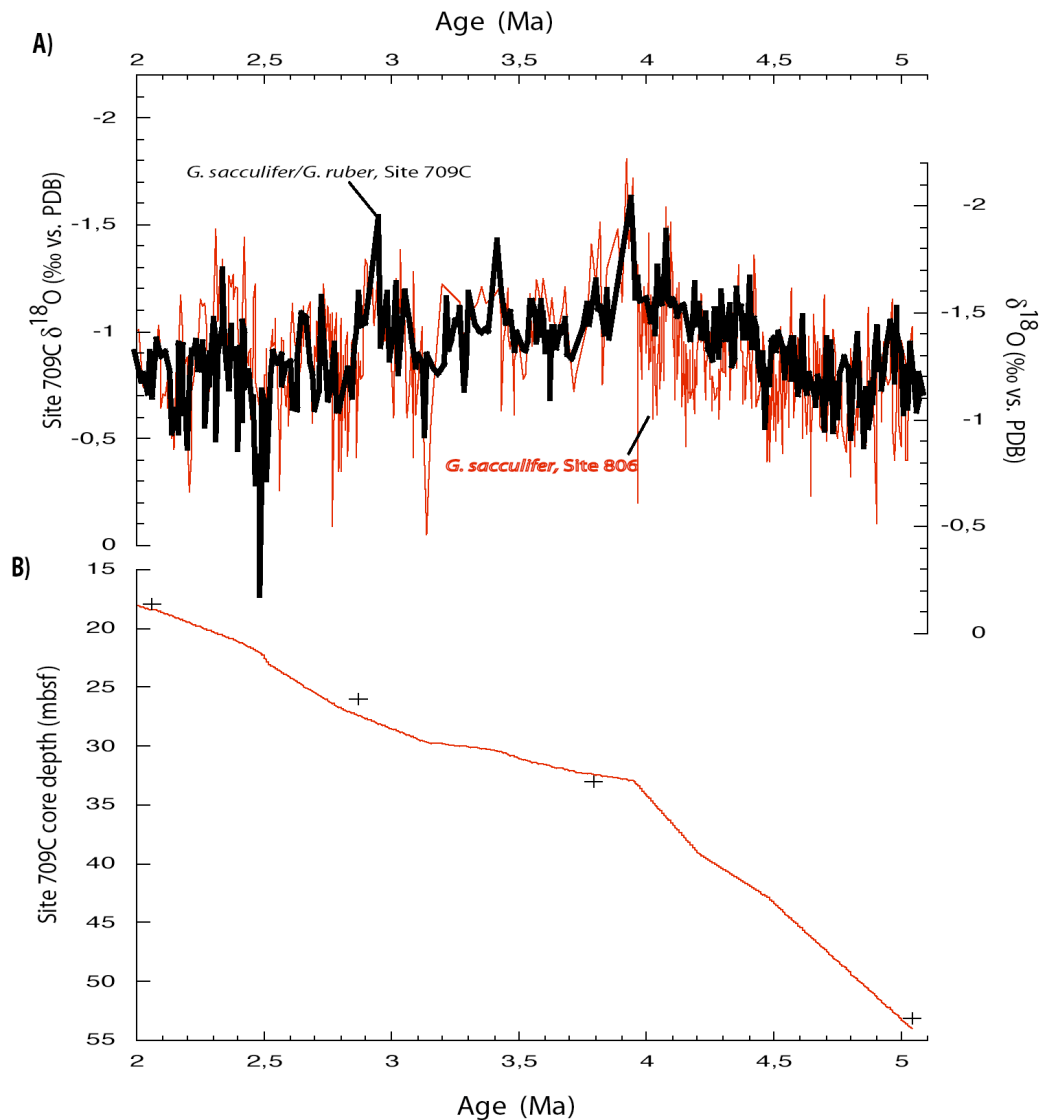


Figure 4.2 Revised stratigraphic framework of Site 709C. (A) Tuning of the high resolution planktonic *G. ruber*/*G. sacculifer* $\delta^{18}\text{O}$ record (thick black; *G. ruber* values were adjusted to *G. sacculifer*; Shackleton and Hall, 1990) to the *G. sacculifer* $\delta^{18}\text{O}$ record of Site 806 (Wara et al., 2005; red). (B) Diagram showing the age/depth relationship of Site 709C (red line). Nannofossil datums (Shackleton and Hall, 1990) are indicated (black crosses).

Site 763A

For an initial age control of Site 763A, we selected those magnetic reversal ages (depths from Tang, 1992; ages were updated to the ATNTS 2004 time scale; Lourens et al., 2004), which lie on the already established depth-age plot for this site based on both magnetic reversal ages and foraminiferal biodatums (Sinha and Singh, 2008). To considerably improve the age model especially during the critical time period 3.5-3 Ma, we generated a high-resolution (~ 5.5 kyr) benthic $\delta^{18}\text{O}_{C. wuellerstorfi}$ record during ~ 3.8 -3.1 Ma, which was then fine-tuned to the LR04 stack (Lisiecki and Raymo, 2005; Fig. 4.3A). Both records correspond well. To further check our established age control during 3.8-3.1 Ma, we performed

astronomical tuning. Indeed the obliquity (41 kyr) filtered components of the benthic $\delta^{18}\text{O}_{\text{C. wuellerstorfi}}$ record are in good accordance to the obliquity solution of Laskar et al. (1993) (Fig. 4.3B) supporting our age model. We observed and corrected a phase lag of 8 kyr between obliquity and obliquity-controlled variations in the benthic $\delta^{18}\text{O}_{\text{C. wuellerstorfi}}$ record. The resulting depth/age curve for the whole studied time period matches very well the magnetic reversal ages (Fig. 4.3C).

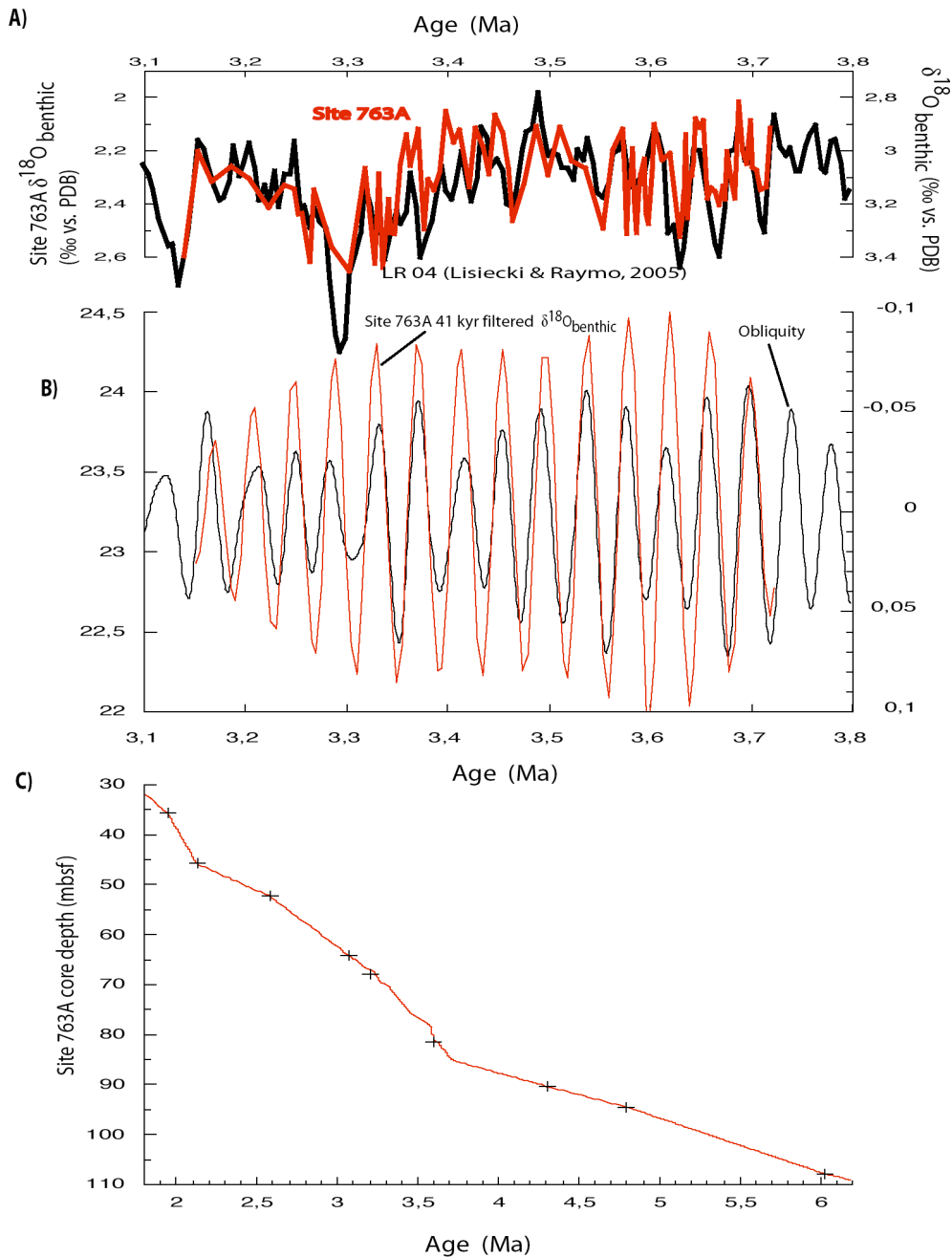


Figure 4.3 Stratigraphic framework of ODP Site 763A. (A) Tuning of the high resolution benthic $\delta^{18}\text{O}_{\text{C. wuellerstorfi}}$ record (thick red) to the global benthic reference stack LR04 (Lisiecki and Raymo, 2005). (B) Showing the filtered 41 kyr components of the benthic $\delta^{18}\text{O}_{\text{C. wuellerstorfi}}$ record (red) being in good accordance to the obliquity solution (Laskar et al., 1993; black). (C) Diagram showing the age/depth relationship (red line) of Site 763A. Crosses indicate magnetic reversal datums (Tang, 1992; Sinha and Singh, 2008) that were updated to the ATNTS 2004 time scale (Lourens et al., 2004).

2.2. $\delta^{18}\text{O}$ and Mg/Ca analysis

For stable oxygen isotope and Mg/Ca analyses, ~30 specimens were selected from shallow dwelling planktonic foraminifera *G. sacculifer* (without sac-like chamber), which calcify in the upper 50 m water depth (Anand et al., 2003). From the deep dwelling planktonic foraminifera *G. crassaformis*, which calcify below the seasonal thermocline (calcification depth of ~300-450 m; Elderfield et al., 2002) 20-40 specimens were selected. Only in a few cases, the number had to be reduced to ~10 specimens. Specimens were selected from the 315-355 μm size fraction to avoid size effects in $\delta^{18}\text{O}$ values and Mg/Ca (Elderfield et al., 2002). The size fraction had to be widened to the 315-400 μm size fraction when only insufficient foraminiferal tests were within the narrow fraction. Subsequently, sample material was gently crushed, mixed and divided into two thirds used for Mg/Ca analyses, and one third for stable isotope measurements. Isotope measurements were either conducted on a Finnigan MAT-252 (at IFM-GEOMAR, Kiel) or on a Finnigan MAT-251 mass spectrometer (at the Leibniz-Laboratory for Radiometric Dating and Stable Isotope Research, Kiel), both equipped with a fully automated carbonate preparation device. Both machines had an analytical precision better than $\pm 0.07\%$ for $\delta^{18}\text{O}$; $\pm \sigma$. All values are reported relative to Pee Dee Belemnite (PDB, based on calibration directly to National Bureau of Standards (NBS-19)). From Site 709C, we used the published $\delta^{18}\text{O}$ record from Shackleton and Hall (1990), who selected in the older part of the core ($> 4\text{Ma}$) *G. sacculifer* and in the younger part *G. ruber* specimens. In order to make the $\delta^{18}\text{O}$ values from both species comparable, we added 0.25‰ to the $\delta^{18}\text{O}_{G. ruber}$ record, being consistent to studies at the same site (Shackleton and Hall, 1990) and in the tropical eastern Indian Ocean Site 214 (Karas et al., 2009).

For Mg/Ca analyses, samples were cleaned according to the established cleaning protocol of Barker et al. (2003) (non reductive). Measurements were performed on a simultaneous, radially viewing ICP-OES (Ciros CCD SOP, Spectro A.I., Germany, Inst. of Geosciences, Univ. of Kiel). The analytical error for the Mg/Ca ratios was ~0.17% (~900 samples). Replicate analysis on the same samples, cleaned and analysed during different sessions, showed a standard deviation of <0.1 mmol/mol (rel. std. dev. $<3\%$). Monitoring of Fe/Ca and Mn/Ca indicated that contamination with clays or Mn-carbonates after cleaning was not an issue. This is supported by the Fe/Mg values, which were commonly significantly lower than 0.1 mmol/mol indicative for negligible contamination of silicate phases (Barker et al., 2003). However, at Site 763A we rejected 8 samples, because these samples showed Fe/Mg ratios >0.15 mmol/mol accompanied by relatively high Mg/Ca ratios (~4 mmol/mol)

which might be related to silicate contamination. We converted Mg/Ca ratios of *G. sacculifer* into temperatures by using the multispecies calibration of Anand et al. (2003): $\text{Mg/Ca} = 0.38 \exp(0.09 \times \text{SST})$. The conversion of *G. crassaformis* Mg/Ca ratios into temperatures was conducted by using a species-specific calibration of Regenberg et al. (2009): $\text{Mg/Ca} = 0.83 \exp(0.082 \times T)$.

2.3. Dissolution effects on Mg/Ca values

When interpreting $\text{SST}_{\text{Mg/Ca}}$, it is crucial to assess possible calcite dissolution, which is known to considerably affect foraminiferal Mg/Ca (e.g., Regenberg et al., 2006). From core-top studies, Regenberg et al. (2006) suggested that Mg^{2+} loss starts below critical ΔCO_3^{2-} threshold values of $\sim 20 \mu\text{mol/kg}$ and proposed species-specific correction equations. As Site 763A location (1367 m water depth) is situated well above the present lysocline in that region (deeper than ~ 3900 m; Martinez et al., 1999) and indeed, lies above critical ΔCO_3^{2-} levels of $\sim 20 \mu\text{mol/kg}$ (Dekens et al., 2002; Regenberg et al., 2006; Data from World Ocean Circulation Experiment-transect 110 were used to calculate ΔCO_3^{2-} levels; Lewis and Wallace, 1998), we did not correct the initial Mg/Ca values (Fig. 4.4C). Although Site 709C (3041 m water depth) is also situated above the present lysocline (~ 4400 m in the central tropical Indian Ocean; Banakar et al., 1998) and carbonates are well preserved throughout the studied time interval (Backman et al., 1988), ΔCO_3^{2-} values are on average at $\sim 10 \mu\text{mol/kg}$ (Data from World Ocean Circulation Experiment-transect 102E/W was used to calculate ΔCO_3^{2-} levels; Lewis and Wallace, 1998) clearly below critical levels where dissolution starts. We therefore applied the species-specific correction equation for *G. sacculifer* (Regenberg et al., 2006) to correct the initial Mg/Ca values (Fig. 4.4C).

2.4. Calculation of $\delta^{18}\text{O}_{\text{seawater}}$

To assess changes in ancient sea (sub)surface salinities, we used the combined $\delta^{18}\text{O}$ and Mg/Ca temperature records from the surface dwelling planktonic species *G. sacculifer* and from the deep dwelling *G. crassaformis*. Accordingly, we calculated $\delta^{18}\text{O}_{\text{seawater}}$ (Shackleton, 1974), which reflects a combination of ice-volume controlled $\delta^{18}\text{O}_{\text{seawater}}$ changes plus local variations in $\delta^{18}\text{O}_{\text{seawater}}$ due to regional hydrological changes. As $\delta^{18}\text{O}_{\text{seawater}}$ records from different core locations are equally influenced by variations in global ice volume, the relative changes between them reflect the regional hydrological changes, which we aim to resolve in this study. We are aware that this approach introduces slight errors, but provides a reliable approximation of changes in ocean salinity.

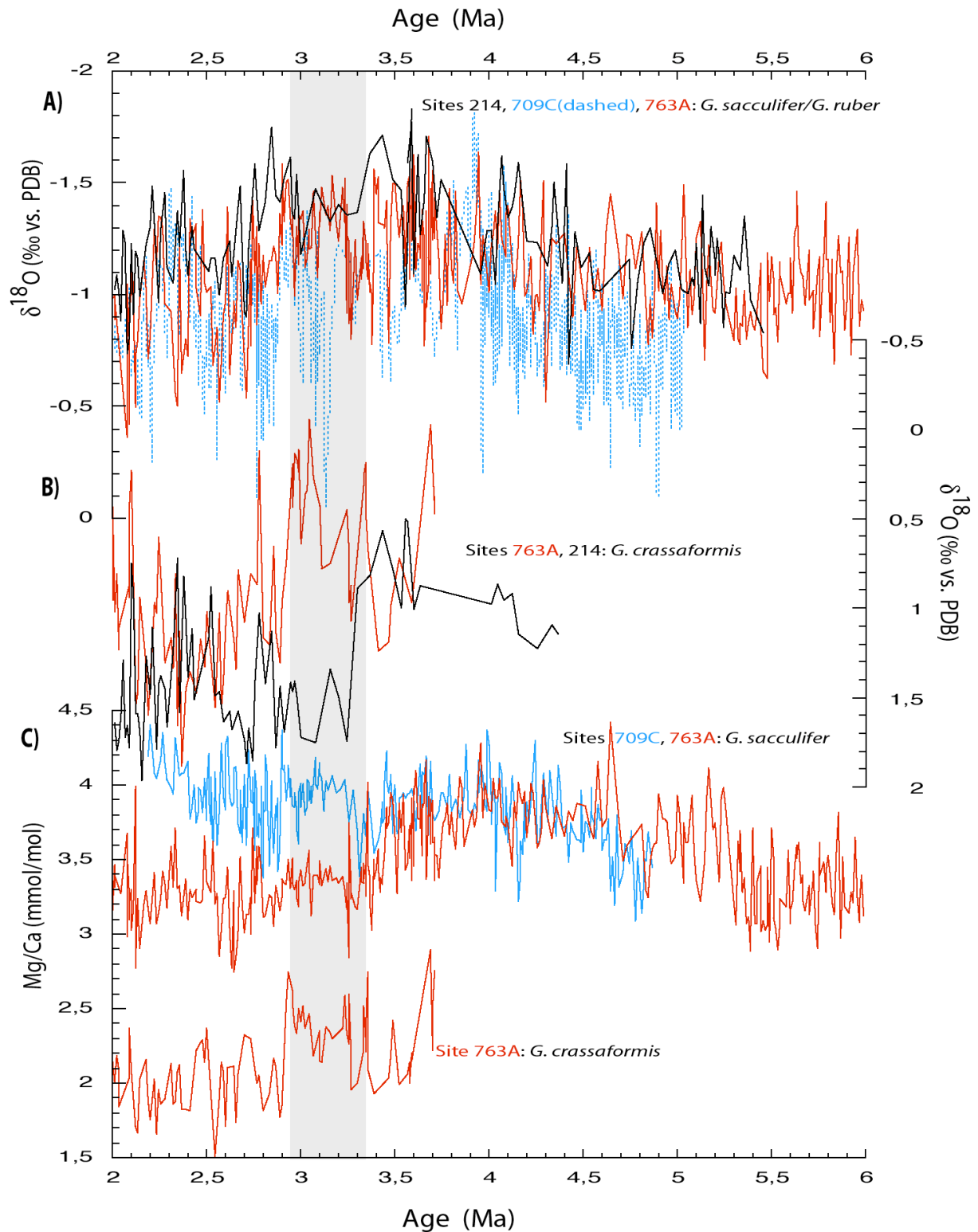


Figure 4.4 (A) Surface layer *G. ruber/G. sacculifer* $\delta^{18}\text{O}$ records from Site 214 (black; Karas et al., 2009), Site 709C (dashed blue; Shackleton and Hall, 1990) and Site 763A (red, this study). (B) subsurface *G. crassaformis* $\delta^{18}\text{O}$ records from sites 214 (black) and 763A (red). (C) *G. sacculifer* and *G. crassaformis* Mg/Ca records from sites 763A (red) and 709C (blue) used to calculate (sub)surface temperatures. Note that Mg/Ca ratios from Site 709C were corrected after Regenberg et al. (2006) (see section 2.3).

3. Results and Discussion

3.1. Development of (sub)surface hydrography

The *G. ruber*/*G. sacculifer* $\delta^{18}\text{O}$ records of Site 709C from the tropical western Indian Ocean (Shackleton and Hall, 1990), of Site 763A from the subtropical eastern Indian Ocean, and of Site 214 from the tropical eastern Indian Ocean (Fig. 4.4A; Karas et al., 2009) show similar long-term trends with decreasing values from the early Pliocene until ~ 3.5 Ma, changing towards more positive values during mid-Pliocene global cooling (Ravelo et al., 2004). However, absolute $\delta^{18}\text{O}$ values differ between cores. $\delta^{18}\text{O}$ values at Site 709C are commonly more positive than those at sites 214 and 763A, possibly indicating higher salinities there. Since ~ 3.5 Ma, $\delta^{18}\text{O}$ values at Site 763A start to deviate showing at times more positive values compared to Site 214. Foraminiferal Mg/Ca implies similar $\text{SST}_{\text{Mg/Ca}}$ during the early Pliocene at all sites with a long-term warming trend of $\sim 2^\circ\text{C}$ towards the mid-Pliocene at ~ 4 - 3.6 Ma (Figs 4.4C, 4.5A). This observation is in accordance with Brierley et al. (2009), who showed that during the early Pliocene the tropical warm pool was expanded with a reduced temperature gradient between the equator and the subtropics. During the mid-Pliocene, $\text{SST}_{\text{Mg/Ca}}$ from the tropical western Indian Ocean Site 709C remained stable at $\sim 26^\circ\text{C}$ (Fig. 4.5A) and broadly resemble those from tropical eastern Indian Ocean Site 214 (Karas et al. 2009). The long term decrease of $\sim 1^\circ\text{C}$, which is evident at sites 214 and 806 (Wara et al., 2005; Karas et al., 2009), is not seen at Site 709C implying that the tropical western Indian Ocean might have been less influenced by mid-Pliocene global cooling (Ravelo et al., 2004). From ~ 3.3 Ma onwards, $\text{SST}_{\text{Mg/Ca}}$ at Leeuwin Current Site 763A became significantly cooler by 2 - 3°C than at tropical sites 214 and 709C from the present-day Indian Ocean Warm Pool. This gradient in $\text{SST}_{\text{Mg/Ca}}$ is comparable to modern conditions with an annual SST difference of $\sim 2^\circ\text{C}$ between sites (Locarnini et al., 2006), implying that present-day SST conditions were already reached during the mid-Pliocene.

Within the critical time period at 3.5 - 3 Ma, we not only observe at the ocean surface a different hydrographic development between sites 214 and 763A, but also at the subsurface level. In particular at ~ 3.3 - 3 Ma, the *G. crassaformis* $\delta^{18}\text{O}$ record from Site 763A shows significantly lower values of up to $\sim 1.5\text{‰}$ than those from Site 214 (Fig. 4.4B). Also, both deep-dwelling *G. crassaformis* $\delta^{18}\text{O}_{\text{seawater}}$ records approximating past salinity conditions deviate from each other pointing to more saline conditions at Site 214 (Fig. 4.5D). After ~ 3 Ma, both *G. crassaformis* $\delta^{18}\text{O}_{\text{seawater}}$ records converge, suggesting at times fresher conditions at Site 214 (Fig. 4.5D). The more saline subsurface conditions during ~ 3.3 - 3.1 Ma at tropical eastern Indian Ocean Site 214 (Fig. 4.5D) were interpreted as a consequence of the tectonic

reorganization of the Indonesian Gateway (Karas et al., 2009). Either the contribution of cooler and fresher ITF waters to this site was reduced and replaced by warmer and saltier tropical Indian Ocean waters or a switch back to more warm and saline South Pacific source waters occurred (Karas et al., 2009). The Site 763A $\delta^{18}\text{O}_{\text{seawater}}$ record does not show such high saline conditions during ~3.3-3.1 Ma most likely because Site 763A is outside the present main throughflow of cold and fresh AAMW (Tomczak and Godfrey, 1994). A change in the subsurface throughflow, thus, would have affected Site 763A much less than Site 214. After ~2.95 Ma, the change in ITF subsurface waters from a South to a dominant North Pacific source finalized (Karas et al., 2009) indicated by fresher and cooler conditions at the subsurface level at Site 214 (Fig. 4.5B). This switch is not such pronounced at Site 763A with on average ~2°C warmer subsurface Mg/Ca derived temperatures and occasionally saltier conditions, implying that a modern-like hydrographic front between the cold and fresh AAMW from the Indonesian region and the warmer Indian Ocean Central Water from the southern Indian Ocean (Tomczak and Godfrey, 1994) developed since then (Fig. 4.5B, D). This setting is consistent with modern conditions showing a similar gradient in subsurface temperatures at ~400m water depth between both core sites (Fig. 4.1B; Locarnini et al., 2006).

3.2. Pliocene changes in the Leeuwin Current

It is important to note, however, that at Site 763A the surface ocean definitely cooled before the switch of ITF source waters finalized at ~2.95 Ma. Surface cooling began at ~3.5 Ma, and after ~3.3 Ma the impact of warm tropical waters diminished compared to the tropical eastern and western Indian Ocean sites 214 and 709C (Fig. 4.5A). At the same time, subsurface waters at Site 214 became more saline in line with a reduction of the ITF (Fig. 4.5D; Karas et al., 2009). Both, the more saline conditions at the subsurface level at Site 214 and the cooler surface conditions at Site 763A suggest a significant reduction of the ITF at 3.3-3.1 Ma. As today the Leeuwin Current is controlled mainly by the ITF (e.g., Feng et al., 2003), we suspect that it was clearly reduced during the mid-Pliocene when the ITF declined due to the new tectonic setting in the Indonesian Gateway (Cane and Molnar, 2001; Gaina et al., 2007). We presuppose in this respect that the Leeuwin Current was present also during the mid-Pliocene indicated by *G. sacculifer* $\delta^{18}\text{O}_{\text{seawater}}$ records from sites 214 and 763A, which are very similar and imply a common ITF source water (Fig. 4.5D).

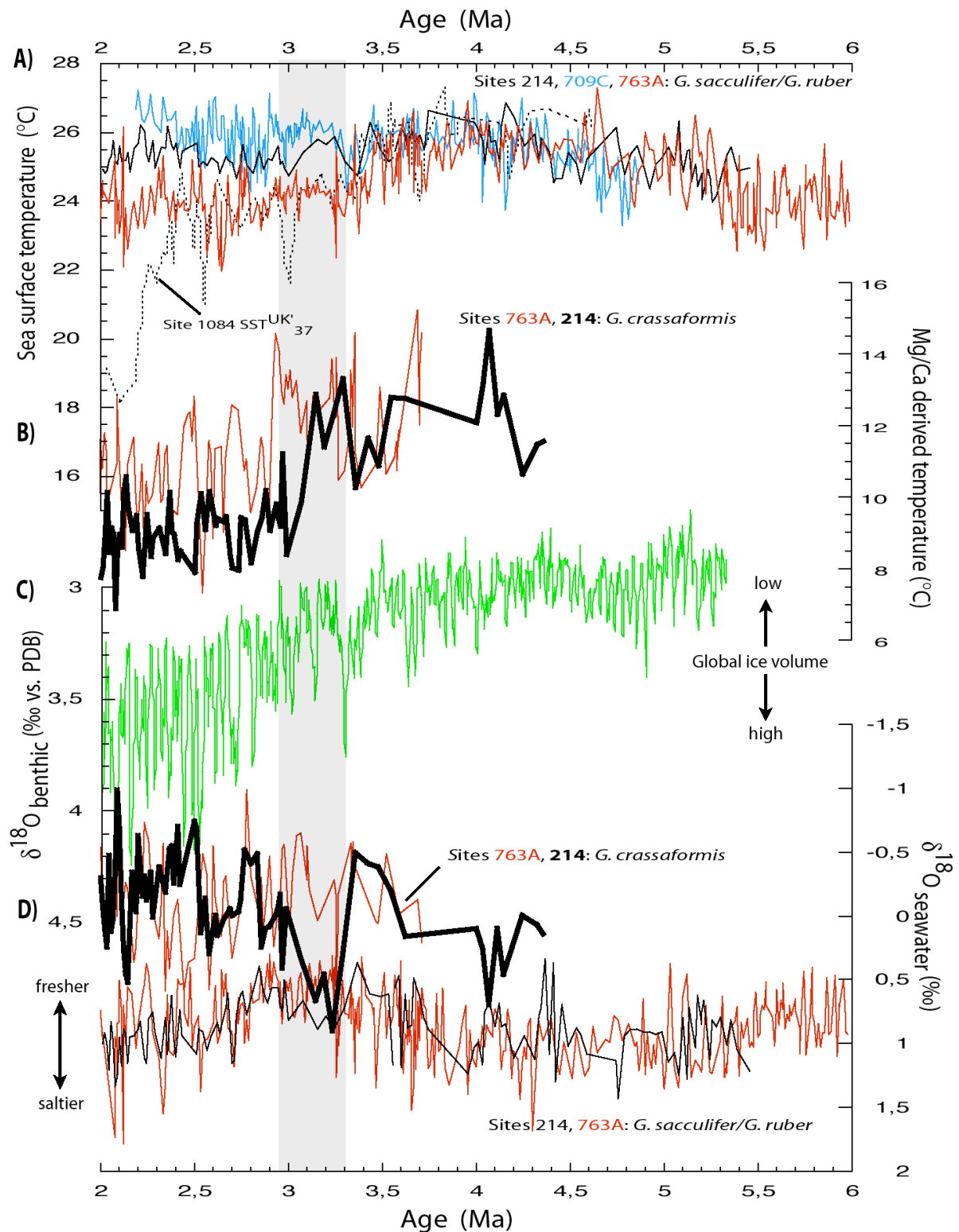


Figure 4.5 (A) *G. ruber/G. sacculifer* SST_{Mg/Ca} from Site 214 (black; Karas et al., 2009), Site 709C (blue, this study), Site 763A (red, this study), and alkenone derived SST from Site 1084 in the Benguela upwelling system (Marlow et al., 2000; Etourneau et al., 2009). (B) Comparison of *G. crassaformis* Mg/Ca derived temperatures at the subsurface level from sites 214 (thick black; Karas et al., 2009) and 763A (red; this study). (C) The LR04 global ice volume record from Lisiecki and Raymo (2005). (D) *G. sacculifer* (Site 214, black; Site 763A, red) and subsurface *G. crassaformis* (Site 214, thick black; Site 763A).

Various modelling studies in fact pointed out the effects of the mid-Pliocene ITF reduction (Hirst and Godfrey, 1993; Godfrey, 1996; Lee, 2002). With an entirely closed Indonesian Gateway, these models generate scenarios quite similar to our reconstructions. Our observed SST_{Mg/Ca} pattern in the Indian Ocean suggests a weaker Leeuwin Current being ~2°C cooler, while SST_{Mg/Ca} at the tropical eastern and western Indian Ocean sites 214 and 709C remain rather stable. In this respect, a cooling of surface ITF waters during this time interval causing the SST_{Mg/Ca} decline in the Leeuwin Current area seems rather unlikely as the SST_{Mg/Ca} at Site 214 (and at Site 806; Wara et al., 2005) are hardly changing (Fig. 4.5A; Karas et al., 2009). We therefore consider the reduction in ITF and not just a cooling as causative for the cooling at Leeuwin Current Site 763A. This notion is further supported by tectonic reconstructions of the ITF region, which propose a shoaling of the Indonesian Gateway with the emergence of small islands like Timor (Cane and Molnar, 2001; Gaina et al., 2007; Kuhnt et al., 2004), and in consequence, a restricted throughflow (Kuhnt et al., 2004).

The tectonic reorganization might indeed have reduced the surface throughflow volume since ~3.3 Ma, whereas the subsurface ITF after ~3.1 Ma again started to cool and freshen due to the switch to North Pacific source waters (Karas et al., 2009). This switch might have supported the surface layer cooling of Site 763A through mixing processes of the cold and fresh subsurface waters from the Indonesian region (Hirst and Godfrey, 1993; Song and Gordon 2004). In contrast, changes in the monsoon systems (Indian and Asian monsoon), driving oceanographic changes in that area today and possibly on glacial-interglacial timescales (Gordon et al., 2003; Xu et al., 2008), are unlikely of having cooled the (sub)surface during the mid-Pliocene time period ~3.5-3 Ma, when Indonesian surface and subsurface flow changed. Significant changes in the monsoon systems and in South China SST clearly appeared after 3 Ma (Gupta and Thomas, 2003; Jia et al., 2008).

Our findings of a reduced Leeuwin Current are consistent with marine and terrestrial palynological studies off northwestern Australia and from southwestern Australia, respectively (Martin et al., 1994; Dodson et al., 2004). These studies suggest the expansion of aridity around 3 Ma in the southwest, the disappearance of rainforest and the development of shrub/grasslands in northwestern Australia. Indeed cooler SST in that area through a reduced Leeuwin Current would have caused a significant reduction in precipitation in the coastal areas of western and southwestern Australia (Feng et al., 2003).

3.3. Implications for the poleward heat transport

Apart from climatic effects on western Australia, we observe from 3.5-3 Ma a similar surface layer cooling at Site 1084 in the Benguela upwelling system (Marlow et al., 2000) as we registered at Site 763A (Fig. 4.5A). Both temperature records show an almost identical development until 2.4 Ma, when alkenone-derived SST from Site 1084 further drop significantly. The good match of both SST records until late Pliocene times supports our notion that the restriction of the Indonesian Gateway possibly contributed to the cooling of the Benguela upwelling system (Karas et al., 2009). Such cooling most likely resulted not only from the proposed cooling of subsurface waters in the tropical eastern Indian Ocean (Karas et al., 2009), but also from the reduced surface throughflow of Indonesian waters. Support comes from modelling studies (Hirst and Godfrey, 1993; Godfrey, 1996), which suggest both a weaker Leeuwin Current when the ITF is closed, and a weaker Agulhas Current resulting in a significant cooling of the Agulhas outflow region close to Site 1084. In consequence, the poleward heatflux would have been considerably reduced (Hirst and Godfrey, 1993; Gordon, 2005) explaining the enhanced meridional temperature gradient in the Indian Ocean and the cooling of the Benguela upwelling system. Global Pliocene cooling by itself seems to be unlikely to have initiated the cooling of both the Leeuwin Current and the Benguela upwelling system. In fact, no other studies, which calculated meridional temperature gradients show such an abrupt SST decline at ~3.3 Ma (Jia et al., 2008; Brierley et al., 2009). We further suspect that an enlarged meridional temperature gradient between the tropics and subtropics, if initially caused by a “cooling from the south”, would have promoted cooling at higher southern latitudes. However at Site 1084, which is located ~5° more southward than Site 763A, we do not observe a more pronounced cooling than at Site 763A (Figs 4.1A, 4.5A). This is consistent with the planktonic $\delta^{18}\text{O}$ record from the subantarctic southeast Atlantic Ocean Site 704 (Hodell and Venz, 1992), which neither exhibit pronounced cooling at ~3.5-3 Ma. We therefore suggest that the constriction of the Indonesian Gateway was an important regional process reducing the poleward heat flux (Brierley et al., 2009) and strengthening the global meridional atmospheric circulation (Hadley circulation). After ~2.4 Ma, the significant cooler alkenone SST at Site 1084 (Marlow et al., 2000) compared to the $\text{SST}_{\text{Mg/Ca}}$ at Site 763A are most likely related to the intensification of the trade winds and marked cooling of the Southern Ocean, which initiated the modern-like Benguela upwelling system (Fig. 4.5A; Etourneau et al., 2009). At the same time, $\text{SST}_{\text{Mg/Ca}}$ at Site 763A remained relatively warm caused by a still flowing Leeuwin Current. Even though it was cooler and/or reduced, it

prevented strong coastal upwelling, which would likely have developed without the presence of the Leeuwin current (Smith et al., 1991; Morrow et al., 2003).

4. Conclusions

We reconstructed the Pliocene surface and subsurface hydrography of the tropical western and subtropical eastern Indian Ocean. While in the tropical eastern Indian Ocean, the restriction of the Indonesian Gateway caused a switch in ITF source waters at the subsurface level showing a distinct cooling/freshening (Karas et al., 2009) at ~3.5-2.95 Ma, subsurface waters at Site 763A are less affected showing on average ~2°C warmer subsurface temperatures. This implies the development of a modern-like hydrographic front between the cold and fresh AAMW stemming from the Indonesian region and the warmer Indian Ocean Central Water from the southern Indian Ocean since ~3 Ma (Tomczak and Godfrey, 1994). Ocean surface temperatures from the eastern and western tropical Indian Ocean sites 214 (Karas et al., 2009) and 709C remained rather constant during this time period, while those at Site 763A significantly dropped, indicating a reduced Leeuwin Current. We suggest that the weakening of the Leeuwin Current since ~3.3 Ma was caused by the tectonically reduced surface ITF, possibly supported by mixing processes with the cold and fresh subsurface waters from the Indonesian region. Most likely the reduced surface ITF led to a diminished poleward heat transport resulting in a weakened Leeuwin Current and a cooling of the Benguela upwelling system. Thereby, this mechanism amplified the mid-Pliocene global development towards increased meridional temperature differences (Brierley et al., 2009).

Acknowledgements

Samples for this study were provided by the IODP. Funding of this research was provided by the German Science Foundation (DFG) within project Nu60/14-2. We thank N. Gehre, K. Kiesling, L. Haxhijaj, A. Bahr, M. Regenberg, J. Etourneau and J. Groeneveld for valuable comments and technical support.

References

- Anand, P., H. Elderfield, and M. H. Comte (2003), Calibration of Mg/Ca thermometry in planktonic foraminifera from a sediment trap time series, *Paleoceanography*, 18, doi:10.1029/2002PA000846.
- Backman, J., et al. (1988), Site 709, in Proceedings ODP, Initial Reports, v. 115, Backman, J., et al., Eds., Shipboard Scientific Party (College Station, Texas, 1988).

- Banakar, V. K., G. Parthiban, and P. Jauhari (1998), Chemistry of surface sediments along a north-south transect across the equator in the central Indian basin: An assessment of biogenic and detrital influences on elemental burial on the seafloor, *Chem. Geology*, *147*, 217-232.
- Barker, S., M. Greaves, and H. Elderfield (2003), A study of cleaning procedures used for foraminiferal Mg/Ca paleothermometry, *Geochem., Geophys., Geosyst.*, *4* (9), doi:10.1029/2003GC000559.
- Brierley, C. M., A. V. Fedorov, Z. Liu, T. D. Herbert, K. T. Lawrence, and J. P. LaRiviere (2009), Weakened Hadley Circulation and Greatly Expanded Tropical Warm Pool in the Early Pliocene, *Science*, *323*, 1714-1718.
- Cane, M., and P. Molnar (2001), Closing of the Indonesian seaway as a precursor to east African aridification around 3-4 million years ago, *Nature*, *411*, 157-162.
- Dekens, P. S., D. W. Lea, D. K. Pak, and H. J. Spero (2002), Core top calibration of Mg/Ca in tropical foraminifera: Refining paleotemperature estimation, *Geochem., Geophys., Geosyst.*, *3*, doi: 10.1029/2001GC000200.
- Dodson, J. R., and M. K. Macphail (2004), Palynological evidence for aridity events and vegetation change during the Middle Pliocene, a warm period in Southwestern Australia, *Global Planet. Change*, *41*, 285-307.
- Elderfield, H., M. Vautravers, and M. Cooper (2002), The relationship between shell size and Mg/Ca, Sr/Ca, $\delta^{18}\text{O}$, and $\delta^{13}\text{C}$ of species of planktonic foraminifera, *Geochem., Geophys., Geosyst.*, *3*, doi: 10.1029/2001GC000194.
- Etourneau, J., P. Martinez, T. Blanz, and R. Schneider (2009), Pliocene-Pleistocene variability of upwelling activity, productivity, and nutrient cycling in the Benguela Region, *Geology*, *37*, 871-874, doi: 10.1130/G25733A.1.
- Feng, M., G. Meyers, A. Pearce, and S. Wijffels (2003), Annual and interannual variations of the Leeuwin Current at 32°S, *J. Geophys. Res.*, *108*, NO. C11, 3355, doi:10.1029/2002JC001763.
- Gaina, C., and D. Müller (2007), Cenozoic tectonic and depth/age evolution of the Indonesian gateway and associated back-arc basins, *Earth Sci. Rev.*, *83*, 177-203.
- Godfrey, J. S. (1996), The effect of the Indonesian Throughflow on ocean circulation and heat exchange with the atmosphere: A review, *J. Geophys. Res.*, *101*, 12217-12237.
- Gordon, A. L., R. D. Susanto, and K. Vranes (2003), Cool Indonesian throughflow as a consequence of restricted surface layer flow, *Nature*, *425*, 824-828.

- Gordon, A. L. (2005), Oceanography of the Indonesian Seas and their throughflow, *Oceanography*, 18(4), 14-27.
- Gupta, A. K., and E. Thomas (2003), Initiation of northern hemisphere glaciation and strengthening of the northeast Indian monsoon: Ocean drilling program site 758, eastern equatorial Indian ocean, *Geology*, 31, 47-50.
- Hirst, A. C., and J. S. Godfrey (1993), The role of Indonesian Throughflow in a Global Ocean GCM, *J. Phys. Oceanogr.*, 23, 1057-1086.
- Hodell, D. A., and K. Venz (1992), Toward a high-resolution stable isotopic record of the Southern Ocean during the Pliocene-Pleistocene (4.8 to 0.8 Ma), in Kennett, J.P., and D.A. Warnke, Eds., *The Antarctic Paleoenvironment: A Perspective on Global Change*, 1, Antarctic Research Series, v. 56, p. 265-310.
- Jia, G., F. Chen, and P. Peng (2008), Sea surface temperature differences between the western equatorial Pacific and northern South China Sea since the Pliocene and their paleoclimatic implications, *Geophys. Res. Lett.*, 35, doi: 10.1029/2008GL034792.
- Karas, C., D. Nürnberg, A. K. Gupta, R. Tiedemann, K. Mohan, and T. Bickert (2009), Mid-Pliocene climate change amplified by a switch in Indonesian subsurface throughflow, *Nature Geoscience*, 2, 434-438.
- Kuhnt, W., A. Holbourn, R. Hall, M. Zuvela, and R. Käse (2004), Neogene History of the Indonesian Throughflow, in Clift, P., D. Hayes, W. Kuhnt, and P. Wang eds., *American Geophysical Union Monograph*, Washington, p. 299-320.
- Laskar, J. (1993), The chaotic motion of the solar system: a numerical estimate of the chaotic zones, *Icarus*, 88, 266-291.
- Lee, T., I. Fukumori, D. Menemenlis, Z. Xing, and L. L. Fu (2002), Effects of the Indonesian Throughflow on the Pacific and Indian Oceans, *J. Phys. Oceanogr.*, 32, 1404-14290.
- Lewis, E., and D. W. R. Wallace (1998), co2sys -Program Developed for CO2System Calculations, oRNL/CDIAC-105, Carbon Dioxide Information Analysis Center, Oak Ridge Natl. Lab., (U.S. Dep. of Energy, Oak Ridge, Tenn., 1998).
- Lisiecki, L. E., and M. E. Raymo (2005), A Pliocene-Pleistocene stack of 57 globally distributed benthic $\delta^{18}\text{O}$ records, *Paleoceanography*, 20, PA1003, doi:10.1029/2004PA001071.
- Locarnini, R. A. et al. (2006), *World Ocean Atlas 2005*, in Vol. 1: Temperature. S. Levitus, Eds., NOAA Atlas NESDIS 61, (U.S. Government Printing Office, Washington, D.C., 2006) 182 pp.

- Lourens, L. J. et al. (2004), in *A Geologic Time Scale 2004*: Cambridge. Gradstein, F. M., J. Ogg et al., Eds. (Cambridge Univ. Press, 2004), Appendix 2.
- Marlow, J. R., C. B. Lange, G. Wefer, and A. Rosell-Melé (2000), Upwelling intensification as part of the Pliocene-Pleistocene climate transition, *Science*, *290*, 2288-2291.
- Martin, H. A., and A. McMinn (1994), Late Cainozoic Vegetation History of North-western Australia, from the Palynology of a Deep Sea Core (ODP Site 765), *Aust. J. Bot.*, *42*, 95-102.
- Martinez, J. I., P. De Deckker, and T. T. Barrows (1999), Palaeoceanography of the last glacial maximum in the eastern Indian Ocean: Planktonic foraminiferal evidence, *Palaeogeogr., Palaeoclim., Palaeoecol.*, *147*, 73-99.
- Morrow, R., F. Fang, M. Fieux, and R. Molcard (2003), Anatomy of three warm-core Leeuwin Current eddies, *Deep-Sea Res. II*, *50*, 2229-2243.
- Mudelsee, M., and M. E. Raymo (2005), Slow dynamics of the Northern Hemisphere glaciation, *Paleoceanography*, *20*, PA4022, doi:10.1029/2005PA001153.
- Paillard, D., L. Labeyrie, and P. Yiou (1996), Macintosh program performs time-series analysis, *Eos, Transactions AGU*, *77*, 379.
- Ravelo, A. C., D. H. Andreasen, M. Lyle, A. O. Lyle, and M. W. Wara (2004), Regional climate shifts caused by gradual global cooling in the Pliocene epoch, *Nature*, *429*, 263-267.
- Regenberg, M., D. Nürnberg, S. Steph, J. Groeneveld, D. Garbe-Schönberg, R. Tiedemann, and W.-C. Dullo (2006), Assessing the effect of dissolution on planktonic foraminiferal Mg/Ca ratios: Evidence from Caribbean core tops, *Geochem., Geophys., Geosyst.*, *7*, doi: 10.1029/2005GC001019.
- Regenberg, M., S. Steph, D. Nürnberg, R. Tiedemann, and D. Garbe-Schönberg (2009), Calibrating Mg/Ca ratios of multiple planktonic foraminiferal species with $\delta^{18}\text{O}$ -calcification temperatures: Paleothermometry for the upper water column, *Earth Planet. Sci. Lett.*, *278*, 324-336, doi:10.1016/j.epsl.2008.12.019.
- Shackleton, N. J. (1974), Attainment of isotope equilibrium between ocean water and the benthonic foraminiferal genus *Uvigerina*. Isotopic changes in the ocean during the last glacial, *Cent. Nat. Rech. Sci. Colloq. Int.*, *219*, 203.
- Shackleton, N. J., and M. A. Hall (1990), in Proceedings ODP, Science Results, v. 115, Duncan, R. A., J. Backman, and L. C. Peterson Eds. (College Station, Texas, 1990).

- Sinha, D. K., and A. K. Singh (2008), Late Neogene planktic foraminiferal biochronology of the ODP Site 763A, Exmouth Plateau, Southeast Indian Ocean, *J. Foram. Res.*, 38, 251-270.
- Smith, R. L., A. Huyer, J. S. Godfrey, and J. A. Church (1991), The Leeuwin Current off western Australia 1986–87, *J. Phys. Oceanogr.*, 21, 323-345.
- Song, Q., and A. L. Gordon (2004), Significance of the vertical profile of the Indonesian Throughflow transport to the Indian Ocean, *Geophys. Res. Lett.*, 31, L16307, doi:10.1029/2004GL020360.
- Talley, L. (2003), Shallow, intermediate, and deep overturning components of the global heat budget, *J. Phys. Oceanogr.*, 33, 530-560.
- Tang, C. (1992), in Proceedings ODP, Science Results, v. 122, von Rad, U., B. U. Haq et al., Eds., Paleomagnetism of cenozoic sediments in holes 762B and 763A, Central Exmouth Plateau, northwest Australia. (College Station, Texas, 1992).
- Tomczak, M., and J. S. Godfrey (1994), Regional Oceanography: an Introduction (Pergamon, Oxford, England; New York 1994) 422pp.
- Wara, M. W., A. C. Ravelo, and M. L. Delaney (2005), Permanent El Niño-Like Conditions During the Pliocene Warm Period, *Science*, 309, 758-761.
- Xu, J., A. Holbourn, W. Kuhnt, Z. Jian, and H. Kawamura (2008), Changes in the thermocline structure of the Indonesian outflow during Terminations I and II, *Earth Planet. Sci. Lett.*, 273, 152–162.

Chapter V

Pliocene climate change of the southwest Pacific and the impact of ocean gateways

Pliocene climate change of the southwest Pacific and the impact of ocean gateways

Cyrus Karas¹, Dirk Nürnberg¹, Ralf Tiedemann² and Dieter Garbe-Schönberg³

¹ Leibniz Institute of Marine Sciences (IFM-GEOMAR), University of Kiel, Wischhofstrasse 1-3, D-24148 Kiel, Germany

² Alfred Wegener Institute for Polar and Marine Research, Am Alten Hafen 26, D-27568 Bremerhaven, Germany

³ Institute of Geosciences, University of Kiel, D-24118 Kiel, Germany

The transition from the early Pliocene “Warmhouse” towards the present “Icehouse” climate and the role of gateway dynamics are currently intensively debated. Both, the closing of the Central American Seaway and the constriction of the Indonesian Gateway took place during the Pliocene epoch with far reaching effects on ocean circulation and climate. Here, we present Pliocene upper ocean temperature and salinity reconstructions from the southwestern Pacific ODP Site 590B from 6.5-2.5 Ma. Our data suggest a gradual cooling of ~2°C and freshening of the sea surface during ~4.6-4 Ma with an increased meridional temperature gradient when the closing of the Central American Seaway reached a critical threshold. After ~3.5 Ma, the restricted Indonesian Gateway might have amplified the East Australian Current, allowing enhanced heat transport towards the southwestern Pacific with reduced meridional temperature gradients when the global climate gradually cooled. At the same time our data suggest a cooling and freshening of Subantarctic Mode Water (SAMW) or/and an increased northward flow of SAMW towards Site 590B location, possibly a first step towards the present Antarctic Frontal System.

1. Introduction

Earth’s climate was considerably warmer during the early Pliocene with higher sea level than today and less ice shields in the high northern latitudes (Mudelsee and Raymo, 2005; Dowsett et al., 1996). The tropical warm pool was greatly expanded with a weaker global atmospheric circulation that maintained “permanent El Nino- like” or “El Padre” conditions in the tropical Pacific Ocean (Brierley et al., 2009) with no or less east-west SST gradient and a deep thermocline in the east (Wara et al., 2005). Also, subsurface waters seemed to have been warmer than today with distinctly warmer SST at present eastern boundary upwelling regions

in the (sub)tropics (e.g., Marlow et al., 2000; Lawrence et al., 2006). However, owing to different forcing mechanisms these conditions have not changed synchronously when earth experienced gradual global cooling towards the late Pliocene (Ravelo et al., 2004; Mudelsee et al., 2005). Important driving mechanisms during the Pliocene epoch, which influenced global climate, were the closure and restriction of the Central American and Indonesian Seaways (e.g., Haug et al., 1999; Cane and Molnar et al., 2001; Karas et al., 2009). Whereas the closure of the Central American Seaway had primarily effects on the eastern Pacific tropical thermocline and oceanic heat transport from the Southern to the Northern Hemisphere during the early Pliocene (~4.6-4 Ma; e.g., Haug et al., 1999; Haug et al., 2001, Steph et al., in press) the restriction of the Indonesian Seaway led to a distinct cooling of tropical Indian Ocean subsurface waters and to reduced southward heatflux in the Indian and Atlantic Oceans during the mid-Pliocene (~3.5-3 Ma; Karas et al., 2009; Karas et al., in review, Chapter IV). Modelling studies also suggested changes in the southwest Pacific Ocean, namely a distinct weakening of the warm East Australian Current (EAC) upon closing of the Indonesian Gateway (Hirst and Godfrey, 1993; Godfrey, 1996).

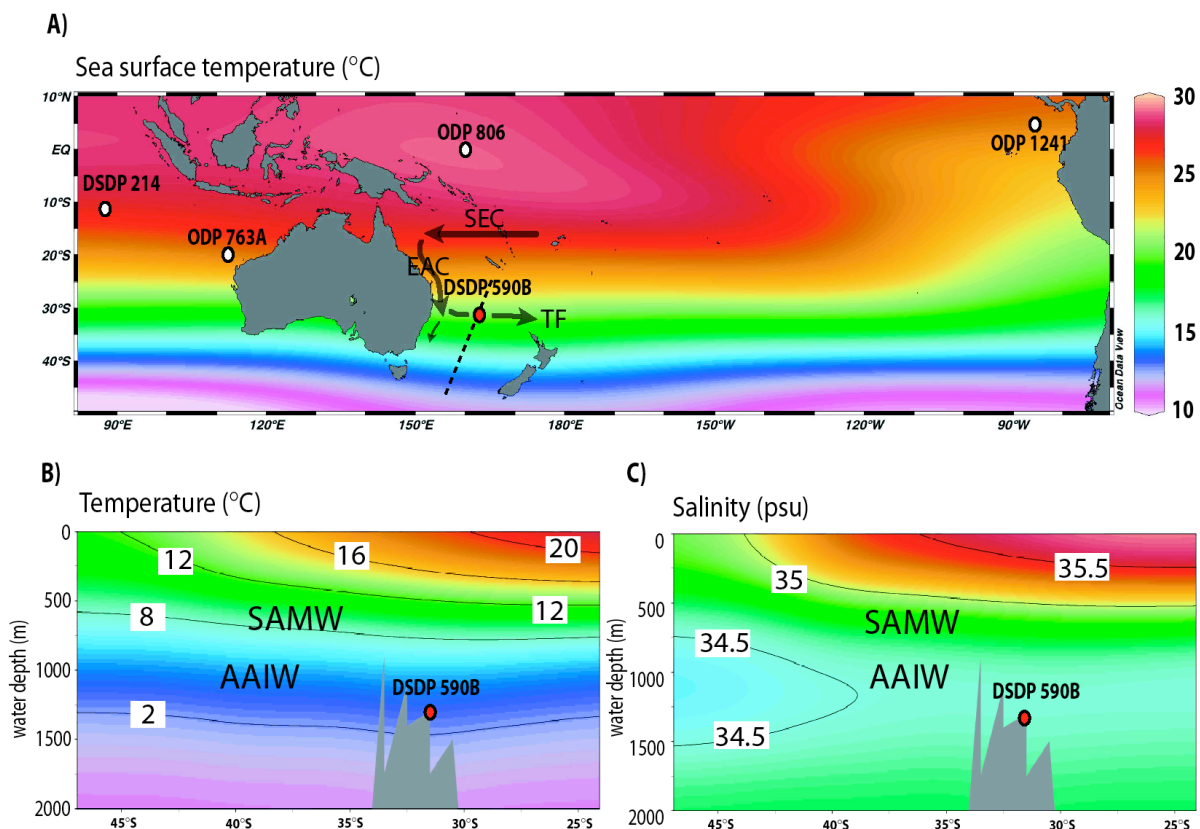


Figure 5.1 (A) Chart of annual ocean temperatures (in °C) at 20 m water depth (Locarnini et al., 2006). Paleooceanographic proxy data were generated for DSDP Site 590B. The South Equatorial Current (SEC), East Australian Current (EAC) and Tasman Front (TF) as well as locations of sediment cores discussed in the text are indicated. Dashed line indicates SW-NE cross-section through Site 590B. Cross sections showing annual temperatures (B) and salinities (C) (Locarnini et al., 2006; Antonov et al., 2006). Site 590B location and water masses are indicated: Antarctic Intermediate Water (AAIW), Subantarctic Mode Water (SAMW).

At modern times the EAC, being a branch of the South Equatorial Current fed the Tasman Front, which is a thermal front separating warm subtropical waters to the north from temperate waters to the south (Stanton, 1981; Elmstrom and Kennett, 1986). This front, which lies just within Site 590B, partially separates from the Australian coast at $\sim 31^\circ$ extending to the North Cape of New Zealand (Fig. 5.1A; Stanton, 1981; Mulhearn et al., 1986). However, some water is occasionally transported along the east coast of Australia towards Tasmania (Hamilton, 2006) forming warm eddies there (Cresswell, 1987). Consequently, together with West Pacific Warm Pool Site 806B (Wara et al., 2005), Site 590B ($31^\circ 10.02'S$; $163^\circ 21.51'E$; 1308 m water depth) is ideally located to infer changes in the meridional heat gradient, which is directly related to changes of the Tasman front and the EAC. At subsurface and bottom depths, Site 590B lies within the influence of fresh and less saline Subantarctic Mode Water (SAMW) and Antarctic Intermediate Water (AAIW), which can be found at ~ 400 -600 m and ~ 500 -1500 m water depth, respectively (Mc Cartney, 1977; Martinez, 1997; Fig. 5.1B, C). For these depths, Site 590B location is useful to infer the development of AAIW and SAMW, which reflect climate variations in the Southern Ocean (Martinez et al., 1997). The importance of these water masses is evident as they spread far into the North Atlantic Ocean (Sloyan and Rintoul, 2001) and are a main source for nutrients (Sarmiento et al., 2003).

Here, we present combined planktonic foraminiferal Mg/Ca and $\delta^{18}O$ data from 6.5 to 2.7 Ma to infer temperature and salinity changes in the (sub)surface layer of southwest Pacific Ocean Site 590B. We selected surface dwelling planktonic foraminifera *Globigerinoides sacculifer* and subsurface dwelling species *Globorotalia crassaformis* (habitat depth of ~ 300 -450 m; Elderfield et al., 2002) indicative for changes related changes in SAMW.

2. Materials and Methods

2.1. Age model

For an initial age control of Site 590B, we selected those magnetic reversal and nannofossil ages (updated to the ATNTS 2004 time scale; Lourens et al., 2004), which were either used or which were very close to the already established depth-age relationship for this site (Grant and Dickens, 2002). To considerably improve the age model during the critical time period of ~ 4.5 -2.7 Ma, when both Indonesian and Central American Gateways had important effects on ocean circulation (Haug et al., 1999; Karas et al., 2009; Steph et al., in press), we generated a benthic $\delta^{18}O_{U. peregriana}$ record with an average resolution of ~ 15 kyr. We then fine-tuned our benthic $\delta^{18}O_{U. peregriana}$ record to the LR04 stack (Lisiecki and Raymo, 2005; Fig. 5.2A) using Analyseries 1.2 (Paillard et al., 1996). Both records show a good

correspondency. The resulting depth/age curve for the entire studied time period matches well to the initial age model based on nannofossil and magnetic reversal ages from Grant and Dickens (2002) (Fig. 5.2B).

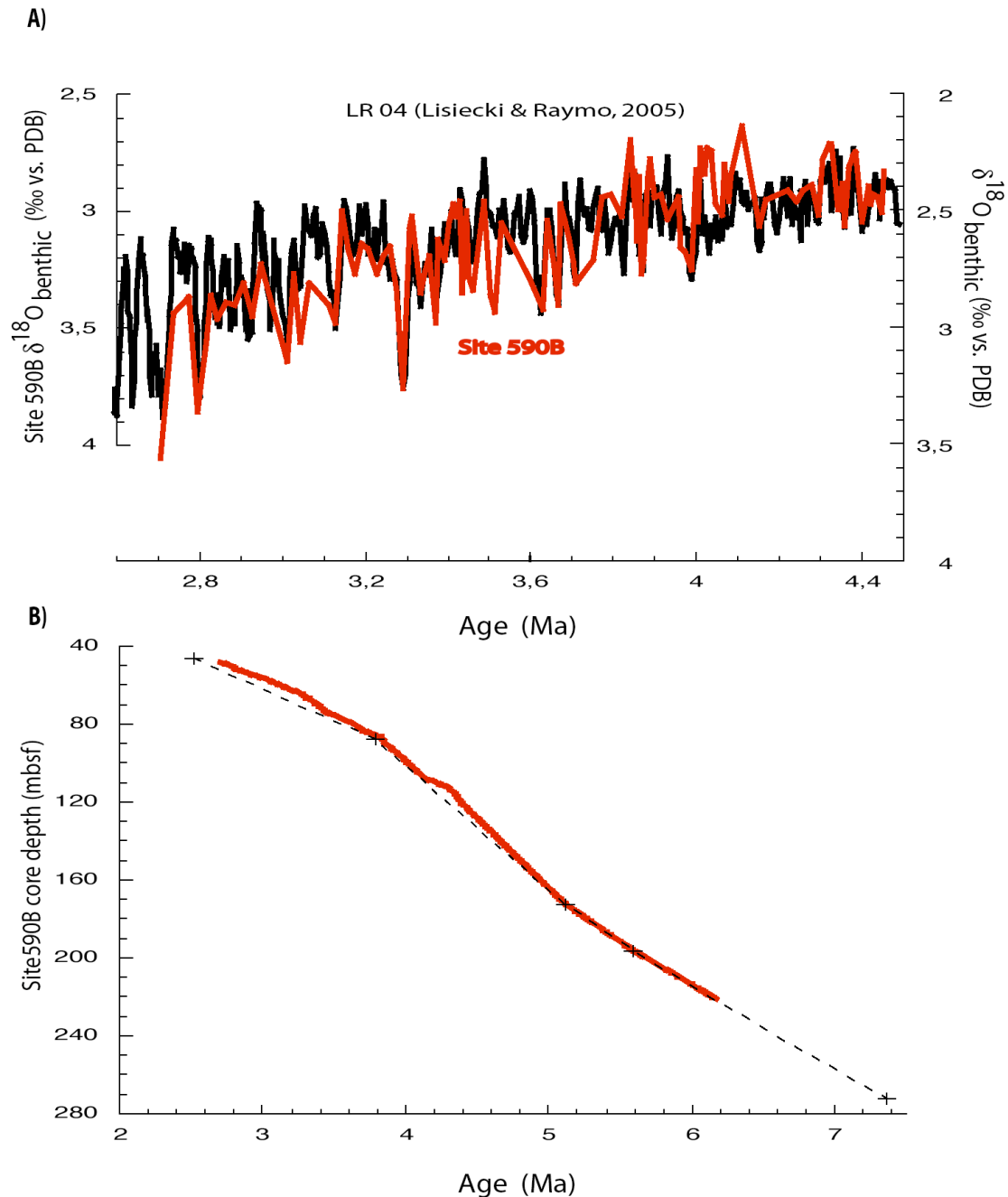


Figure 5.2 Stratigraphic framework of Site 590B. (A) Correlation of the benthic $\delta^{18}\text{O}_{U. peregriana}$ record (black line) from 4.5-2.7 Ma to the benthic LR04 stack (Lisiecki and Raymo, 2005; red line) according for this study. (B) Age/depth relationship of Site 590B (red line). Crosses indicate nannofossil datums (updated to the ATNTS 2004 time scale; Lourens et al., 2004) lying on the previous age model of Grant and Dickens (2002; dashed line).

2.2. Sample preparation and analyses of foraminiferal stable oxygen isotopes and Mg/Ca ratios

Before selection of foraminifera, bulk samples were freeze-dried, weighted and washed over a 63 μm sieve. Dry weights of bulk sediments and the $>63 \mu\text{m}$ fraction were used to calculate weight percentages of the sandfraction. For stable oxygen isotope and Mg/Ca analyses, ~ 30 specimens were selected from shallow dwelling planktonic foraminifera *G. sacculifer* (without sac-like chamber), which calcify in the upper 50 m water depth (Anand et al., 2003). From the deep dwelling planktonic foraminifera *G. crassaformis* (calcification depth of $\sim 300\text{-}450$ m; Elderfield et al., 2002), 20-40 specimens were selected. In a few cases the number had to be reduced to ~ 10 specimens. For benthic isotope stratigraphy 1-4 specimens of *Uvigerina peregrina* were used. Specimens were selected from the narrow 315-355 μm size fraction to avoid size effects in $\delta^{18}\text{O}$ and Mg/Ca (Elderfield et al., 2002). The size fraction was widened to 315-400 μm in a few cases due to insufficient numbers of specimens. Subsequently, sample material was gently crushed, mixed and optically divided into two thirds used for Mg/Ca analyses, and one third for stable isotope measurements. Isotope measurements were either conducted on a Finnigan MAT-252 (at IFM-GEOMAR, Kiel) or on a Finnigan MAT-251 mass spectrometer (at the Leibniz-Laboratory for Radiometric Dating and Stable Isotope Research, Kiel), both equipped with a fully automated carbonate preparation device. Both machines exhibit an analytical precision better than $\pm 0.07\%$ for $\delta^{18}\text{O}$; $\pm \sigma$. All values are reported relative to Pee Dee Belemnite (PDB, based on calibration directly to National Bureau of Standards (NBS-19)).

For Mg/Ca analyses, samples were cleaned according to the established cleaning protocol of Barker et al. (2003) (non reductive). Measurements were performed on a simultaneous, radially viewing ICP-OES (Ciros CCD SOP, Spectro A.I., Germany, Inst. of Geosciences, Univ. of Kiel) with an analytical error for the Mg/Ca ratios of $\sim 0.1\%$. Replicate analysis on the same samples, cleaned and analysed during different sessions, showed a standard deviation of ~ 0.1 mmol/mol (rel. std. dev. $< 3\%$). Monitoring of Fe/Ca and Mn/Ca indicated no contamination with clays or Mn-carbonates after cleaning. Also Fe/Mg values were significantly lower than 0.1 mmol/mol indicative for negligible contamination by silicate phases given by Barker et al. (2003).

2.3. Calculation of $\text{SST}_{\text{Mg/Ca}}$ and meridional temperature gradients

We converted Mg/Ca ratios of *G. sacculifer* into temperatures by using the multispecies calibration of Anand et al. (2003): $\text{Mg/Ca} = 0.38 \exp(0.09 \times \text{SST})$, which is almost identical

to the species-specific equation from Dekens et al. (2002) without the dissolution correction part of that equation. The conversion of *G. crassaformis* Mg/Ca ratios into temperatures was conducted by using a species-specific calibration of Regenberg et al. (2009): $\text{Mg/Ca} = 0.83 \exp(0.082 \times T)$. We did not apply a dissolution correction on our foraminiferal Mg/Ca due to following reasons: First, the Site 590B location (1308 m water depth) is far above the present lysocline in that region (~3100 m water depth; Martinez et al., 1994). Second, core-top studies suggested in general accordance (Dekens et al., 2002; Regenberg et al., 2006) that Mg^{2+} loss first starts below critical ΔCO_3^{2-} levels of ~20 $\mu\text{mol/kg}$, and Site 590B location is above the critical ΔCO_3^{2-} levels of ~20 $\mu\text{mol/kg}$ (data from World Ocean Circulation Experiment-transect P06W were used to calculate ΔCO_3^{2-} levels; Lewis and Wallace, 1998).

To infer the meridional temperature gradient between WPWP Site 806 and Site 590B, which are at comparable longitudes, we calculated a 15 point smooth deviation of both temperature records. We here kept in mind the problems of comparing different Mg/Ca data sets, which include the cleaning techniques applied, the temperature vs. Mg/Ca calibrations used and differences in calcite dissolution. We indeed considered the most important disturbing factor on foraminiferal Mg/Ca, which is calcite dissolution. The other both factors produce constant offsets between various Mg/Ca derived temperature records (e.g., Dekens et al., 2002; Barker et al., 2003; Anand et al., 2003; Regenberg et al., 2009). Consequently, the relative changes between both $\text{SST}_{\text{Mg/Ca}}$ records are neither influenced by using different cleaning methods nor by various calibrations, which we aim to resolve in this study.

2.4. Calculation of $\delta^{18}\text{O}_{\text{ivc-seawater}}$

To assess ancient sea surface salinities from different water depths, we used the combined $\delta^{18}\text{O}$ and Mg/Ca-temperature records from surface and deep dwelling planktonic foraminifera *G. sacculifer* and *G. crassaformis*. These values allowed us to calculate $\delta^{18}\text{O}_{\text{seawater}}$, (Fig. 5.3A) which reflects a combination of ice-volume controlled $\delta^{18}\text{O}_{\text{seawater}}$ changes plus local variations in $\delta^{18}\text{O}_{\text{seawater}}$ due to regional hydrological changes (Shackleton, 1974). Variations in local sea surface salinities expressed as ice volume corrected records ($\delta^{18}\text{O}_{\text{ivc-seawater}}$) were deduced by subtracting an estimation of the Pliocene global ice volume signal. Here we used the benthic $\delta^{18}\text{O}$ record of Lisiecki and Raymo (2005) (Fig. 5.3B), which was normalized to the modern value. The benthic $\delta^{18}\text{O}$ record with its last glacial/interglacial amplitude of ~1.6‰, being in accordance to observations from the east Pacific (Tiedemann et al., 2006), was subsequently reduced to 75% to account for the ~1.2‰

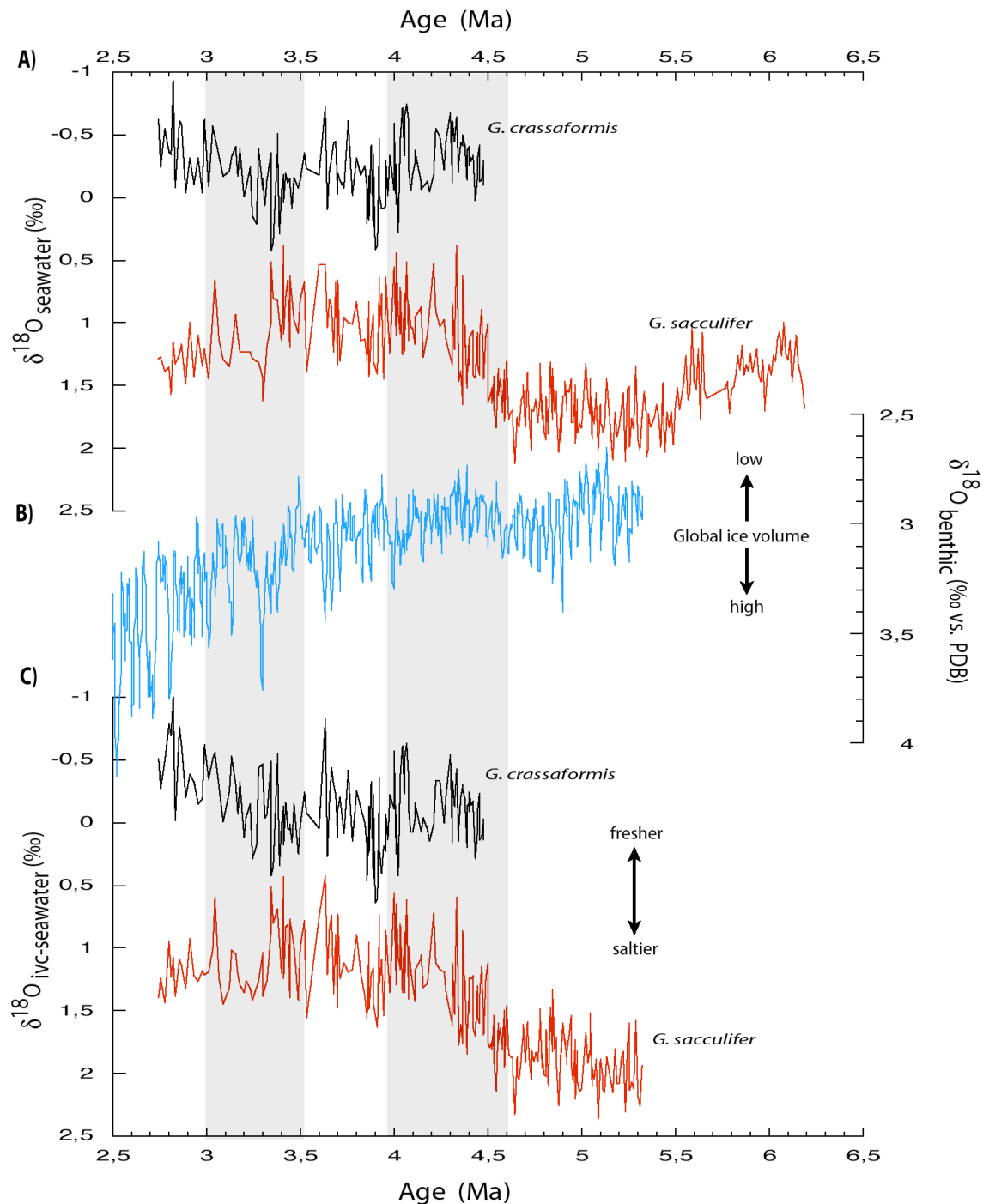


Figure 5.3 Site 590B records of $\delta^{18}\text{O}_{\text{ivc-seawater}}$ as an approximation of sea (sub)surface salinities. (A) *G. sacculifer* (red) and *G. crassaformis* (black) $\delta^{18}\text{O}_{\text{seawater}}$ values calculated according to Shackleton et al. (1974). (B) The benthic LR04 record (Lisiecki and Raymo, 2005) was taken as an appropriate estimation of changes in the global ice volume. (C) The subtraction of our estimation of the global ice volume led to $\delta^{18}\text{O}_{\text{ivc-seawater}}$ records for *G. sacculifer* (red) and *G. crassaformis* (black).

last glacial/interglacial difference in global ice volume. We presuppose that the relationship between global ice volume, sea surface salinity and temperature holds for the Pliocene. Finally, we subtracted the modified benthic $\delta^{18}\text{O}$ record from our $\delta^{18}\text{O}_{\text{seawater}}$ records leading

to $\delta^{18}\text{O}_{\text{ivc-seawater}}$ values (Fig. 5.3C). We are aware that this approach introduces slight errors, but it provides a reliable approximation for calculating ice volume free $\delta^{18}\text{O}$ seawater values for the Pliocene.

3. Results and Discussion

3.1. Mg/Ca derived (sub)surface temperatures and salinities

The $\text{SST}_{\text{Mg/Ca}}$ record from the southwest Pacific Ocean Site 590B shows a gradual warming of $\sim 2^\circ\text{C}$ from the latest Miocene to the early Pliocene at ~ 5 Ma, and then relatively stable $\text{SST}_{\text{Mg/Ca}}$ of $\sim 24\text{--}25^\circ\text{C}$ until ~ 4.5 Ma (Fig. 5.4A). This late Miocene to early Pliocene warming trend is not reflected in the corresponding *G. sacculifer* $\delta^{18}\text{O}$ record, which shows high values of 0 to -0.5‰ . From ~ 4.6 to 4 Ma, when the closing history of the Central American seaway reached a critical threshold (Haug et al., 1999; Steph et al., 2006), we observe a gradual $\text{SST}_{\text{Mg/Ca}}$ cooling of $\sim 2^\circ\text{C}$ towards $\sim 21\text{--}22^\circ\text{C}$. Such temperatures, being the coolest observed during the studied time period are comparable to the modern annual SST of $\sim 21^\circ\text{C}$ (Fig. 5.1A; Locarnini et al., 2006) in the Site 590B region suggesting that most Pliocene $\text{SST}_{\text{Mg/Ca}}$ were commonly warmer than today. Synchronously to the $\text{SST}_{\text{Mg/Ca}}$ drop, *G. sacculifer* $\delta^{18}\text{O}$ values decrease and reach most negative values (Fig. 5.4A). Subsequently the *G. sacculifer* $\delta^{18}\text{O}$ record broadly follows the $\text{SST}_{\text{Mg/Ca}}$ record, which culminates with $\sim 24^\circ\text{C}$ at 3.8–3.5 Ma, and then declines by $\sim 1^\circ\text{C}$ towards 3 Ma.

The Mg/Ca temperature record of the subsurface dwelling *G. crassaformis* broadly varies between 9°C and 15°C showing low temperatures during the early Pliocene between ~ 4.3 Ma and ~ 4 Ma (Fig. 5.4A). In contrast to the $\text{SST}_{\text{Mg/Ca}}$ record, the subsurface Mg/Ca temperatures exhibit a warming trend of $\sim 2^\circ\text{C}$ from ~ 4.2 to 3.8 Ma, with maximum temperatures of $\sim 14\text{--}15^\circ\text{C}$. Most distinctly after ~ 3.5 Ma, Mg/Ca derived temperatures gradually drop to $10\text{--}11^\circ\text{C}$ towards the late Pliocene. In contrast to the *G. sacculifer* $\delta^{18}\text{O}$ record, the *G. crassaformis* $\delta^{18}\text{O}$ record is corresponding to the Mg/Ca derived temperatures, implying that the $\delta^{18}\text{O}$ signal to a large part mirrors past ocean temperatures.

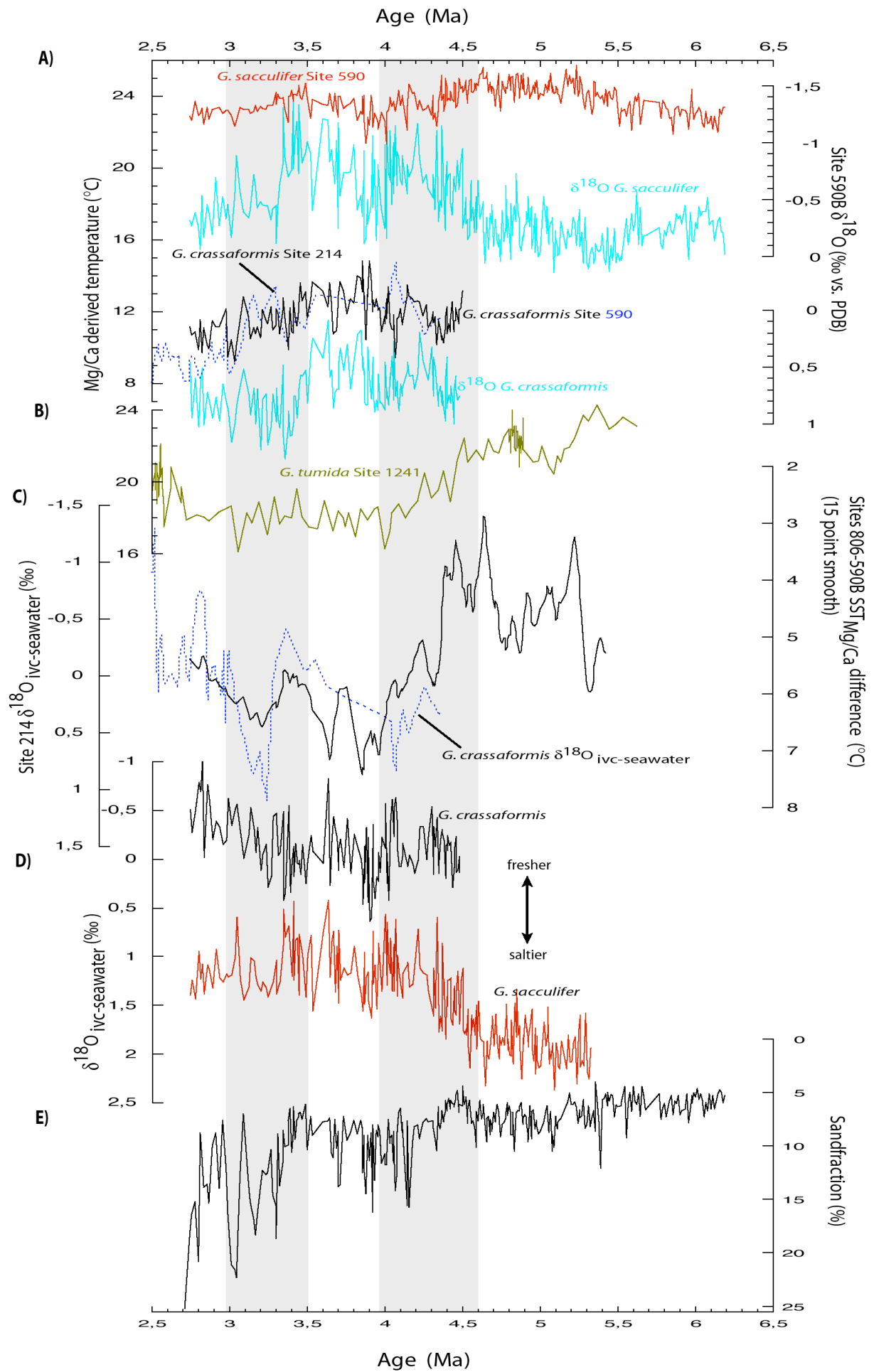
In order to approximate salinity changes in the upper water column, we calculated $\delta^{18}\text{O}_{\text{ivc-seawater}}$ records of *G. sacculifer* and *G. crassaformis* (Fig. 5.4D; see section 2.4). The *G. sacculifer* $\delta^{18}\text{O}_{\text{ivc-seawater}}$ record shows high values during 5.5–4.5 Ma, in line with increasing or high $\text{SST}_{\text{Mg/Ca}}$ pointing to both more saline and warm conditions. This development supports the recent study of Brierley et al. (2009) proposing that during the early Pliocene the meridional temperature differences were clearly reduced with a great expansion

of the tropical warm pool. Apparently, these surface ocean properties seemed to have changed in the southwest Pacific earlier than assumed (Brierley et al., 2009) namely during ~4.6-4 Ma, (Fig. 5.4A, D), synchronously to the closing of the Central American Seaway (Haug et al., 1999; Steph et al., 2009). Since then, *G. sacculifer* $\delta^{18}\text{O}_{\text{ivc-seawater}}$ values are consistently lower by ~1‰ than before (Fig. 5.4D). After ~3.3 Ma, *G. sacculifer* $\delta^{18}\text{O}_{\text{ivc-seawater}}$ values of ~1.2 ‰ tend to more saline conditions. The subsurface *G. crassaformis* $\delta^{18}\text{O}_{\text{ivc-seawater}}$ record, instead, does not suggest considerable changes during the early Pliocene, but slightly saltier conditions between ~4.3 and 3.8 Ma, when Mg/Ca derived subsurface temperatures increase (Fig. 5.4A, D). Most notably after ~3.5 Ma, when there is evidence for a major reorganization in the Indonesian throughflow (Karas et al., 2009; Cane and Molnar 2001), we observe a distinct freshening and cooling in the subsurface layer at southwest Pacific Ocean Site 590B.

3.2 The Central American Seaway and the Tasman Front

From these temporally succeeding events we infer that the hydrography at the Site 590B location was subsequently influenced by both, the Central American and the Indonesian Gateway constrictions. The tectonic closure of the Central American Seaway showed most intensive oceanic impacts during ~4.6-4 Ma (Haug et al., 1999; Steph et al., 2006). It was suggested that during this time, a critical threshold was reached with a significantly restricted Caribbean–Pacific surface water exchange. This induced thermocline shoaling in the equatorial east Pacific (Steph et al., 2006) indicated by subsurface cooling at Site 1241 (Fig. 5.4B; Steph et al., 2006). Early Pliocene thermocline shoaling was also registered at equatorial east Pacific sites 847 and 851 based on *G. sacculifer* and *G. tumida* $\delta^{18}\text{O}$ records (Cannariato and Ravelo, 1997; Chaisson and Ravelo, 2000; Wara et al., 2005). The surface cooling/freshening at Site 590B covaries to the shoaling/cooling of the thermocline at Site 1241 (Fig. 5.4A, B; Steph et al., 2006), although $\text{SST}_{\text{Mg/Ca}}$ records from tropical Pacific Ocean sites 806 and 1241 indicate increasing or high temperatures (Wara et al., 2005; Steph et al., 2006). In consequence, the cooling of the southwest Pacific Site 590B led earlier than assumed to an increased meridional temperature gradient of up to 4°C compared to equatorial West Pacific Site 806 (Fig. 5.4C).

Both, the observed surface cooling/freshening at Site 590B and changes in the depth of the thermocline in the equatorial east Pacific may be related to the oceanographic changes in response to the closing of the Central American Seaway. A model study of Lunt et al. (2008) confirmed that the formation of the Isthmus of Panama could have cooled the Southern



Hemisphere through “heat piracy” of the Northern Hemisphere. This heat piracy was explained in terms of a strengthened Atlantic thermohaline circulation transporting more surface heat to high northern latitudes. The apparent sensitivity of Site 590B to heat piracy from the Northern Hemisphere might have been favoured by the still wide Indonesian Passage during this time (4.6-4 Ma; Karas et al., 2009) with a weak EAC and a reduced southward heat transport in the Tasman Sea area (Godfrey et al., 1996). Under these conditions, the closing of the Central American Seaway might have initiated cooling/freshening of the south Pacific Ocean and in consequence the northward shift of the “Paleo Tasman Front”. Analogous to modern times, relatively cool and fresh waters from the south would have gradually replaced the warmer waters from the north (Andrews et al., 1980). However, some southern Indian and Atlantic Ocean paleoclimatic records do not show a cooling during this time period (Marlow et al., 2000; Karas et al., 2009; Karas et al., in review, Chapter IV), suggesting that this phenomenon was regionally limited and not apparent in the whole Southern Hemisphere. The notion of the northward shift of the Tasman Front is further supported by the increasing coarse carbonate fraction starting at ~4.4 Ma and culminating with maximum values of ~15% at ~4 Ma (Fig. 5.4E). The coarse carbonate fraction is almost entirely composed of foraminiferal shells and most likely reflects an increase in foraminiferal productivity. A change towards enhanced primary productivity at ~4 Ma is also observed at the close-by Site 591 (Gardner et al., 1986). Increasingly high primary productivity at cooler and fresher sea surface conditions is best explained by the northward shift of the Tasman Front with the increasing influence of cool and high-nutrient waters from the south (e.g., Baird et al., 2006). Alternatively, upwelling could have brought cooler and more productive waters to the surface, when the Tasman Front was situated near Site 590B. (e.g., Gardner et al., 1986; Elmstrom and Kennett, 1986). From our point of view, the Tasman Front only occasionally reached the Site 590B location during ~4-3.8 Ma - when SST_{Mg/Ca} were lowest and the subsurface *G. crassaformis* Mg/Ca derived temperatures were increasing (Fig. 5.4A).

◀ **Figure 5.4** Late Miocene to Pliocene proxy records of southwest Pacific Ocean Site 590B in relation to other ocean areas (A) *G. sacculifer* SST_{Mg/Ca} (red) and subsurface *G. crassaformis* Mg/Ca derived temperatures (black) as well as corresponding $\delta^{18}\text{O}$ values (light blue). Dashed line indicates the *G. crassaformis* Mg/Ca derived subsurface temperatures from equatorial eastern Indian Ocean Site 214 (Karas et al., 2009). (B) *G. tumida* Mg/Ca derived subsurface temperatures from Site 1241 (Steph et al., 2009). (C) SST_{Mg/Ca} difference (black line; 15 point smooth) between Site 590B and West Pacific Warm Pool Site 806B (Wara et al., 2005). Also shown is the $\delta^{18}\text{O}_{\text{IVC-seawater}}$ record from Site 214 (Karas et al., 2009). (D) *G. sacculifer* (red) and *G. crassaformis* (black) $\delta^{18}\text{O}_{\text{IVC-seawater}}$ values from Site 590B. (E) Site 590B sandfraction data.

The small temperature difference between the surface and the subsurface layer during this time interval suggests a deeper thermocline and hence, deep reaching eddies, which could have mixed the upper water column (Grant and Dickens, 2002), typical for the Tasman Front region (e.g., Baird et al., 2008). We denote, however, that the Tasman Front did not cross the Site 590B location (Fig. 5.4A), as $SST_{Mg/Ca}$ remained equal or even higher during $\sim 4.6-4$ Ma relative to today's conditions.

3.3. Indonesian Gateway dynamics: Effects on the EAC and Mode Water variability

After ~ 3.8 Ma, the Tasman Front removed southward of the Site 590B location, indicated by increasing $SST_{Mg/Ca}$ and a gradually declining meridional $SST_{Mg/Ca}$ gradient between tropical Site 806 and subtropical Site 590B (Fig 5.4A, C). The warming trend starting at ~ 3.8 Ma was presumably triggered by different mechanisms. First, the primary oceanic and climatic effects from the closing Central American Seaway terminated (Haug et al., 1999; Steph et al., 2006), which might have allowed a slight warming trend during a globally warm climate. Second, starting at 3.8 Ma subsurface freshening in the equatorial eastern Indian Ocean (Site 214) initiated by a throughflow change in the Indonesian Gateway (Karas et al., 2009) is accompanied by the decreasing meridional SST gradient between Sites 806 and 590B (Fig. 5.4C). In consequence, the tectonic restriction of the Indonesian Gateway might have amplified the EAC and hence, relative warming of Site 590B. The EAC, which today effectively triggers the position of the Tasman Front (Stanton, 1981; Kennett, 1986) is quite sensitive to changes in the Indonesian Throughflow. Model simulations, indeed, suggest a strengthening of the EAC upon closing the Indonesian Throughflow (Godfrey et al., 1996). We therefore suppose that mainly after ~ 3.5 Ma, the strengthened EAC maintained the relative high $SST_{Mg/Ca}$ at Site 590B and reduced the meridional SST gradient towards the West Pacific Warm Pool Site 806, when the global climate gradually cooled with the onset of a significant meridional temperature gradient in the subtropical south Indian Ocean (Ravelo et al., 2004; Brierley et al., 2009; Karas et al., 2009). In this respect, the trend to more saline surface conditions since ~ 3.3 Ma at Site 590B might be related to a still strong influence of the EAC transferring saline and warm waters from the Coral Sea southward, when surface Indonesian Throughflow waters became increasingly restricted (Karas et al., 2009; Karas et al., in review, Chapter IV).

In contrast to the surface layer, the subsurface water masses at Site 590B exhibit a gradual cooling/freshening trend since 3.5 Ma inline to subsurface cooling and freshening at equatorial eastern Indian Ocean Site 214 (Fig. 5.4A, C, D; Karas et al., 2009). The subsurface

Mg/Ca temperatures from Site 590B, however, show a more gradual decline than at Site 214 with at least $\sim 2^{\circ}\text{C}$ warmer temperatures after $\sim 3\text{Ma}$, when the change in subsurface flow through the Indonesian Gateway from the South Pacific to the North Pacific finalized (Fig. 5.4A; Karas et al., 2009). The simultaneous subsurface cooling and freshening trend since $\sim 3.5\text{ Ma}$ at Site 590B rather implies the increasing dominance of northward expanding SAMW or/and a cooling and freshening of SAMW itself. Today, the fresh and cool SAMW is at $\sim 400\text{-}600\text{ m}$ water depths north of the Subantarctic Front (Fig. 5.1B, C; Mc Cartney, 1977; Martinez, 1997) which is within the presumed depth habitat of *G. crassaformis* (Elderfield et al., 2002: $\sim 300\text{-}450\text{ m}$).

Support for the overtaking presence of highly dynamic intermediate water masses stems from the increasing portion of sand by $\sim 15\%$ in Site 590B since $\sim 3.5\text{ Ma}$ (Fig. 5.4E), also seen at other sites from Lord Howe Rise (Stein et al., 1986; Gardner et al., 1986) and best explained in terms of sediment winnowing. At Site 590B, which is well-bathed within AAIW ($\sim 500\text{-}1500\text{ m}$ water depth; Martinez, 1997; Fig. 5.1B, C), the coarsening of the sediment suggests the ongoing northward migration of AAIW. As today, SAMW and AAIW are closely related (Martinez, 1997), SAMW waters most likely followed the northward migration of AAIW since $\sim 3.5\text{ Ma}$. Cooling and freshening of SAMW, as indicated by subsurface salinity and temperature changes at Site 590B, most likely resulted from a climatic change in the formation area of SAMW and AAIW, which today is located between the Polar Front and the Subtropical Front in the Southern Ocean (McCartney, 1977; Sarmiento et al., 2003) during winter (Sarmiento et al., 2003). Cooling of the SAMW/AAIW formation area would have changed the meridional heat gradient and hence, would have changed Southern Hemisphere atmospheric circulation (Ribbe, 2001). The Antarctic Frontal System with its westerly wind field, in fact, is essential for the formation and widespread dispersal of Mode Waters (Ribbe, 2001; Liu et al., 2008). Such conditions might have started since $\sim 4\text{ Ma B.P.}$ when earth climate began to cool (Ravelo et al., 2004).

The reduced heat transport into the southern Indian Ocean caused by the change in Indonesian Throughflow (Karas et al., in review, Chapter IV) could have served as a viable mechanism for cooling the southern latitude ocean areas and for the northward migration of SAMW/AAIW during the critical time span from $3.5\text{-}3\text{ Ma}$, when there is evidence for less global ice volume (Lisieki and Raymo, 2005; Mudelsee et al., 2005; Raymo et al., 2006). SST reconstructions from the southern Indian and Atlantic ocean areas indeed suggest a cooling of $\sim 2^{\circ}\text{C}$ during this time period (Karas et al., in review, Chapter IV; Etourneau et al., 2009). These findings are further supported by modelling studies showing that a blocked Indonesian

Throughflow might have caused cooling of up to 1°C of a large ocean area reaching from Australia to southern Africa between ~55°S and 30°S, where Mode Waters form today (Hirst and Godfrey, 1993; Godfrey, 1996). Hence, the reconstructed cooling of Indonesian Throughflow subsurface waters in the equatorial eastern Indian Ocean (Karas et al., 2009) might have contributed to the cooling of the southern Indian and Atlantic oceans through mixing and upwelling processes (Karas et al., 2009; Karas et al., in review, Chapter IV). Cooling of the subtropical and high southern latitude ocean areas would have amplified the meridional temperature gradients and the Hadley cells leading to the strengthening and possibly to the northward shift of the westerly wind belt. These oceanographic and atmospheric modifications might have been a first step towards the present Antarctic Frontal System and in consequence, the northward circulation of Mode Waters.

4. Conclusions

Our proxy results on DSDP Site 590B shed light on the climatic evolution of the southwest Pacific Ocean from the late Miocene to the late Pliocene. We found a gradual cooling of ~2°C and freshening of the sea surface during ~4.6-4 Ma with increasing meridional temperature gradients when the closing of the Central American Seaway reached a critical threshold (Haug et al., 1999). The Tasman Front migrated northward, in close temporal correspondence to the closing of the Central American Seaway, and favoured by the still wide –open Indonesian Seaway, which apparently led to a cooling of the southwest Pacific through heat piracy by the Northern Hemisphere (e.g., Lunt et al., 2008). The northward migrating Tasman Front started to return southward since ~3.8 Ma, presumably related to the ceased oceanic and climatic effects from the closed Central American Seaway and early influences from the Indonesian Gateway (Haug et al., 1999; Steph et al., 2006; Karas et al., 2009). We argue that mainly after ~3.5 Ma, the ongoing restriction of the Indonesian Gateway might have amplified the southward heading EAC, allowing enhanced heat transport towards the Site 590B location, and there maintaining the relative warm SST. This allowed reduced meridional temperature gradients when the global climate gradually cooled (Ravelo et al., 2004), synchronously to the development of significant meridional temperature gradients in the subtropical south Indian Ocean (Karas et al., in review, Chapter IV). In contrast to the surface ocean, subsurface water masses at Site 590B gradual cooled/freshened since ~3.5 Ma, in line with a marked increase in the sandfraction pointing to the increasing dominance of SAMW/AAIW. We suspect that the continuous restriction of the Indonesian Seaway might have contributed through cooling of the southern Indian and

Atlantic oceans (Karas et al., 2009; Karas et al., in review, Chapter IV) to the development of the present Antarctic Frontal System with stronger westerly winds leading to a cooling and or/northward migration of Mode Waters.

Acknowledgements

Samples for this study were provided by the IODP. Funding of this research was provided by the German Science Foundation (DFG) within project Nu60/14-2. We thank N. Gehre, K. Kiesling, L. Haxhijaj, A. Bahr and M. Regenberg, for valuable comments and technical support.

References

- Anand, P., H. Elderfield, and M. H. Comte (2003), Calibration of Mg/Ca thermometry in planktonic foraminifera from a sediment trap time series, *Paleoceanography*, 18, doi:10.1029/2002PA000846.
- Andrews, J. C., M. W. Lawrence, and C. S. Nilsson (1980), Observations of the Tasman Front, *J. Phys. Oceanogr.* 10, 1854-1869.
- Antonov, J. I., R. A. Locarnini, T. P. Boyer, A. V. Mishonov, and H. E. Garcia (2006), World Ocean Atlas 2005, vol. 2, Salinity, NOAA Atlas NESDIS, vol. 62, S. Levitus Ed., (U.S. Government Printing Office, Washington, D.C., 2006) 182 pp.
- Baird, M., P. G. Timko, J. H. Middleton, T. J. Mullaney, D. R. Cox, and I. M. Suthers (2008), Biological properties across the Tasman Front off southeast Australia, *Deep-Sea Res. I* 55, 1438-1455.
- Barker, S., M. Greaves, and H. Elderfield (2003), A study of cleaning procedures used for foraminiferal Mg/Ca paleothermometry, *Geochem., Geophys., Geosyst.*, 4 (9), doi:10.1029/2003GC000559.
- Brierley, C. M., A. V. Fedorov, Z. Liu, T. D. Herbert, K. T. Lawrence, and J. P. LaRiviere (2009), Weakened Hadley Circulation and Greatly Expanded Tropical Warm Pool in the Early Pliocene. *Science* 323, 1714-1718.
- Cane, M., and P. Molnar (2001), Closing of the Indonesian seaway as a precursor to east African aridification around 3-4 million years ago, *Nature*, 411, 157-162.
- Cannariato, K. G., and A. C. Ravelo (1997), Pliocene-Pleistocene Evolution of Eastern Tropical Pacific Surface Water Circulation and Thermocline Depth, *Paleoceanography* 12(6), 805-820.

- Chaisson, W., and A. C. Ravelo (2000), Pliocene development of the East-West hydrographic gradient in the Equatorial Pacific. *Paleoceanography* 15, 497-505.
- Cresswell, G. (1987), The East Australian Current. CSIRO Mar. Lab. Inf. Sheet, 3.
- Dekens, P. S., D. W. Lea, D. K. Pak, and H. J. Spero (2002), Core top calibration of Mg/Ca in tropical foraminifera: Refining paleotemperature estimation, *Geochem., Geophys., Geosyst.*, 3, doi: 10.1029/2001GC000200.
- Dowsett, H., J. Barron, and R. Poore (1996), Middle Pliocene sea surface temperatures: a global reconstruction, *Mar. Micropaleontol.* 27, 13-26.
- Elderfield, H., M. Vautravers, and M. Cooper (2002), The relationship between shell size and Mg/Ca, Sr/Ca, $\delta^{18}\text{O}$, and $\delta^{13}\text{C}$ of species of planktonic foraminifera, *Geochem., Geophys., Geosyst.*, 3, doi: 10.1029/2001GC000194.
- Elmstrom, K. M., and J. P. Kennett (1986), Late Neogene paleoceanographic evolution of site 590: Southwest Pacific. In: Kennett, J. P., C. C. von der Borch, et al., Eds., in Initial Reports of the DSDP, U.S. Government Printing Office, Washington D.C., pp. 1361-1381.
- Etourneau, J., P. Martinez, T. Blanz, and R. Schneider (2009), Pliocene-Pleistocene variability of upwelling activity, productivity, and nutrient cycling in the Benguela Region, *Geology*, 37, 871-874, doi: 10.1130/G25733A.1.
- Gardner, J. V., W. E. Dean, L. Bisagno, and E. Hemphill (1986), Late Neogene and Quaternary coarse-fraction and carbonate stratigraphies for Site 586 on Ontong-Java Plateau and Site 591 on Lord Howe Rise. In: Kennett, J. P., C. C. von der Borch et al., Eds., in Init. Repts. DSDP, 90: Washington (U.S. Govt. Printing Office).
- Godfrey, J. S. (1996), The effect of the Indonesian Throughflow on ocean circulation and heat exchange with the atmosphere: A review, *J. Geophys. Res.* 101, 12217-12237.
- Grant, K. M., and G. R. Dickens (2002), Coupled productivity and carbon isotope records in the southwest Pacific Ocean during the late Miocene-early Pliocene biogenic bloom, *Palaeogeogr., Palaeoclim., Palaeoecol.* 187, 61-82.
- Hamilton, L. J. (2006), Structure of the Subtropical Front in the Tasman Sea. *Deep-Sea Res. I*, 53, 1989-2009.
- Haug, G. H., D. M. Sigman, R. Tiedemann, T. F. Pedersen, and M. Sarnthein (1999), Onset of permanent stratification in the subarctic Pacific, *Nature* 401, 779-782.
- Haug, G. H., R. Tiedemann, R. Zahn, and A. C. Ravelo (2001), Role of Panama uplift on oceanic freshwater balance, *Geology* 29, 207-210.
- Hirst, A. C., and J. S. Godfrey (1993), The role of Indonesian Throughflow in a Global Ocean GCM, *J. Phys. Oceanogr.*, 23, 1057-1086.

- Karas, C., D. Nürnberg, A. K. Gupta, R. Tiedemann, K. Mohan, and T. Bickert (2009), Mid-Pliocene climate change amplified by a switch in Indonesian subsurface throughflow, *Nature Geoscience*, 2, 434-438.
- Lawrence, K. T., Z. Liu, T. D. Herbert (2006), Evolution of the eastern tropical Pacific through Plio-Pleistocene glaciation, *Science* 312, 79-83.
- Lewis, E., and D. W. R. Wallace (1998), co2sys -Program Developed for CO2System Calculations, oRNL/CDIAC-105, Carbon Dioxide Information Analysis Center, Oak Ridge Natl. Lab., (U.S. Dep. of Energy, Oak Ridge, Tenn., 1998).
- Lisiecki, L. E., and M. E. Raymo (2005), A Pliocene-Pleistocene stack of 57 globally distributed benthic $\delta^{18}\text{O}$ records, *Paleoceanography*, 20, PA1003, doi:10.1029/2004PA001071.
- Liu, Z., M. A. Altabet, and T. D. Herbert (2008), Plio-Pleistocene denitrification in the eastern tropical North Pacific: Intensification at 2.1 Ma. *Geochem., Geophys., Geosyst.* 9 (11), Q11006. doi:10.1029/2008GC002044.
- Locarnini, R. A. et al. (2006), *World Ocean Atlas 2005*, Vol. 1: Temperature. S. Levitus, Eds. NOAA Atlas NESDIS 61, (U.S. Gov. Printing Office, Washington, D.C., 2006) 182 pp.
- Lourens, L. J. et al. (2004), in *A Geologic Time Scale 2004*: Cambridge. Gradstein, F.M., J. Ogg et al., Eds. (Cambridge Univ. Press, 2004), Appendix 2.
- Lunt, D. J., P. J. Valdes, A. Haywood, and I. C. Rutt (2008), Closure of the Panama Seaway during the Pliocene: implications for climate and Northern Hemisphere glaciation, *Clim. Dyn.* 30, 1-18. doi:10.1007/s00382-007-0265-6.
- Marlow, J. R., C. B. Lange, G. Wefer, and A. Rosell-Melé (2000), Upwelling intensification as part of the Pliocene-Pleistocene climate transition, *Science*, 290, 2288-2291.
- Martinez, J. I. (1994), Late Pleistocene palaeoceanography of the Tasman Sea: Implications for the dynamics of the warm pool in the western Pacific, *Palaeogeogr., Palaeoclim., Palaeoecol.* 112, 19-62.
- Martinez, J. I. (1997), Decreasing influence of Subantarctic Mode Water north of the Tasman Front over the past 150 kyr, *Palaeogeogr., Palaeoclim., Palaeoecol.* 131, 355-364.
- McCartney, M. S. (1977), Subantarctic Mode Water, in Angel, M., Ed., *A Voyage of Discovery*. Pergamon, Oxford, pp. 103-119.
- Mudelsee, M., and M. E. Raymo (2005), Slow dynamics of the Northern Hemisphere glaciation. *Paleoceanography*, 20, PA4022, doi:10.1029/2005PA001153.

- Mulhearn, P. J., J. H. Filloux, F. E. M. Lilley, N. L. Bindoff, and I. J. Fergusson (1986), Abyssal currents during the formation and passage of a warm-core ring in the East Australian Current, *Deep-Sea Res.* 33, 1563-1576.
- Paillard, D., L. Labeyrie, and P. Yiou (1996), Macintosh program performs time-series analysis, *Eos, Transactions AGU*, 77, 379.
- Ravelo, A. C., D. H. Andreasen, M. Lyle, A. O. Lyle, and M. W. Wara (2004), Regional climate shifts caused by gradual global cooling in the Pliocene epoch, *Nature*, 429, 263-267.
- Raymo, M. E., L. E. Lisiecki, and K. H. Nisancioglu (2006), Plio-Pleistocene Ice Volume, Antarctic Climate, and the Global $\delta^{18}\text{O}$ Record, *Science* 313, 492-495.
- Regenberg, M., D. Nürnberg, S. Steph, J. Groeneveld, D. Garbe-Schönberg, R. Tiedemann, and W.-C. Dullo (2006), Assessing the effect of dissolution on planktonic foraminiferal Mg/Ca ratios: Evidence from Caribbean core tops, *Geochem., Geophys., Geosyst.*, 7, doi: 10.1029/2005GC001019.
- Regenberg, M., S. Steph, D. Nürnberg, R. Tiedemann, and D. Garbe-Schönberg (2009), Calibrating Mg/Ca ratios of multiple planktonic foraminiferal species with $\delta^{18}\text{O}$ -calcification temperatures: Paleothermometry for the upper water column, *Earth Planet. Sci. Lett.*, 278, 324-336, doi:10.1016/j.epsl.2008.12.019.
- Ribbe, J. (2001), Intermediate Water Mass production controlled by southern hemisphere winds, *Geophys. Res. Lett.* 28, 535-538.
- Sarmiento, J. L., N. Gruber, M. A. Brzezinski, and J. P. Dunne (2003), High-latitude controls of thermocline nutrients and low latitude biological productivity, *Nature* 427, 56-60.
- Shackleton, N. J. (1974), Attainment of isotopic equilibrium between ocean water and the benthonic foraminifera genus *Uvigerina*: isotopic changes in the ocean during the last glacial, *Colloq. Int. Cent. Natl. Rech. Sci.* 219, 203-209.
- Sloyan, B. M., and S. R. Rintoul (2001), Circulation, Renewal and Modification of Antarctic Mode and Intermediate Water, *J. Phys. Oceanogr.* 31, 1005-1030.
- Stanton, B. R., (1981) An oceanographic survey of the Tasman Front. New Zealand. *J. Mar. Freshw. Res.* 15, 289-297.
- Stein, R. (1986), Late Neogene evolution of paleoclimate and paleoceanic circulation in the Northern and Southern Hemispheres, *Geologische Rundschau* 75/1, 125-138.
- Steph, S., R. Tiedemann, J. Groeneveld, A. Sturm, and D. Nürnberg (2006), Pliocene changes in tropical east Pacific upper ocean stratification: response to tropical gateways? In *Proc.*

ODP, Sci. Results, 202 Tiedemann, R., A. C. Mix, C. Richter, and W.F. Ruddiman, Eds. (College Station, TX 2006) pp. 1–51.

Steph, S., R. Tiedemann, M. Prange, J. Groeneveld, M. Schulz, A. Timmermann, D. Nürnberg, C. Rühlemann, C. Saukel, and G. Haug 2009, Early Pliocene increase in thermohaline overturning preconditioned the development of the modern equatorial Pacific cold tongue, *Paleoceanography* (in press).

Tiedemann, R., A. Sturm, S. Steph, S. P. Lund, and J. S. Stoner (2006), Astronomically calibrated timescales from 6 to 2.5 Ma and benthic isotope stratigraphies, Sites 1236, 1237, 1239 and 1241, in Tiedemann, R., A. C. Mix, C. Richter, and W. F. Ruddiman, Eds., *Proceedings of the Ocean Drilling Program, Sci. Res. 202*.

Wara, M. W., A. C. Ravelo, and M. L. Delaney (2005), Permanent El Niño-Like Conditions During the Pliocene Warm Period, *Science*, *309*, 758-761.

Chapter VI

General conclusions and perspectives

General Conclusions

This study reconstructed Pliocene (6-2 Ma) surface and subsurface foraminiferal Mg/Ca derived temperatures and changes in paleosalinity (expressed as $\delta^{18}\text{O}_{(\text{ivc-})\text{seawater}}$) from Indian Ocean DSDP/ODP sites 214, 709C, 763A and Pacific Ocean DSDP Site 590B. The results shed new light on the sequence of events associated with the transition from the early Pliocene warm period towards the late Pliocene cooling. This study in fact deciphered the role of the narrowing Indonesian Gateway on climate and ocean circulation during the mid-Pliocene and provided for the first time a well-founded basis to test various model studies, which predicted oceanographic changes due to the constriction of the Indonesian Gateway (e.g., Godfrey, 1996; Rodgers et al., 2000; Cane and Molnar, 2001). Furthermore, this study differentiated between oceanographic effects resulting from the closing Central American Seaway during the early Pliocene, and the constriction of the Indonesian Gateway during the mid-Pliocene. The discoveries made here further underlined the importance of subsurface water masses in the climate system.

Here, I briefly summarize the main conclusions presented in the chapters before and give some perspectives for future studies:

- The proxy results from tropical eastern Indian Ocean Site 214 support the hypothesis of Cane and Molnar (2001) that the constriction of the Indonesian Seaway (4-3 Ma) led to a major reorganization in the ITF. Although the proposed drop in tropical eastern Indian Ocean SST was not found, the subsurface level revealed a pronounced cooling of $\sim 4^\circ\text{C}$ and freshening from ~ 3.5 -2.95 Ma pointing to a switch in ITF source waters from initially South Pacific to North Pacific (Fig. 6.1). The cooled tropical Indian Ocean subsurface waters and the associated changes in the thermocline might have preconditioned the cooling of the Benguela Upwelling system in the southwest Atlantic at ~ 3.2 Ma, and contributed to the global cooling of the thermocline. It was further speculated that the plate tectonic constellation of the Indonesian region after 2.95 Ma allowed for bringing a larger portion of Subantarctic Mode Water via “ocean tunnels” into the Equatorial Undercurrent of the Pacific, thereby supporting the final formation of the equatorial east Pacific cold tongue.

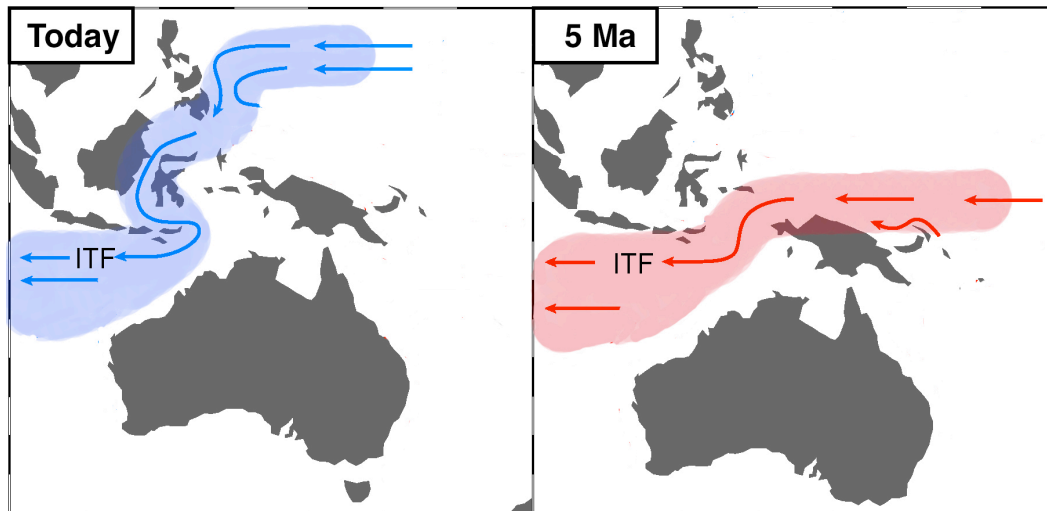


Figure 6.1 Schematic pattern of subsurface ITF for today and 5 Ma. Scenarios are based on model studies (Rogers et al., 1999; 2000; Cane and Molnar, 2000). ITF=Indonesian Throughflow.

- Since ~3.3 Ma, significant surface cooling of Leeuwin Current Site 763A compared to tropical Indian Ocean Sites 214 and 709C was registered, which was interpreted in terms of a weakened Leeuwin Current. It was suggested that the Leeuwin current weakened due to the tectonically reduced surface ITF, which led in agreement to model studies (e.g., Hirst and Godfrey 1993; Godfrey, 1996) to a diminished poleward heat transport and to a cooling of the Benguela Upwelling System. This mechanism might have amplified the mid-Pliocene development towards increased meridional temperature differences (Brierley et al., 2009) in the Southern Hemisphere. In consequence, a reduced poleward heat transport would have induced stronger westerly winds, leading to the development of the present Antarctic Frontal System with an increased northward flow of AAIW/SAMW (Fig. 6.2).
- At the southwest Pacific Ocean Site 590B, a gradual cooling of ~2°C and freshening of the sea surface was detected pointing to a northward shifting of the Tasman Front during ~4.6-4 Ma, synchronous to the closing of the Central American Seaway. The closing of the Central American Seaway was described as a viable mechanism for cooling the southwest Pacific through heat piracy of the Northern Hemisphere when the Indonesian Gateway was still wide-open. After ~3.5 Ma, the restricted Indonesian Gateway might have amplified the EAC, allowing enhanced heat transport towards southwestern Pacific Site 590B, maintaining relative warm SST there. In contrast, the

subsurface level of Site 590B shows a gradual cooling/freshening trend since ~3.5 Ma, suggesting an increasing northward circulation of SAMW/AAIW, indicative for the development of the present Antarctic Frontal System (Fig. 6.2).

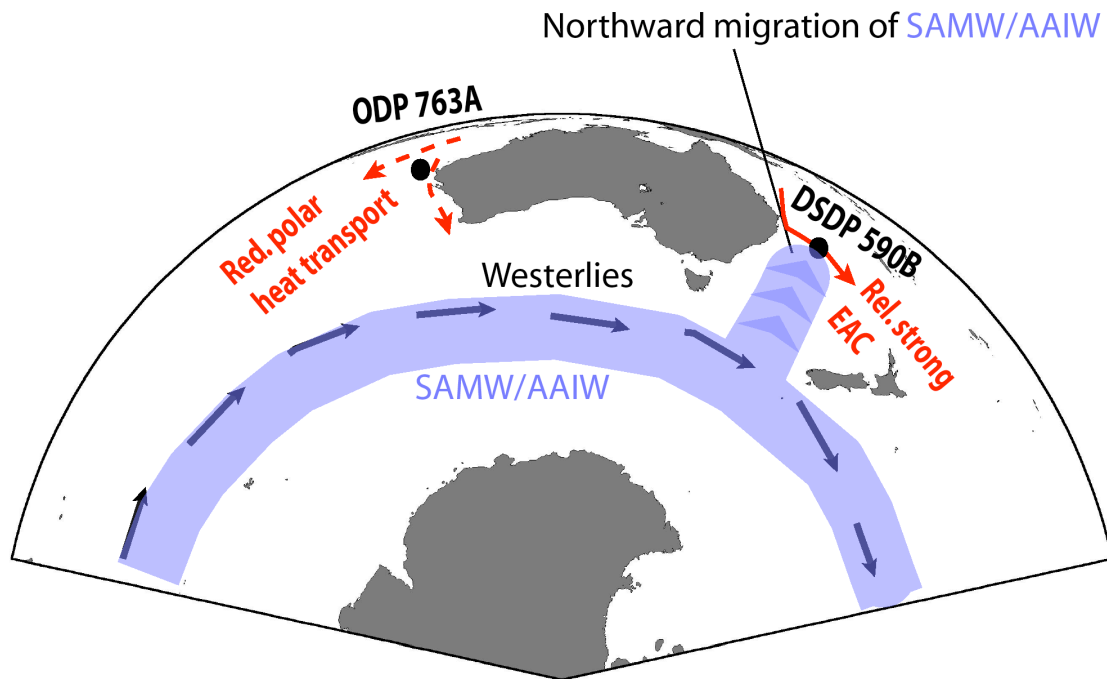


Figure 6.2 Schematic pattern of intensified northward migration of Subantarctic Mode Water (SAMW) and Antarctic Intermediate Water (AAIW) during the mid-Pliocene. Surface currents (red) affected due to the restricted Indonesian Gateway and location of Site 590B (black) are indicated. EAC= East Australian Current. For further explanation see text.

Perspectives

Future studies should concentrate on proving the findings of this study in a better spatial resolution and should differentiate between effects from the narrowed Indonesian Gateway and other climatic drivers like the “global” cooling trend over the last 4 Million years (Ravelo et al., 2004). Hence, two strategies appear most important: First, the selection of more suitable core sites and the generation of proxy records at potentially sensitive regions influenced by the narrowed gateway. Second, the development of sophisticated model simulations, showing the oceanographic and climatic impacts of the narrowed seaway. Especially, the first strategy could confirm the hypothesis of a switched ITF by reconstructing changes in the subsurface level at high northern latitudes and at tropical locations in the west Pacific Ocean. This would bring more information on how North Pacific subsurface waters developed during the closing history of the Indonesian Gateway. The second strategy of developing high-resolution ocean

circulation models was already stimulated by this study, the preliminary results of which indeed verified important parts of the conclusions presented here (Krebs-Kanzow et al., in prep.). The Kiel Climate Model (KCM) predict a robust cooling of the subsurface waters near the tropical eastern Indian Ocean Site 214 upon closing the Indonesian Gateway (Figs 6.3, 6.4). The climate simulation was improved by a higher geographical resolution (up to $2^\circ \times 0.5^\circ$ in the Indonesian region) and a longer run time (1000 years) compared to former model studies (e.g., Rodgers et al., 2000; Jochum et al., 2009; with run times between 30 and 250 years). In particular, the need for higher resolution in coupled ocean climate models became evident as the coarse resolution study of Jochum et al. (2009) described the entire ITF just by one grid point in their simulations. With the northward drift of New Guinea, this study showed miniscule ocean temperature changes with opposite patterns than all former model studies (e.g., Rodgers et al., 2000; Cane and Molnar, 2001) and the paleoceanographic evidences of this study.

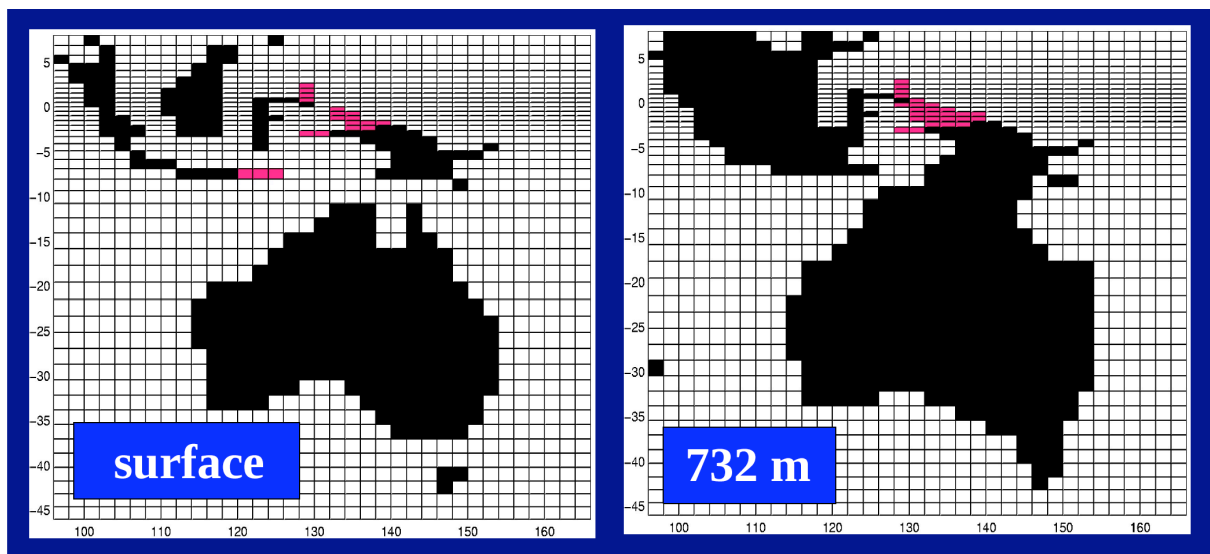


Figure 6.3 Coastline and bathymetry in Kiel Climate Model for Pliocene and modern conditions at surface (left) and at deep water depths (right). Note that the red indicated landmass is removed during Pliocene conditions, opening the Seaway to the south (Krebs-Kanzow et al., in prep.).

We therefore need more high-resolution ocean models that also incorporate Pliocene climate conditions to further test the effects of the narrowed gateway on surface currents like the warm Leeuwin current off western Australia and changes in precipitation at adjacent land areas.

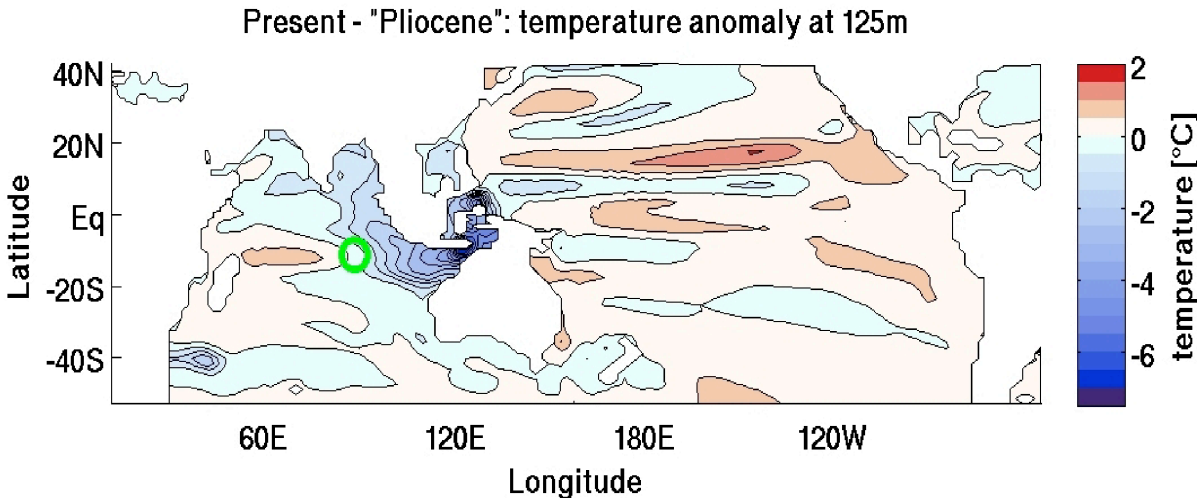


Figure 6.4 Modelled differences in ocean temperatures at 125m water depth for Pliocene and modern conditions (Krebs-Kanzow et al., in prep.). Note distinct cooling in the equatorial eastern Indian Ocean near Site 214 (red circle).

References for chapters I, II and VI

- Anand, P., H. Elderfield, and M. H. Comte (2003), Calibration of Mg/Ca thermometry in planktonic foraminifera from a sediment trap time series, *Paleoceanography*, 18, doi:10.1029/2002PA000846.
- Barker, S., M. Greaves, and H. Elderfield (2003), A study of cleaning procedures used for foraminiferal Mg/Ca paleothermometry, *Geochem., Geophys., Geosyst.*, 4 (9), doi:10.1029/2003GC000559.
- Brierley, C. M., A. V. Fedorov, Z. Liu, T. D. Herbert, K. T. Lawrence, and J. P. LaRiviere (2009), Weakened Hadley Circulation and Greatly Expanded Tropical Warm Pool in the Early Pliocene, *Science*, 323, 1714-1718.
- Cane, M., and P. Molnar (2001), Closing of the Indonesian seaway as a precursor to east African aridification around 3-4 million years ago, *Nature*, 411, 157-162.
- Cresswell, G. (1987), The East Australian Current. CSIRO Mar. Lab. Inf. Sheet, 3.
- Dowsett, H., J. Barron, and R. Poore, (1996), Middle Pliocene sea surface temperatures: a global reconstruction. *Mar. Micropaleontol.* 27, 13-26.
- Elderfield, H., M. Vautravers, and M. Cooper (2002), The relationship between shell size and Mg/Ca, Sr/Ca, $\delta^{18}\text{O}$, and $\delta^{13}\text{C}$ of species of planktonic foraminifera, *Geochem., Geophys., Geosyst.*, 3, doi: 10.1029/2001GC000194.
- Gasperi, J. T., and J. P. Kennett (1993), Vertical thermal structure of Miocene surface waters: Western equatorial Pacific DSDP Site 289, *Mar. Micropaleontology* 22, 235-254.
- Godfrey, J. S. (1996), The effect of the Indonesian Throughflow on ocean circulation and heat exchange with the atmosphere: A review, *J. Geophys. Res.*, 101, 12217-12237.
- Hamilton, L. J. (2006), Structure of the Subtropical Front in the Tasman Sea. *Deep-Sea Res. I*, 53, 1989-2009.
- Haug, G. H., D. M. Sigman, R. Tiedemann, T. F. Pedersen, and M. Sarnthein (1999), Onset of permanent stratification in the subarctic Pacific, *Nature* 401, 779-782.
- Haug, G. H., R. Tiedemann, R. Zahn, and A. C. Ravelo (2001), Role of Panama uplift on oceanic freshwater balance, *Geology* 29, 207-210.
- Hill, K. C., and R. Hall (2003), Mesozoic–Cainozoic evolution of Australia's New Guinea margin in a West Pacific context, in *Defining Australia: The Australian Plate*, Hillis, R. and R. D. Müller, Eds., *Planet Earth. Geol. Soc. Australia Spec. Pub.*, 22 and *GSA Spec. Paper*, 372, 259-283.

- Hirst, A. C., and J. S. Godfrey (1993), The role of Indonesian Throughflow in a Global Ocean GCM, *J. Phys. Oceanogr.*, 23, 1057-1086.
- Jochum, M., B. Fox-Kemper, P. H. Molnar, and C. Shields (2009), Differences in the Indonesian seaway in a coupled climate model and their relevance to Pliocene climate and El Niño, *Paleoceanography*, 24, PA1212, doi:10.1029/2008PA001678.
- Karas, C., D. Nürnberg, A. K. Gupta, R. Tiedemann, K. Mohan, and T. Bickert (2009), Mid-Pliocene climate change amplified by a switch in Indonesian subsurface throughflow, *Nature Geoscience*, 2, 434-438.
- Kennett, J. P., G. Keller, and M. S. Srinivasan (1985), Miocene planktonic foraminiferal biogeography and paleoceanographic development of the Indo-Pacific region, in J. P. Kennett, *The Miocene Ocean: Paleoceanography and Biogeography*, *Geol. Soc. Am. Mem.* 163, 197-236.
- Kennett, J. P., (1986), Miocene to early Pliocene oxygen and carbon isotope stratigraphy in the southwest Pacific, DSDP Leg 90, *Init. Repts. DSDP*, 90, 1383-1412.
- Kuhnt, W., A. Holbourn, R. Hall, M. Zuvela, and R. Käse (2004), Neogene History of the Indonesian Throughflow, in Clift, P., D. Hayes, W. Kuhnt, and P. Wang Eds., *American Geophysical Union Monograph*, Washington, p. 299-320.
- Lawrence, K. T., Z. Liu, and T. D. Herbert (2006), Evolution of the eastern tropical Pacific through Plio-Pleistocene glaciation, *Science* 312, 79-83.
- Locarnini, R. A. et al. (2006), *World Ocean Atlas 2005*, in Vol. 1: Temperature. S. Levitus, Eds., NOAA Atlas NESDIS 61, (U.S. Government Printing Office, Washington, D.C., 2006) 182 pp.
- Lourens, L. J. et al. (2004), in *A Geologic Time Scale 2004*: Cambridge. Gradstein, F. M., J. Ogg et al., Eds. (Cambridge Univ. Press, 2004), Appendix 2.
- Lisiecki, L. E., and M. E. Raymo (2005), A Pliocene-Pleistocene stack of 57 globally distributed benthic $\delta^{18}\text{O}$ records, *Paleoceanography*, 20, PA1003, doi:10.1029/2004PA001071.
- Marlow, J. R., C. B. Lange, G. Wefer, and A. Rosell-Melé (2000), Upwelling intensification as part of the Pliocene-Pleistocene climate transition, *Science*, 290, 2288-2291.
- Mudelsee, M., and M. E. Raymo (2005), Slow dynamics of the Northern Hemisphere glaciation, *Paleoceanography*, 20, PA4022, doi:10.1029/2005PA001153.
- Nürnberg, D., (2000), Taking the Temperature of Past Ocean Surfaces. *Science*, 289, 1698-1699.

- Pagani, M., Z. Liu, J. LaRiviere, and A. C. Ravelo (2010), High Earth-system climate sensitivity determined from Pliocene carbon dioxide concentrations, *Nature Geoscience*, *3*, 27-30.
- Paillard, D., L. Labeyrie, and P. Yiou (1996), Macintosh program performs time-series analysis, *Eos, Transactions AGU*, *77*, 379.
- Ravelo, A. C., D. H. Andreasen, M. Lyle, A. O. Lyle, and M. W. Wara (2004), Regional climate shifts caused by gradual global cooling in the Pliocene epoch, *Nature*, *429*, 263-267.
- Raymo, M. E., B. Grant, M. Horowitz, and G. H. Rau (1996), Mid-Pliocene warmth: stronger greenhouse and stronger conveyor, *Mar. Micropaleontol.*, *27*, 313–326.
- Regenberg, M., D. Nürnberg, S. Steph, J. Groeneveld, D. Garbe-Schönberg, R. Tiedemann, and W.-C. Dullo (2006), Assessing the effect of dissolution on planktonic foraminiferal Mg/Ca ratios: Evidence from Caribbean core tops, *Geochem., Geophys., Geosyst.*, *7*, doi: 10.1029/2005GC001019.
- Regenberg, M., S. Steph, D. Nürnberg, R. Tiedemann, and D. Garbe-Schönberg (2009), Calibrating Mg/Ca ratios of multiple planktonic foraminiferal species with $\delta^{18}\text{O}$ -calcification temperatures: Paleothermometry for the upper water column, *Earth Planet. Sci. Lett.*, *278*, 324-336, doi:10.1016/j.epsl.2008.12.019.
- Rodgers, K. B., M. A. Cane, and N. H. Naik (1999), The role of the Indonesian Throughflow in equatorial Pacific thermocline ventilation. *J. Geophys. Res.*, *104*, (C9), 20,551-20,570.
- Rodgers, K. B., M. Latif, and S. Legutke (2000), Sensitivity of equatorial Pacific and Indian Ocean watermasses to the position of the Indonesian throughflow, *Geophys. Res. Lett.* *27*, 2941-2944.
- Shackleton, N. J., and M. A. Hall (1990), in Proceedings ODP, Science Results, v. 115, Duncan, R. A., J. Backman, and L. C. Peterson Eds. (College Station, Texas, 1990).
- Srinivasan, M. S., and Sinha, D. K. (1998), Early Pliocene closing of the Indonesian Seaway: evidence from north-east Indian Ocean and Tropical Pacific deep sea cores, *Journal of Asian Earth Sciences*, *1*, 29-44.
- Steph, S., R. Tiedemann, J. Groeneveld, A. Sturm, and D. Nürnberg (2006), Pliocene changes in tropical east Pacific upper ocean stratification: response to tropical gateways? In *Proc. ODP, Sci. Results, 202* Tiedemann, R., A. C. Mix, C. Richter, and W.F. Ruddiman, Eds. (College Station, TX 2006) pp. 1–51.
- Steph, S., R. Tiedemann, M. Prange, J. Groeneveld, M. Schulz, A. Timmermann, D. Nürnberg, C. Rühlemann, C. Saukel, and G. Haug (in press), Early Pliocene increase in

thermohaline overturning preconditioned the development of the modern equatorial Pacific cold tongue, *Paleoceanography*.

Tomczak, M., and J. S. Godfrey (1994), *Regional Oceanography: an Introduction* (Pergamon, Oxford, England; New York 1994) 422pp.

Wara, M. W., A. C. Ravelo, and M. L. Delaney (2005), Permanent El Niño-Like Conditions During the Pliocene Warm Period, *Science*, 309, 758-761.